3 Brain Cortical Mantle and White Matter Core

I Historical Notes and Landmarks

In 1810, François-Joseph Gall initiated the study of the human cerebral cortex. In 1839, Leuret and his pupil, Gratiolet, attempted to classify the fissures of the human brain. However, the first to give a detailed account of the structure of the cerebral cortex was Baillarger (1840), who in addition described the gray and white matter. Meynert (1867, 1868) expanded on this finding and gave a detailed account of the regional variations existing in the cortical mantle and their structural and functional relationships. Following this major contribution, Betz (1874) described the motor area and its giant pyramidal cells which bear his name.

A large body of literature from the second part of the nineteenth and the early twentieth centuries reported on the frequency and variations of the sulcal pattern of the brain. These are found in the works of Zernov (1877), Cunningham and Horsley (1892), Retzius (1896), Kohlbrugge (1906), Landau (1910, 1911, 1914), Shellshear (1926), Van Bork-Feltkamp (1930), Slome (1932), Vint (1934), Chi and Chang (1941), Connolly (1950) and others.

Encephalometry, pioneered by Ariens Kappers (1847; Ariens Kappers et al. 1936), and later by von Economo (1929), was one of the most extensively used methods to study the brain. The brain index, also described by Ariens Kappers, was determined by measuring, on the lateral aspect of the brain, the length of the hemisphere and on the medial side, the occipital and temporal lobe length, (Fig. 3.1). He defined the callosal baseline connecting the basis of the genu to the basis of the splenium of the corpus callosum and measured accordingly the callosal length and height. Many brain indexes were subsequently reported, such as the callosal index, the central or the occipital index, as well as the temporal indexes of frontal height and frontal depth or length.

The relationship between the sulcation pattern of the cerebral hemispheres and genetics is still controversial despite the efforts of several authors (Karplus 1905, 1921; Sano 1916; Rossle 1937; Geyer 1940; Higeta 1940). We have recently reported using MR for in vivo brain morphology and morphometry on a series of patients with specific chromosomal aberrations (Tamraz et al. 1987,1990, 1991a,b, 1993). These preliminary qualitative morphometric results showed a clear cortical and brain phenotype accompanying the clinical syndromes.

The extensive work on racial differences in the early part of this century, aimed at disclosing brain morphological peculiarities, failed to a large extent. The anthropology of the human brain has not been adequately studied, as most series of brains analyzed from an encephalometric aspect are too small to yield significant results. If some racial differences do exist, it seems that they involve more particularly the lunate sulcus, the superior frontal sulcus and the temporal lobe and pole (Bailey and von Bonin 1951).

II Cytoarchitecture and Brain Mapping

Several methodologies were used in the assessment of the surface of the cerebral cortex, and the relative thickness of the cortical mantle in relation to particular anatomical regions, with slightly variable results, averaging 2000–2200 cm^2 (Wagner 1864; Calori 1870; Baillarger 1840; Jensen 1875; Giacomini 1878; Flechsig 1898; Campbell 1905; Benedikt 1906; Brodmann 1909; Henneberg 1910; Ramon y Cajal 1911; Jaeger 1914; Aresu 1914; von Economo and Koskinas 1925; Rose 1926; Kraus et al. 1928; Leboucq 1929; Lorente de No 1933; Filimonoff 1947).

Differences with respect to sex are emphasized by Aresu (1914) who reported values of 2300 cm^2 in males and 2000 cm^2 in females. A difference of about 136 cm^2 between brachicephalics and dolichocephalics in favor of the former was reported by Calori (1870). The ratio between external to buried surface has been reported by Henneberg (1910) and Jensen (1875). Both emphasized the larger development of the buried cortical surface averaging two thirds of the total cortical surface. This shows regional varia-

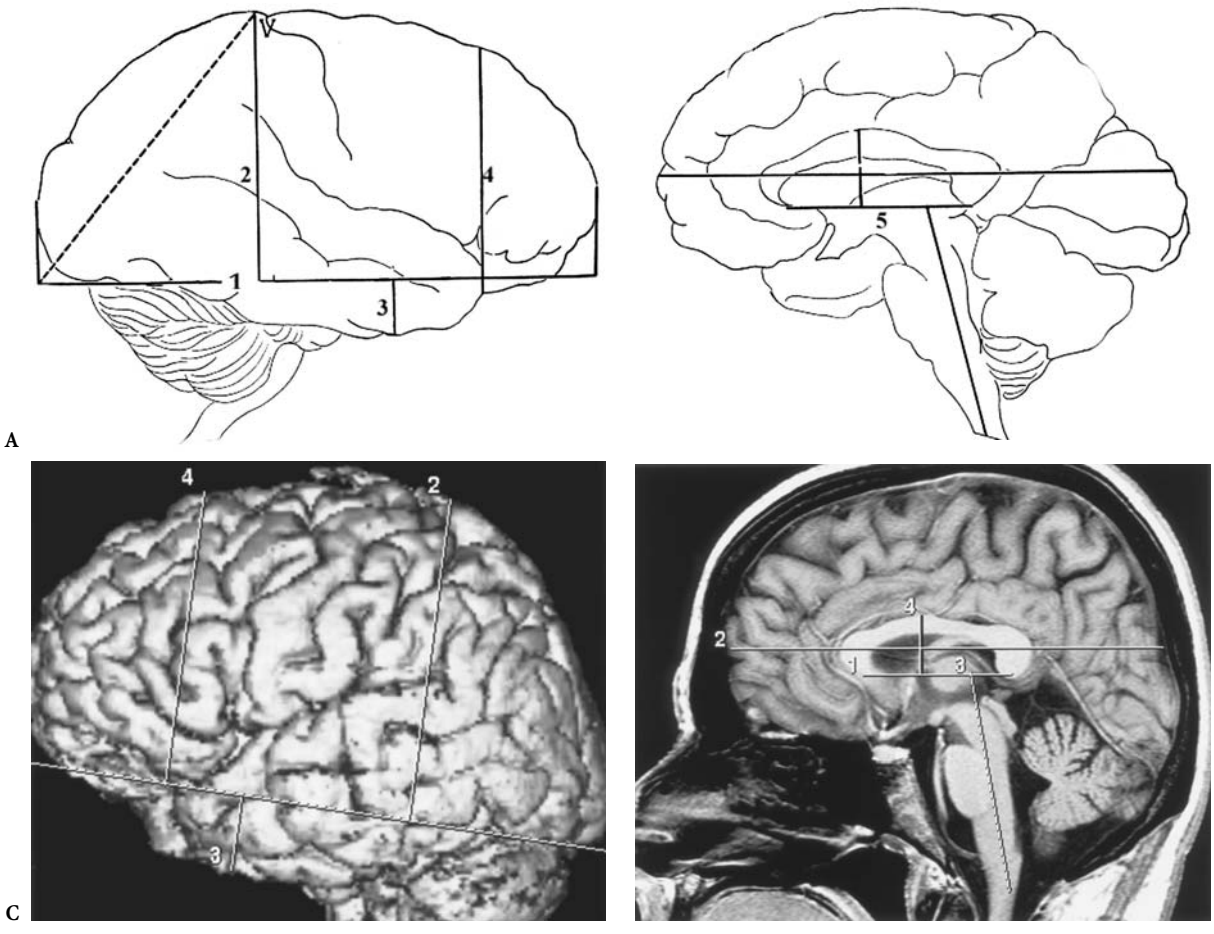

Fig. 3.1A–D. Encephalometry according to the methodology adopted by Ariens Kappers et al. (1936). **A** *1*, The horizontal lateral line, tangent to the ventral aspect of the occipital lobe and the fronto-orbital lobe; *2*, the parietal perpendicular line, from the highest parietal point; *3*, the temporal perpendicular line, from the lowest temporal point. **B** *4*, The callosal basal line tangent inferiorly to the genu and the splenium of the corpus callosum. **C,D** MR correlations

tions, ranging from as much as 4.5 mm in the precentral cortex to 1.5 mm in the depth of the calcarine sulcus. Actually, it increases from the frontal pole to the central cortex (2.2–3.3 mm), then decreases progressively in thickness from the postcentral gyrus toward the occipital pole (3.3–1.5 mm). The cortical thickness of the postcentral bank of the central sulcus is thinner than that of the precentral. The cortical ribbon of the central sulcus is thicker than the remaining part of the precentral gyrus. The cortical thickness decreases with age. The cortex is generally thicker on the apex of the convolution, decreasing in thickness in the depth of the sulci. In the future, high resolution MR, particularly with the use of small dedicated surface coils, will allow in vivo analysis of cortical thickness and will enhance the detection of focal abnormalities.

Jaeger (1914) measured the volume of the cortex at 540–580 cm^3 as compared to that of the white matter, about 400–490 cm^3. The number of cells in the cerebral cortex has been estimated by von Economo and Koskinas (1925) as averaging 15 billion neuronal cells.

The cytoarchitecture of the cortex is not uniform, showing wide variations in its intrinsic structural composition and thickness, as previously reported. Von Economo classifies the cerebral cortex into five fundamental types based on the partitioning of the pyramidal and granular cells. The homotypical type with the widest representation comprises the frontal (type II), the parietal (type III) and the polar (type IV). The heterotypical, limited to particular areas, comprises the agranular (type I) and the granular (type V) cortices. This classification differs from

those previously proposed by Baillarger (1840) or Ramon y Cajal (1911).

Three different conceptual approaches were undertaken to map the human brain. The functional anatomical approach was inaugurated by Broca and followed by Jackson. The cytoarchitectural myelogenetic study was initiated by Baillarger, followed by Ramon y Cajal, and later popularized by Brodmann. The third approach was based on the study of the gyral and sulcal patterns. These three approaches converged as correlations between gross morphology, cytoarchitecture, myelogenesis and function progressively evolved.

Flechsig (1898) used the myelogenetic method based on the investigation of the spatiotemporal distribution of myelination in the immediate subcortical regions. He reported a myelogenetic map of the cerebral cortex with 40 cortical fields grouped into primordial (1–8), intermediate (9–32) and terminal (33–40) areas. The first eight are considered as sensory areas, the intermediate as associative, and the remaining terminal areas are specific to humans, as may be distinguished from the anthropoid brains (Fig. 3.2).

In 1905, Campbell presented his own map of the cerebral cortex based on cytoarchitectural patterns (Fig. 3.3). At the same time, Brodmann also proposed his widely used map of the human brain (Fig. 3.4) based on ontogenesis. Unfortunately, due to his premature death, it was without any accompanying description of the areas indicated on the drawings as he had provided for the cercopithecus.

Continuing in the same trend, Vogt and Vogt described more than 200 different cytoarchitectural ar-

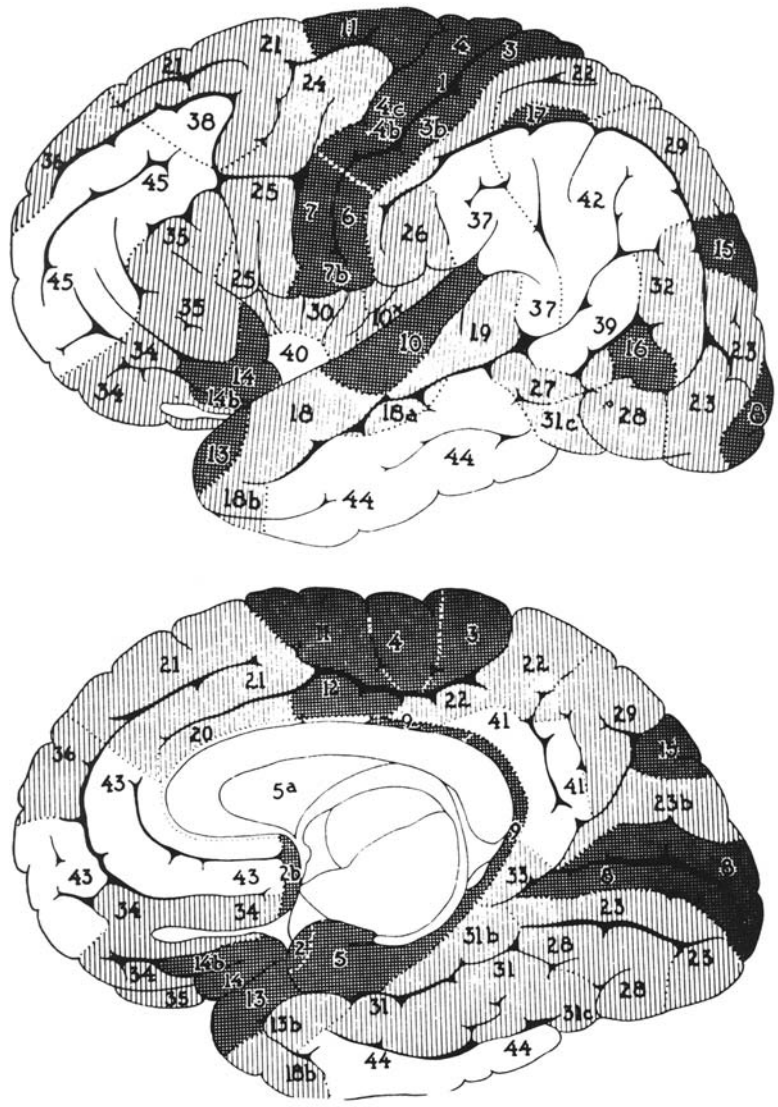

Fig. 3.2. Myelogenetic map of the cerebral cortex. Primordial areas numbered 1–8 (*cross-hatched areas*); terminal areas numbered 30–40 (*open areas*); intermediate areas numbered 9–32 (*lines*). (From Flechsig 1898)

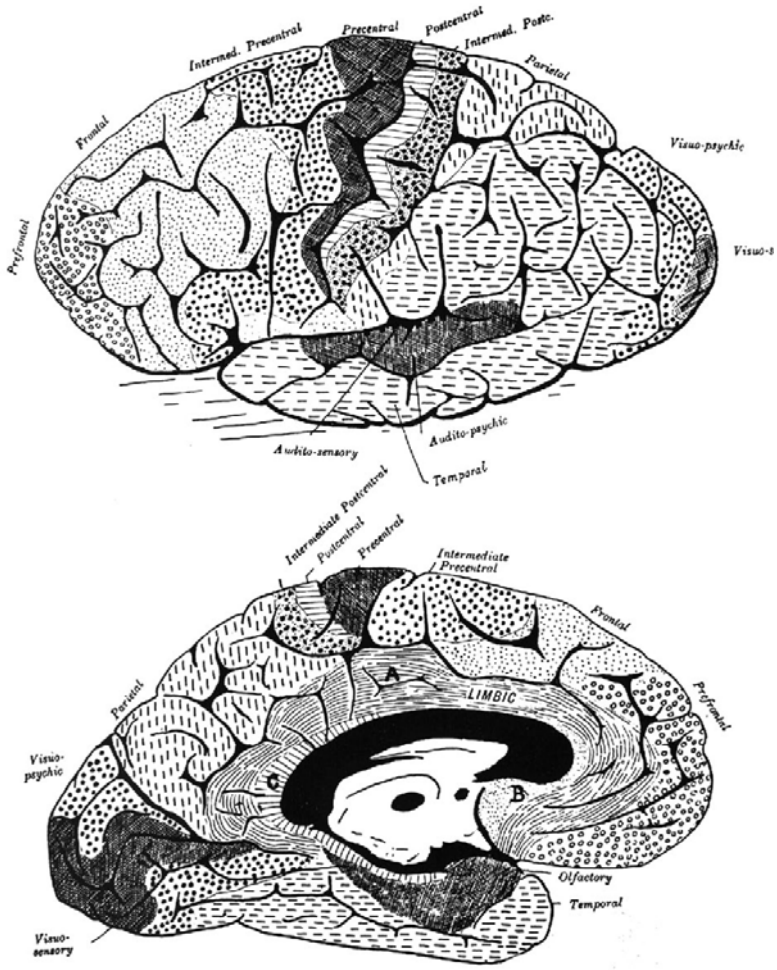

Fig. 3.3. Map of the cerebral cortex. (From Campbell 1905)

eas in the human brain cortex (Fig. 3.5). This attempt to "overparcelize" the cortex was criticized in the 1950s and 1960s. However, the Brodmann map survived these criticisms, and the numbers he used became the standard terminology. Clearly the Brodmann map is the closest to the modern definition of the cortical field, as defined by Jones as an area:

1. With sharp, singular cytoarchitectural boundaries
2. Receiving afferent fibers from a particular nucleus of the thalamus
3. Receiving a set of cortical and commissural axons from a limited, defined and constant set of other cortical areas
4. Giving a constant output to a particular set of cortical, subcortical, and thalamic targets
5. Having a topographic organization of a receptive periphery
6. The deactivation of which may lead to the loss of a particular function

A major contribution to cortical architecture and surface morphology was made by the work of von Economo and Koskinas (1925; von Economo 1927, 1929) (Fig. 3.6), who brought a highly detailed nomenclature of the cortical surface pattern accompanied by a description of cytoarchitectural peculiarities of each region (Fig. 3.7A–D). More recently, Bailey and von Bonin (1951) provided a new cytoarchitectural map (Fig. 3.8A–C). These authors increased our knowledge of cortical patterns following the initial contribution of Eberstaller (1884, 1890) (Fig. 3.9).

Most of the proposed maps, with their variable complexity, lack data concerning the transitional areas. Moreover, several authors have depicted significant inhomogeneities in cytoarchitectural areas considered distinctive.

The evolution of imaging followed a similar path. It progressed from investigation of the ventricular cavities, to opacification of the cerebral vasculature, then to the two dimensional sectional brain anatomy

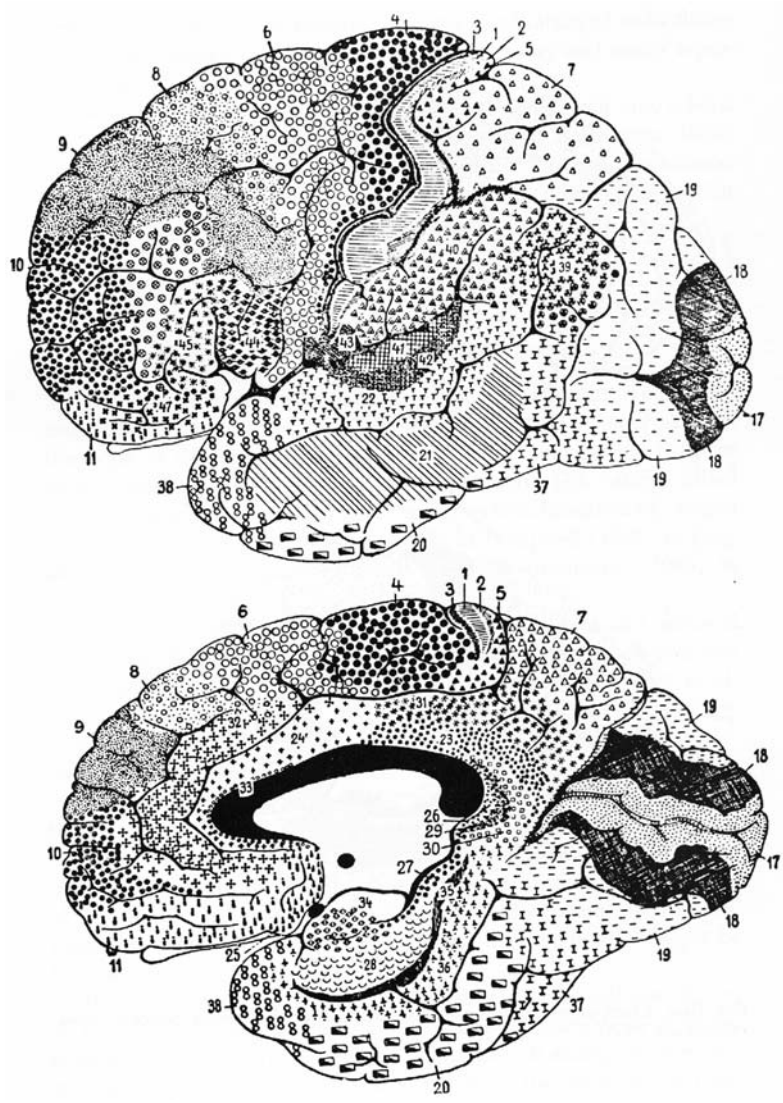

Fig. 3.4. Map of the cerebral cortex in man. Description of the cytoarchitectonic areas has been provided almost exclusively for the cercopithecus (1905), and only a few data concern areas 1, 3, 4, 6, 17, 18. (From Brodmann 1909)

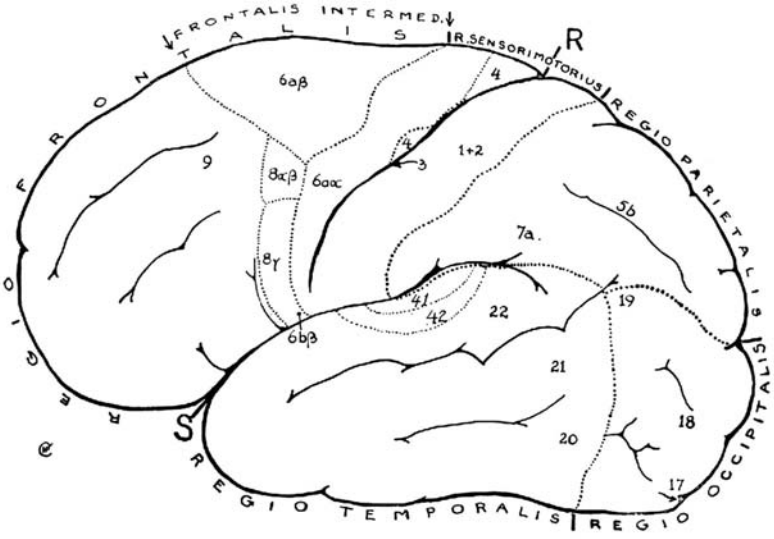

Fig. 3.5. Cytoarchitectonic map of the cortex. (Vogt and Vogt 1926)

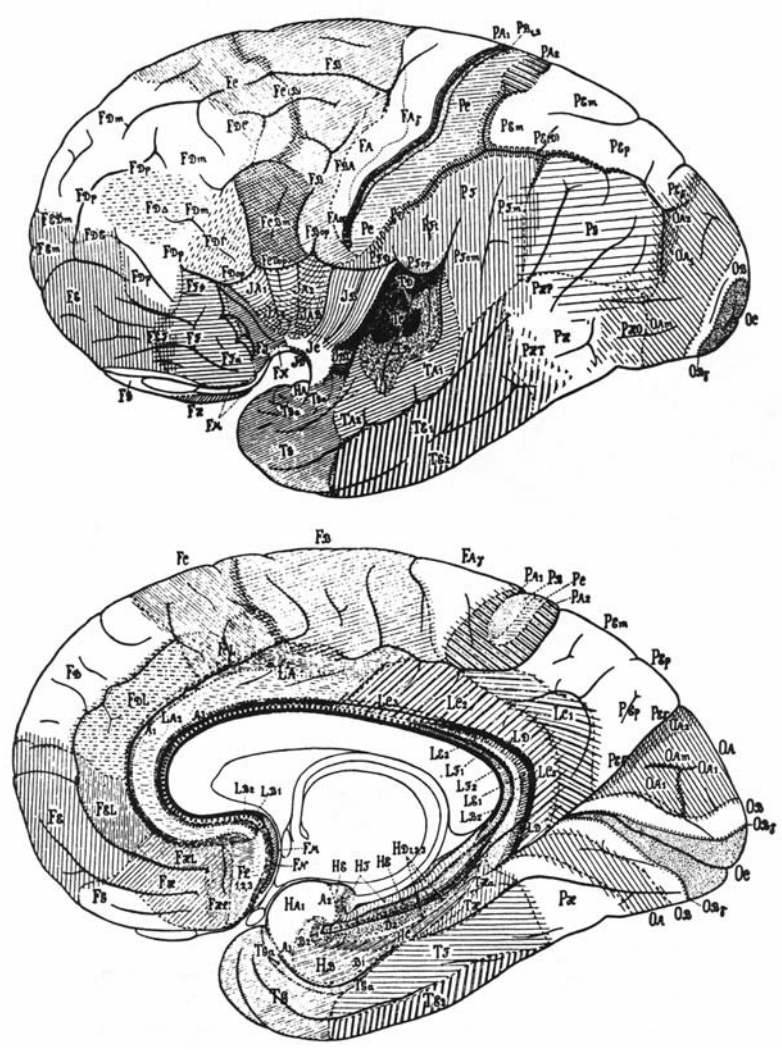

Fig. 3.6.. Cytoarchitectonic map of the cerebral cortex. (After von Economo 1925)

produced by CT scanning, and finally to the multiplanar method of MR, thus providing a sectional atlas of each imaged brain. Further advances in this technique rendered it possible, for the first time, to obtain a routine vision of an entire brain in three dimensions (3D). Furthermore, functional MR is presently available in vivo, allowing the establishment of links between morphology and function. This has in large part corroborated the precise work in brain mapping. The tedious work of the neuroscientists in their laboratories and the neurosurgeons in the operating rooms is progressively being replaced by the work of neuroradiologists, who are integrating data gathered from various metabolic and functional techniques.

This process requires a knowledge of the gyral and sulcal anatomy and its variations. Like the initial anatomists, we need to grasp the complexity of the cortical mantle as studied from various aspects: ontogenetic, phylogenetic, genetic and microscopic. Singly, these different approaches were limited and the results obtained suffered from lack of correlation between morphology and function.

A Gross Morphology and Fissural Patterns of the Brain

1 Gross Morphology

The cerebral hemispheres are ovoid in shape with an anterior-posterior long axis. Each hemisphere presents a base and a convexity. The base lies on the skull base and the convexity is related to the cranial vault and lateral aspects. The two hemispheres are separated by the interhemispheric fissure which pene-

trates deeply to the advent of the corpus callosum. The hemispheres are separated from the brainstem by the cerebral fissure of Bichat, which encircles the upper midbrain and extends posteriorly towards the ambient cistern, and merges anteriorly with the stem of the lateral fissures.

The cerebral hemisphere presents lateral, basal and medial aspects. The lateral and medial aspects are separated by the superior border of the hemisphere, while the lateral border separates the external from the basal aspects, and the medial border corresponds to the junction between the mesial and basal surfaces. Each hemisphere presents three poles: the frontal, occipital and temporal. The superior, mesial and lateral borders of each hemisphere converge towards the frontal and the occipital poles.

2 Brain Sulcation: Classifications

The distinction between fissures and sulci was made by Paul Broca who defined the fissures as folds of the wall pallium with an impression onto the ventricular walls and the sulci as indentations of the cortex. For the purpose of this work we will consider all furrows apart from the interhemispheric fissure as sulci. The classification of sulci into primary, secondary and tertiary has been adopted by most workers in this field.

Primary fissures were described using comparative and ontogenetic approaches The comparative approach was used and developed by Wernicke (1876, 1881–1883), Broca (1878), Turner (1891), Kükenthal and Ziehen (1895), von Bonin and Bailey (1947), and Bailey et al. (1950), among others. The ontogenetic approach was used by Cunningham and Horsley (1892), Retzius (1896) and His (1904).

The distinction made on the basis of comparative anatomy considered the sulci found in all gyrencephalic primates as primary (Fig. 3.10A,B). Embryologically, these fissures appear early in telencephalic development (Figs. 3.11A–C, 3.12). Upon reviewing previous works and the work of Larroche and Feess-Higgins (1987) we classified primary sulci as those appearing before the 30th week of gestation (Fig. 3.13A,B; Table 3.1). Secondary (Table 3.2) and tertiary sulci (Table 3.3) are those giving the brain its adult appearance. The classification of sulci remains controversial given the difficulties associated with the study of the human brain at birth and in infancy (Turner 1948, 1950; Bailey 1948; Bailey et al. 1950; Chi et al. 1977; Huang 1991) (Tables 3.4–3.8). MR data acquired in vivo from children will enable us to understand the progressive nature of sulcal development.

3 Sulcal and Gyral Anatomy

For a better understanding of the sulcal and gyral anatomy, we will first discuss the primary, followed by the secondary sulci. Tertiary sulci are difficult to identify on MRI since they are subject to marked individual variations; only those that are fairly constant will be discussed. In addition, this discussion is further complicated by the variable terminology used by different authors (Tables 3.9–3.11).

B The Lateral Surface of the Cerebral Hemisphere

The lateral aspect of the cerebral hemisphere is most efficiently investigated using 3D MRI surface renderings as reported in a previous work (Comair et al. 1996b). Anatomic correlations may be also achieved indirectly using multiplanar cross-sectional anatomic atlases based on definite reference markings (Déjerine 1895; Delmas and Pertuiset 1959; Talairach et al. 1967; Tamraz 1983; Cabanis et al. 1988; Salamon et al. 1990; Duvernoy et al. 1991) or by using two-dimensional (2D) contiguous MR slices (Naidich et al. 1995) extending from the lateral aspect of the hemisphere to reach the insular level.

1 Lateral Fissure of Sylvius

The lateral or Sylvian fissure, first described by Francois de Le Boë Sylvius (1652), is the major landmark on the lateral surface of the brain (Figs. 3.14–3.21). It is the most important and constant of the cerebral sulci. It is divided into three segments: the first extends from the lateral border of the anterior perforated substance and passes over the limen insulae in a posteriorly concave path that ends at the falciform sulcus, which separates the lateral orbital gyrus from the temporal pole. This part can be simply defined as the hidden or stem segment. The second, or horizontal segment, is the longest and deepest segment on the lateral surface of the hemisphere. We define the third segment as the segment limited anteriorly by the transverse supratemporal sulcus separating Heschl's gyri from the temporal planum and cutting into the superior temporal gyrus. This segment is complex, asymmetrical and correlates with hemispheric dominance. In right-handed individuals, it ascends at an acute angle on the right side and assumes an oblique course superiorly on the left.

Several branches are distinguished on the second or horizontal segment. Two sulci of almost similar

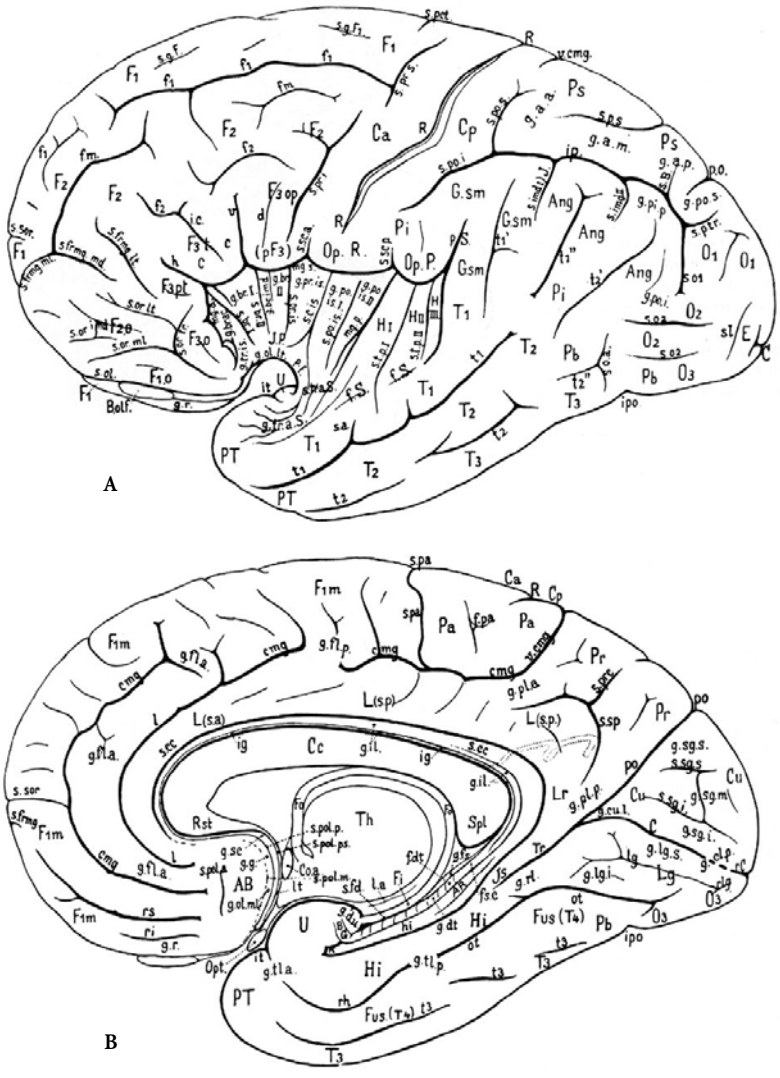

Fig. 3.7A–D. Fissural pattern of the human cerebral cortex. **A,B** Lateral and medial aspects; **C** inferior aspect; **D** superior aspect. (After von Economo and Koskinas 1925)

AB, Area parolfactoria of Broca (carrefour olfactif)
Ang, Lobulus angularis
Aq, Aqueduct
AR, Gyri Andreae Retzii
BB, Broca's band
BG, Bandelette of Giacomini
B.olf, Bulbus olfactorius
C, Fissura calcarina
Ca, Gyrus centralis anterior
Cc, Corpus callosum
Ch, Chiasma nervi optici
Coa, Commissura anterior
Cp, Gyrus centralis posterior
Cu, Cuneus
c, Cap
cmg, Sulcus callosomarginalis
d, Sulcus diagonalis (operculi)
E, Gyrus descendens of Ecker
F1, Gyrus frontalis primus
F2, Gyrus frontalis secundus
F3, Gyrus frontalis tertius
F3o, Pars orbitalis of F3 (F1o, F2o, F3o)
F3op, Pars opercularis of F3
F3pt, Pars praetriangularis of F3
F3t, Pars triangularis of F3 (Cap)
Fi, Fimbria
Fo, Fornix
Fus, Gyrus fusiformis
f1, Sulcus frontalis superior
f2, Sulcus frontalis inferior
f.dt, Fascia dentata
f.m, Sulcus frontalis medius
f.pa, Fossa paracentralis
fs.c, Fasciola cinerea
f.Sy, Fissura Sylvii
Gsm, Lobulus supramarginalis
g.a.a., Gyrus arcuatus anterior lobuli parietalis superioris
g.a.m., Gyrus arcuatus medius lobuli parietalis superioris
g.a.p., Gyrus arcuatus posterior lobuli parietalis superioris
g.amb, Gyrus ambiens
g.ant.o, Gyrus anticentralis operculi
g.ant.d, Gyrus antidiagonalis operculi
g.ant.pr.c, Gyrus antipraecentralis operculi
g.br.ac.(a), Gyrus brevis accessorius (anterior) insulae
<ig.br.I,II,III, Gyrus brevis primus, secundus, tertius, insulae
g.br.imd, Gyrus brevis intermedius insulae
g.cl.p., Gyrus cuneo-lingualis posterior
g.dt., Gyrus dentatus
g.d.u., Gyri digitati unci
g.fl.a, Gyrus frontolimbicus anterior
g.fl.p, Gyrus frontolimbicus posterior
g.fs, Gyrus fasciolaris
g.g, Gyrus geniculatus
g.il, Gyrus intralimbicus
g.imd, Gyrus brevis intermedius insulae
g.lg.s, Gyrus lingualis superior
g.lg.i, Gyrus lingualis inferior
g.ol.lt, Gyrus olfactorius lateralis
g.ol.ml, Gyrus olfactorius medialis
g.pip, Gyrus parietalis inferior posterior
g.pl.a, Gyrus parietolimbicus anterior
g.pl.p, Gyrus parietolimbicus posterior
g.po.i, Gyrus parieto-occipitalis inferior
g.po.s, Gyrus parieto-occipitalis superior
g.po.is.I, Gyrus postcentralis insulae primus
g.po.is.II, Gyrus postcentralis insulae secundus
g.pr.is, Gyrus praecentralis insulae
g.r, Gyrus rectus
g.rl, Gyrus retrolimbicus
g.sc, Gyrus subcallosus
g.sg.i, Gyrus sagittalis cunei inferior
g.sg.m, Gyrus sagittalis cunei medius
g.sg.s, Gyrus sagittalis cunei superior
g.sml, Gyrus semilunaris
g.str, Gyrus subtriangularis operculi
g.tl.a, Gyrus temporolimbicus anterior
g.tl.p, Gyrus temporolimbicus posterior
g.tr.a.S, Gyri temporales transversi anteriores of Schwalbe
g.tr.is, Gyrus transversus insulae
g.tr.op.I, Gyrus transversus operculi parietalis primus
g.tr.op.II, Gyrus transversus operculi parietalis secundus
g.tr.op.III, Gyrus transversus operculi parietalis tertius
H.I, Gyrus Heschl primus
H.II, Gyrus Heschl secundus
Hi, Gyrus hippocampi
h, Ramus horizontalis fissurae Sylvii
hi, Fissura hippocampi
Is, Isthmus
ic, Incisura capiti
ig, Indusium griseum
ip, Sulcus interparietalis
ipo, Incisura praeoccipitalis
it, Incisura temporalis
J, Incisura of Jensen or sulcus intermedius primus
Lg, Lingula
L.s.a, Gyrus limbicus superior pars anterior

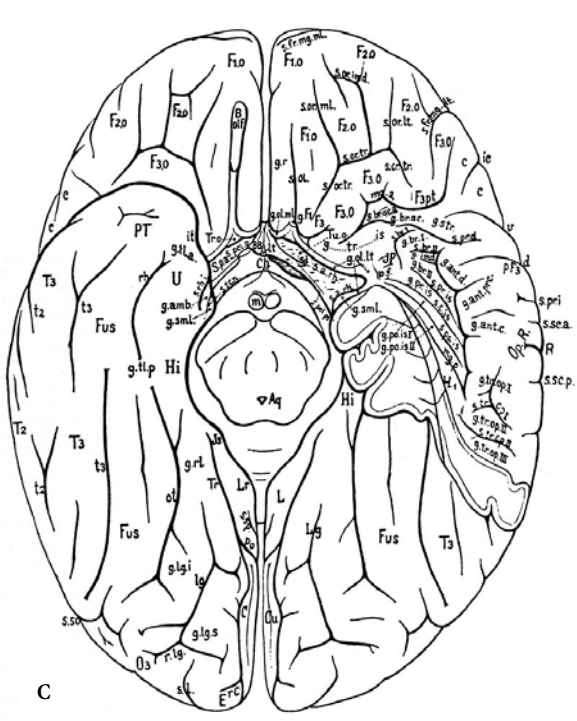

C

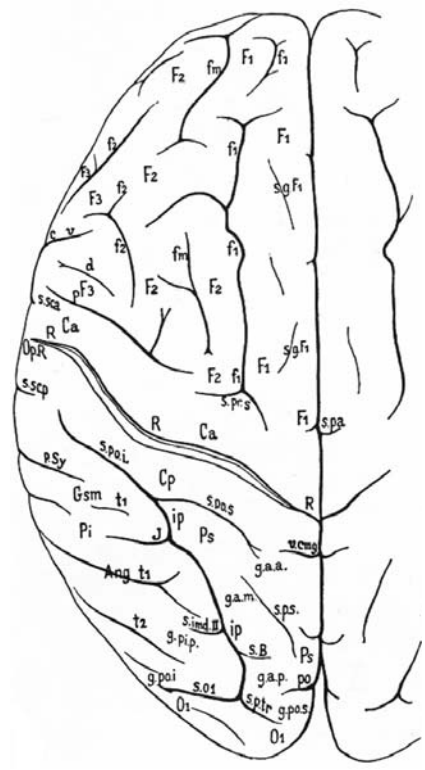

D

L.s.p, Gyrus limbicus superior pars posterior
Lr, Gyri limbici pars retrosplenialis
l, Sulcus intralimbicus
l.a, Lamina affixa
l.g, Sulcus lingualis
lt, Lamina terminalis
m, Corpus mamillare
mg.a, Margo anterior sulci circularis insulae
mg.p, Margo posterior sulci circularis insulae
O1, Gyrus occipitali primus
O2, Gyrus occipitali secundus
O3, Gyrus occipitali tertius
Op.P, Operculum parietale
Op.R, Operculum frontale of Rolando
Opt, Nervus opticus
ot, Fissura occipitotemporalis (collateralis)
Pa, Lobulus paracentralis
Pb, Regio parietalis basalis
Pi, Lobus parietalis inferior
Pr, Praecuneus
Ps, Lobus parietalis superior
PT, Gyrus temporopolaris
p.f, Incisura falciformis
po, Fissura parieto-occipitalis
p.Sy, Ramus posterior fissurae Sylvii
R, Sulcus of Rolando
Rst, Rostrum corporis callosi
rC, Fissura retrocalcarina
rh, Fissura rhinalis
ri, Sulcus rostralis inferior
rl, Sulcus retrolingualis
rs, Sulcus rostralis superior
S.p.a, Substantia perforata anterior
Spl, Splenium corporis callosis
s.a, Sulcus acusticus
s.a.rh, Sulcus arcuatus rhinencephali
s.B, Sulcus of Brissaud
s. br. I, Sulcus brevis primus insulae
s.b. II, Sulcus brevis secundus insulae
s.cc, Sulcus corporis callosi
s.c.is, Sulcus centralis insulae
s.d, Sulcus (parolfactorius) diagonalis
s.fd, Sulcus fimbriodentatus
s. frmg. ml, Sulcus frontomarginalis medialis
s.frmg.md, Sulcus frontomarginalis medius
s.frmg.lt, Sulcus frontomarginalis lateralis
s.g. F1, Sulcus gyri frontalis primi
s.imd.I, Sulcus intermedius primus of Jensen
s.imd.II, Sulcus intermedius secundus
s.l, Sulcus lunatus
so1, Sulcus occipitalis primus (praeoccipitalis, interoccipitalis)
so2, Sulcus occipitalis (secundus) lateralis
s.oa, Sulcus occipitalis (secundus) lateralis
s.ol, Sulcus olfactorius
s.or.lt, Sulcus orbitalis lateralis
s.or.ml, Sulcus orbitalis medialis
s.or.imd, Sulcus orbitalis intermedius
s.or.tr, Sulcus orbitalis transversus
s.pa, Sulcus paracentralis
s.po.i, Sulcus postcentralis inferior
s.po.s, Sulcus postcentralis superior
s.po.is, Sulcus postcentralis insulae
s.pol.a., Sulcus parolfactorius anterior
s.pol.m, Sulcus parolfactorius medius
s.pol.p, Sulcus parolfactorius posterior
s.pol.ps, Sulcus parolfactorius postremus
s.prc, Sulcus praecunei
s.prd, Sulcus praediagonalis
s.pr.i, Sulcus praecentralis inferior
s.pr.s, Sulcus praecentralis superior
s.pr.is, Sulcus praecentralis insulae
s.p.s, Sulcus parietalis superior
s.p.tr, Sulcus parietalis transversus
s.rh.i, Sulcus rhinencephali internus
s.san, Sulcus semiannularis
s.sc.a, Sulcus subcentralis anterior
s.sc.p, Sulcus subcentralis posterior
s.sg.s, Sulcus sagittalis cunei superior
s.sg.i, Sulcus sagittalis cunei inferior
s.so, Sulcus suboccipitalis
s.sor, Sulcus supraorbitalis
s.sp, Sulcus subparietalis
s.tp.I, Sulcus temporalis profundus primus
s.tp.II, Sulcus temporalis profundus secundus
s.tr.a.S, Sulci temporales transversi anteriores of Schwalbe
s.tr.op.I, Sulcus transversus operculi parietalis primus
s.tr.op.II, Sulcus transversus operculi parietalis secundus
T1, Gyrus temporalis primus
T2, Gyrus temporalis secundus
T3, Gyrus temporalis tertius
Th, Thalamus
Tr, Truncus fissurae parietooccipitalis et calcarinae
Tr.o, Trigonum (tuber) olfactorium
Tu.o, Tuberculum olfactorium or colliculus nuclei caudati
t1, Sulcus temporalis superior
t2, Sulcus temporalis medius
t3, Sulcus temporalis internus
U, Uncus
v, Ramus verticalis fissurae Sylvii
v.cmg, Ramus verticalis sulci callosomarginalis

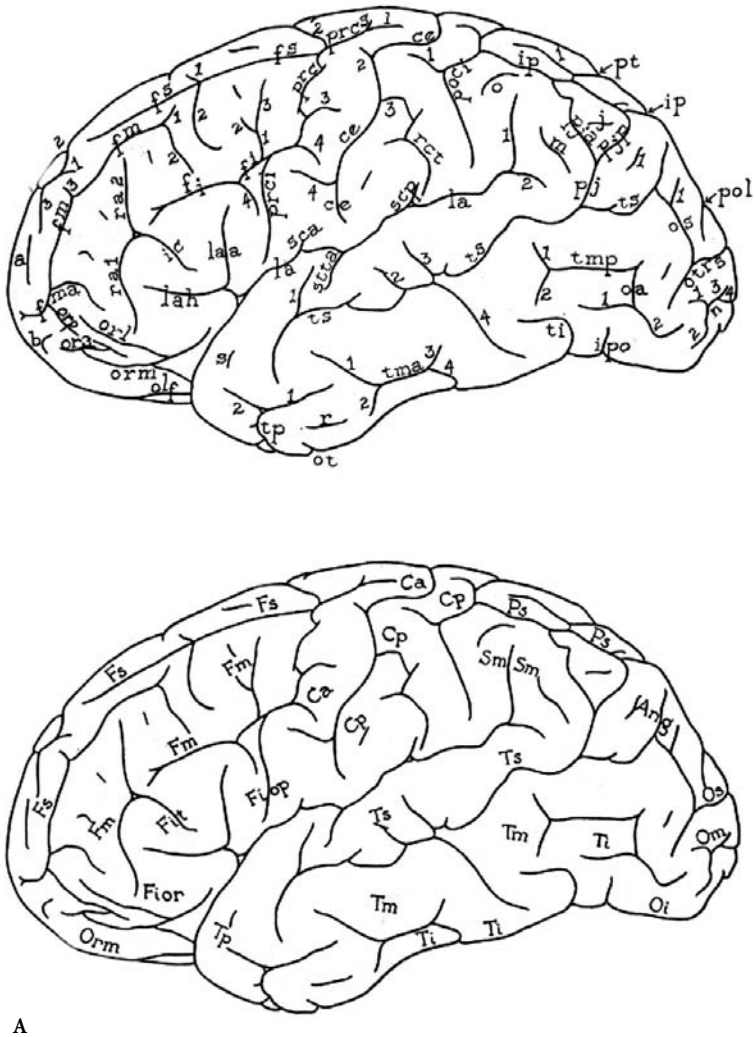

A

Fig. 3.8A–C. Fissural pattern of the human cerebral cortex. **A** Lateral aspect; **B** mesial aspect; **C** superior aspect. (After Bailey and von Bonin 1951)

aic, Sulcus arcus intercuneatus
Ang, Gyrus angularis (Huxley)
ca, Fissura calcarina
Ca, Gyrus centralis anterior
cc, Sulcus corporis callosi
ce, Sulcus centralis (Rolando)
ci, Sulcus cinguli, sive supramarginalis
cim, Sulcus cinguli, pars marginalis
cins, Sulcus centralis insulae
col, Fissura collateralis
Cp, Gyrus centralis posterior
Cu, Cuneus
cu, Sulcus cunei
Fi, Gyrus frontalis inferior
fi, Sulcus frontalis inferior
Fiop, Gyrus frontalis inferior, pars opercularis sive pedalis (Broca)
Fiorb, Gyrus frontalis inferior, pars orbitalis
Fit, Gyrus frontalis inferior, pars triangularis (cap de Broca)
Fm, Gyrus frontalis medius
fm, Sulcus frontalis medius
fma, Sulcus frontomarginalis (Wernicke)
Fs, Gyrus frontalis superior
fs, Sulcus frontalis superior
fsa, Sulcus frontalis superior anterior
ic, Incisura capitis
il, Sulcus intralimbicus
ip, Sulcus intraparietalis
ipo, Sulcus praeoccipitalis (Meynert)
L, Gyrus limbicus (sive cinguli)
La, Gyrus limbicus, pars anterior
Lp, Gyrus limbicus, pars posterior
la, Fissura lateralis (Sylvius)
laa, Fissura lateralis, ramus ascendens
lah, Fissura lateralis, ramus horizontalis
Lg, Gyrus lingualis
lo, Sulcus limitans operculi
mai, Sulcus marginalis anterior insulae
mii, Sulcus marginalis inferior insulae
msi, Sulcus marginalis superior insulae
oa, Sulcus occipitalis anterior (Wernicke)

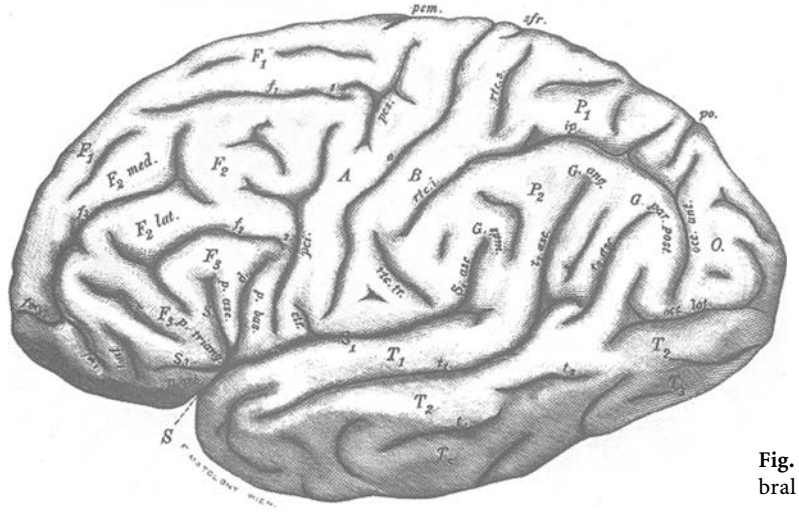

Fig. 3.9. Fissural pattern of the human cerebral cortex. (After Eberstaller 1890)

Oi, Gyrus occipitalis inferior
olf, Sulcus olfactorius
olri, Sulcus occipitalis transversus inferior
olrs, Sulcus occipitalis transversus superior
Om, Gyrus occipitalis medius
oper, Sulcus intraopercularis
ora, Sulcus orbitalis arcuatus
orl, Sulcus orbitalis lateralis
orm, Sulcus orbitalis medialis
orp, Sulcus orbitopolaris
Os, Gyrus occipitalis superior
os, Sulcus occipitalis superior (Ecker)
ot, Sulcus occipitotemporalis
ota, Sulcus occipitotemporalis accessorius
pa, Sulcus polaris anterior
pac, Sulcus paracentralis
Parc, Lobulus paracentralis
Pc, Praecuneus (Foville)
Pim, Gyrus parietalis inferior intermedius
pj, Sulcus parietalis intermedius (Jensen)
pja, Sulcus parietalis intermedius, ramus anterior
pjp, Sulcus parietalis intermedius, ramus posterior
po, Fissura parieto-occipitalis
poci, Sulcus postcentralis inferior
pocs, Sulcus postcentralis superior
pol, Sulcus parieto-occipitalis, pars lateralis
pom, Sulcus parieto-occipitalis, pars medialis
prc, Sulcus praecentralis
prci, Sulcus praecentralis inferior
prcs, Sulcus praecentralis superior
Ps, Lobulus parietalis superior
pt, Sulcus parietalis transversus (Brissaud)
ra, Sulcus radiatus
rct, Sulcus retrocentralis transversus
rh, Sulcus rhinalis
roi, Sulcus rostralis inferior
ros, Sulcus rostralis superior
sca, Sulcus subcentralis anterior
scp, Sulcus subcentralis posterior
Sm, Gyrus supramarginalis (Gratiolet)
sp, Sulcus subparietalis
sro, Sulcus suprarostralis
stta, Sulcus supratemporalis transversus anterior
sttm, Sulcus supratemporalis transversus medius
sttp, Sulcus supratemporalis transversus posterior
ti, Sulcus temporalis inferior
tma, Sulcus temporalis medius anterior
tmp, Sulcus temporalis medius posterior
tp, Sulcus temporopolaris
ts, Sulcus temporalis superior

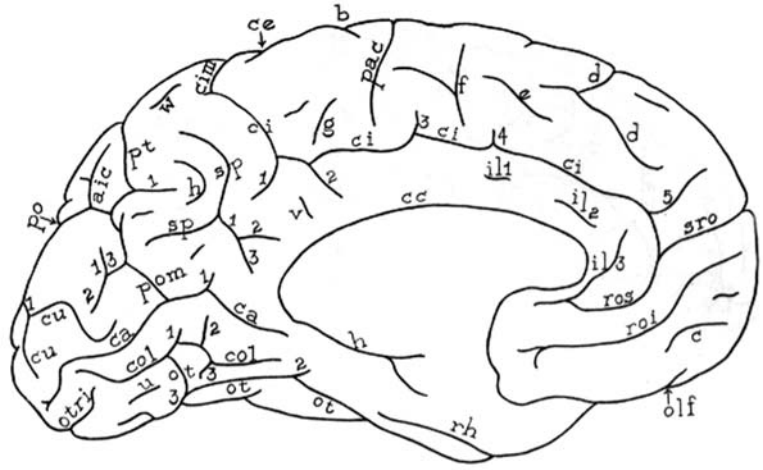

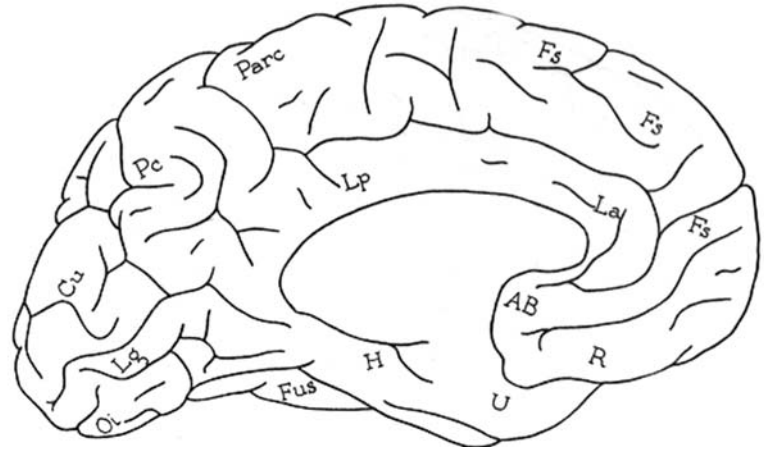

B

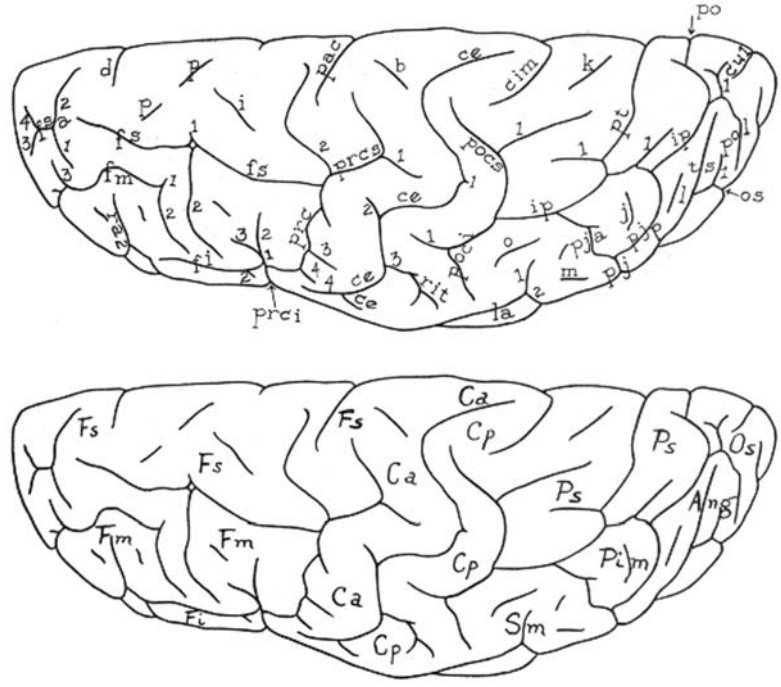

C

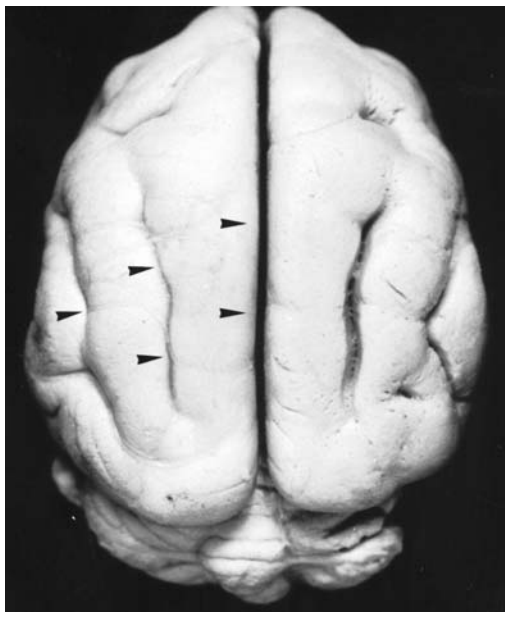

A

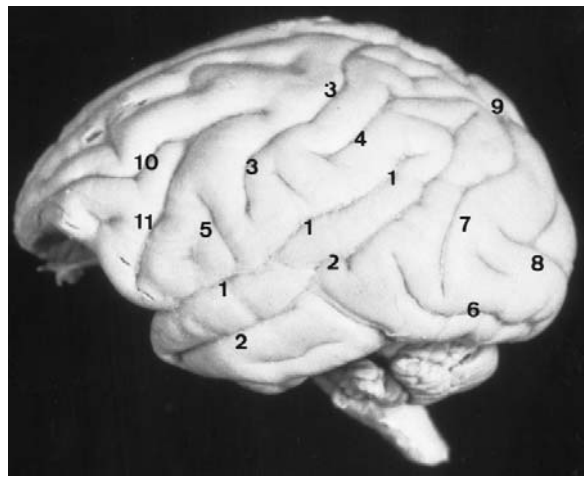

B

C

D

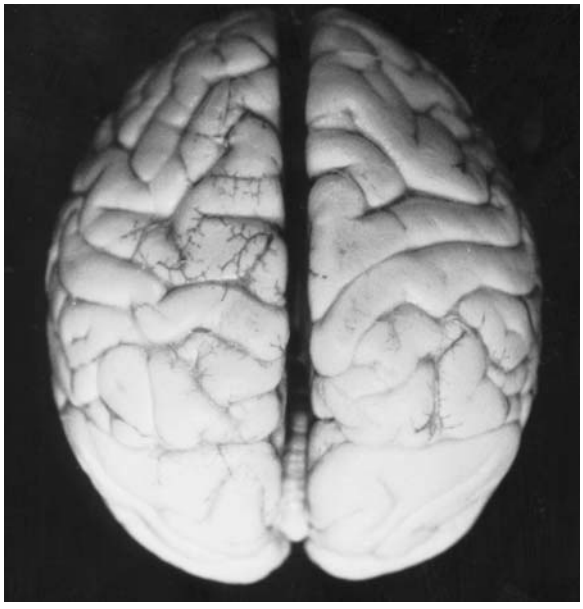

E

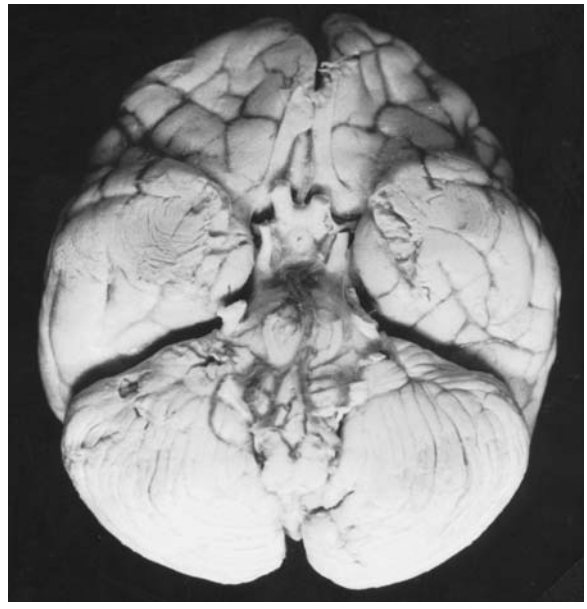

F

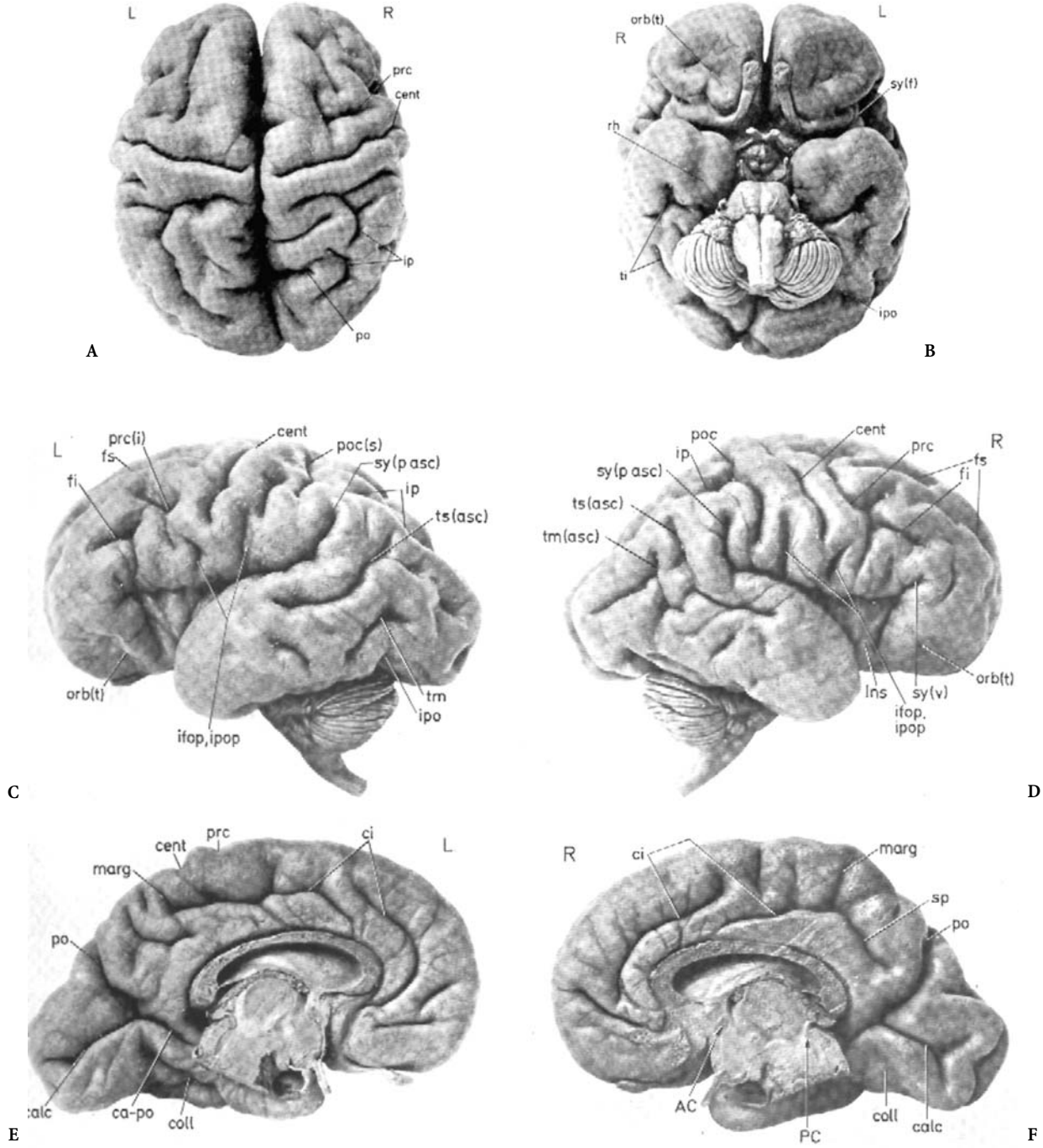

Fig. 3.11A–F. Fissural pattern of the fetal brain at 8 months. (After Retzius 1896)

◁ **Fig. 3.10A–F.** Brain sulcation of primates. **A** *Daubentonia* (lemurian, prosimian): most furrows show parallel orientation to the interhemispheric fissure as well to the sylvian fissure. **B** *Papio* (Cynomorpha): *1*, lateral fissure; *2*, superior temporal sulcus; *3*, central sulcus; 4, intraparietal sulcus; *5*, anterior subcentral sulcus; *6*, Inferior occipital sulcus; *7*, lunate sulcus; *8*, superior occipital sulcus; *9*, parieto-occipital sulcus; *10*, ramus superior of sulcus arcuatus; *11*, ramus infeior of sulcus arcuatus. **C–F** Chimpanzee (Anthropomorpha): *1*, superior temporal (parallel) sulcus; *2*, middle temporal sulcus; *3*, central sulcus; *4*, inferior postcentral and intraparital sulci; *5*, superior precentral sulcus; *6*, inferior precentral sulcus; *7*, sulcus lunatus; *8*, sulcus occipitalis diagonalis; *9*, lateral parieto-occipital incisure; *10*, fronto-orbital "H" (Museum National d'Histoire Naturelle, Paris; courtesy of R. Saban and J. Repérant)

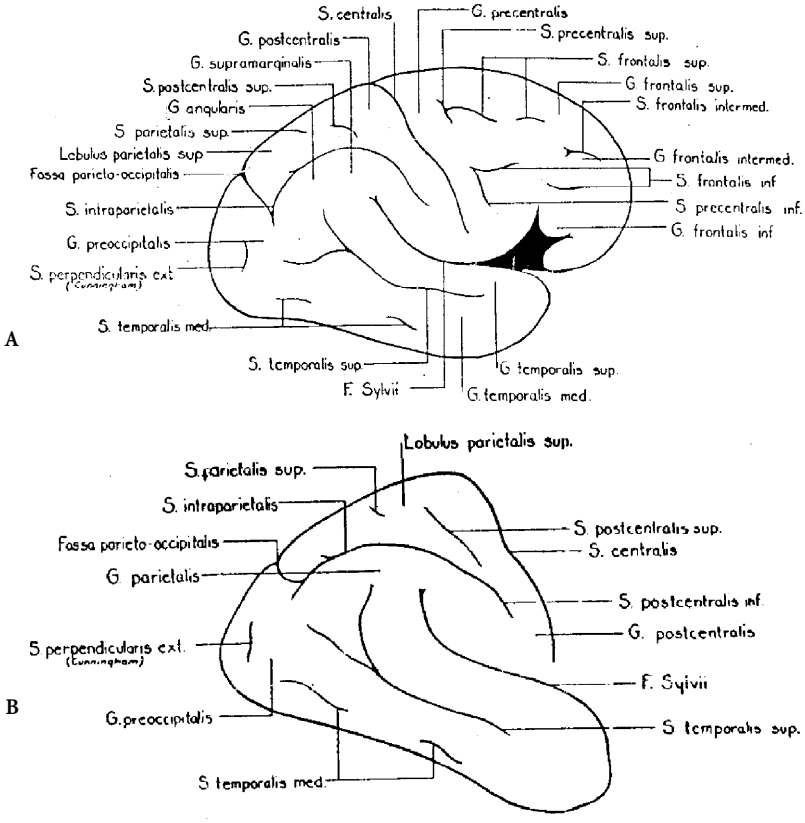

Fig. 3.12A,B. Fissural pattern of the fetal brain from the seventh month to birth. (According to Turner 1948)

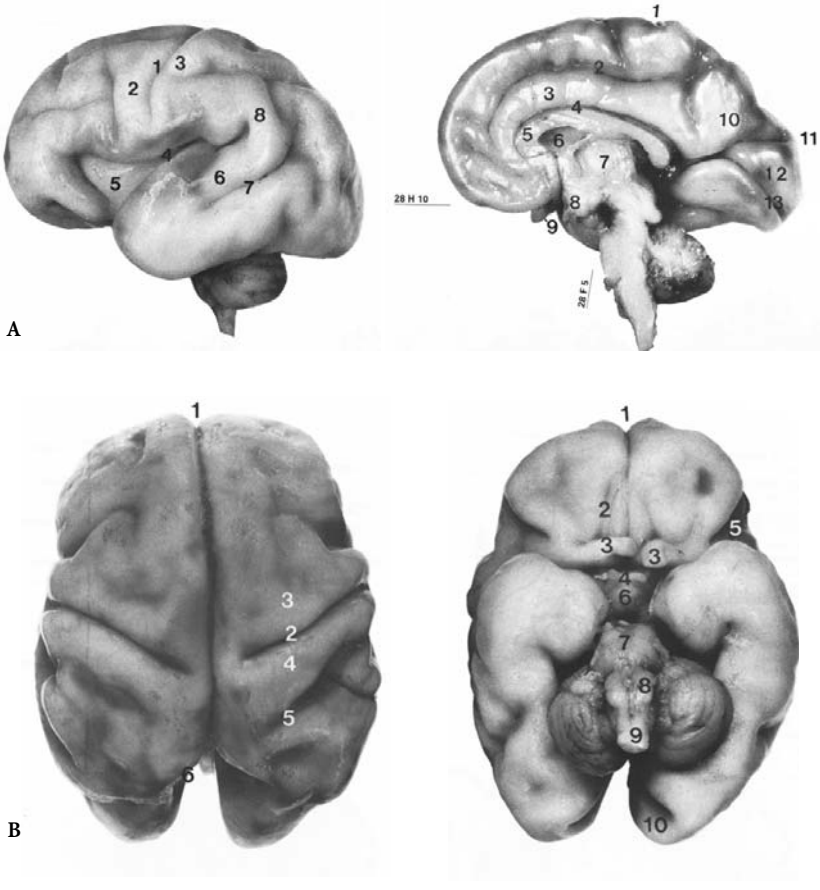

Fig. 3.13A,B. Fetal brain at 28–29 weeks of gestation. **A** Lateral ad mesial aspects. Lateral: *1*, central sulcus; *2*, precentral gyrus; *3*, postcentral gyrus; *4*, lateral sulcus; *5*, insula; *6*, superior temporal gyrus; *7*, superior temporal sulcus; *8*, supramarinal gyrus. Mesial: *1*, central sulcus; *2*, cingulate sulcus; *3*, cingulate gyrus; *4*, callosal sulcus; *5*, corpus callosum; *6*, cavum septi pellucidi; *7*, thalamus; *8*, infundibulum; *9*, olfactory tract; *10*, precuneus; *11*, parieto-occipital sulcus; *12*, cuneus; *13*, calcarine sulcus. **B** Superior and inferior aspects. Superior: *1*, interhemispheric fissure; *2*, central sulcus; *3*, precentral gyru; *4*, postcentral gyrus; *5*, postcentral gyrus; *6*, parieto-occipital sulcus. Inferior: *1*, interhemispheric fissure; *2*, olfactory sulcus; *3*, olfactory tract; *4*, optic chiasm; *5*, lateral fissure; *6*, infundibulum; *7*, pons; *8*, pyramid and uvula; *9*, spinal cod; *10*, calcarine sulcus. (According to Larroche and Feess-Higgins 1987)

Table 3.1. Classification of brain primary sulci

Weeks of gestation	Sulcal maturation
13–15	Early sylvian fissure
16–17	Cingulate sulcus
	Callosal sulcus
	Parieto-occipital sulcus
19–20	Calcarine
22–23	Circular sulcus (operculization)
25–26	Central sulcus
	Superior temporal (left) sulcus
	Superior part of precentral sulcus
	Olfactory sulcus
28–30	Intraparietal sulcus
	Inferior frontal sulcus
	Branching of lateral sulcus
	Paracentral sulcus
	Collateral sulcus
	Superior frontal sulcus

Table 3.2. Classification of brain secondary sulci

Lobe	Sulcus
Frontal lobe	Precentral
	Frontomarginal
	Orbitofrontal
	Rostral (superior, inferior)
Parietal lobe	Subparietal
Occipital lobe	Paracalcarine (ventral and dorsal)
	Lateral occipital
	Transverse occipital
	Lunate
Temporal lobe	Rhinal
	Transverse temporal
	Inferior temporal
Insular lobe	Sulcus centralis insulae

Table 3.3. Classification of fairly constant tertiary brain sulci

Lobe	Sulcus
Frontal Lobe	Intermediate frontal
	Diagonal
	Radiate
	Anterior subcentral
Parietal Lobe	Transverse parietal
	Intermediate (secondary, tertiary)
	Primary intermediate
Temporal lobe	Sulcus acousticus
Occipital lobe	Various individual variations and absence of consensus

Table 3.4. Chronology of sulcal maturation: lateral surface (From Chi et al. 1977)

Weeks of gestation	Sulcal maturation (lateral convexity)
10–15	Sylvian fissure
16–19	Circular sulcus
20–23	Central sulcus, superior temporal sulcus
24–27	Superior frontal sulcus, precentral sulcus, postcentral sulcus, intra-parietal sulcus, lateral occipital sulcus, middle temporal sulcus
28–31	Inferior frontal sulcus, inferior temporal sulcus
32–35	Insular gyri, parietal sulci, secondary frontal sulci, secondary temporal sulci, secondary parietal sulci, superior and inferior occipital sulci
36–39	Secondary transverse temporal sulci, secondary inferior temporal sulci, tertiary frontal sulci, tertiary parietal sulci
40–44	Secondary insular sulci, tertiary inferior temporal sulci, tertiary superior and inferior occipital sulci

Table 3.5. Chronology of sulcal maturation: medial surface (From Chi et al. 1977)

Weeks of gestation	Sulcal maturation (medial surface)
10–15	Interhemispheric fissure
10–15	Hippocampal fissure
10–15	Callosal sulcus
16–19	Cingulate sulcus
16–19	Parieto-occipital sulcus
16–19	Calcarine sulcus
20–23	Collateral sulcus
32–35	Marginal sulcus
36–39	Secondary cingulate sulci
40–44	Secondary callosomarginal sulci

Table 3.6. Chronology of sulcal maturation: basal surface (From Chi et al. 1977)

Weeks of gestation	Sulcal maturation (inferior surface)
16–19	Olfactory sulcus, gyrus rectus
28–31	Medial and lateral orbital gyri
36–39	Anterior and posterior orbital gyri
40–44	Secondary orbital sulci

Table 3.7. Appearance of gyri during gestation (From Chi et al. 1977)

Weeks of gestation	Gyri
27	Middle frontal gyrus, cuneus, medial and lateral occipitotemporal gyri, superior and inferior occipital gyri
28	Callosomarginal gyrus, inferior frontal gyrus, supramarginal gyrus, angular gyrus, medial and lateral orbital gyri
30	Inferior temporal gyrus, external occipital temporal gyrus
31	Transverse temporal gyrus
35	Paracentral gyrus
36	Anterior and posterior orbital gyri

Table 3.9. Sulci of lateral surface. (Modified from Testut and Latarjet 1948, pp 783–785)

Sulci	Eponyms
Lateral fissure	Scissure de Sylvius, grande scissure interlobaire (Chaussier), fissura lateralis (Henle), fissura sive fossa Sylvii (Ecker)
Central sulcus	Scissure de Rolando, sulcus centralis (Ecker), fissura transversa anterior (Pansch), posteroparietal sulcus (Huxley)
Lateral parieto-occipital sulcus	Scissure perpendiculaire externe, sillon occipital transverse (Broca), occipitoparietal fissure (Huxley), parietooccipital fissure (Turner), pars superior sive lateralis fissure parieto-occipitalis (Ecker)
Superior frontal sulcus	Sillon frontal supérieur, scissure frontale supérieure (Pozzi), premier sillon frontal (Broca), superofrontal sulcus (Huxley)
Inferior frontal sulcus	Sillon frontal inférieur, scissure frontale inférieure ou sourcilière (Pozzi), deuxième sillon frontal (Broca), sillon inféro-frontal (Huxley), sillon frontal primaire (Pansch)
Precentral sulcus	Sillon prérolandique, scissure parallèle frontale (Pozzi), sillon antéro-pariétal (Huxley), sulcus precentralis (Ecker), descending ramus of middle frontal sulcus (Pansch)
Intraparietal sulcus	Sillon interpariétal, sillon pariétal (Broca, Pansch), intraparietal fissure (Turner), sulcus occipito-parietalis (Schwalbe), sulcus postcentralis (Ecker), ramus ascendens (Pansch)
Superior temporal sulcus	Sillon parallèle, premier sillon temporal, sillon temporal supérieur (Ecker), sulcus temporalis (Pansch), anterotemporal sulcus (Huxley)
Inferior temporal sulcus	Sillon temporal inférieur, deuxième sillon temporal, sulcus temporalis medius (Ecker), posterotemporal sulcus (Huxley)

Table 3.8. Ultrasound landmarks of cortical maturation at different stages of gestation (From Huang 1991)

Weeks of gestation	Landmarks
24–25	Prominent parieto-occipital sulcus, early branching calcarine sulcus
26–27	Matured calcarine sulcus, anterior cingulate sulcus
28–29	Whole cingulate sulcus, post central sulcus, insula partly covered
30–31	Insula covered completely, cingulate sulcus arcs, curves inferior temporal sulcus, with or without secondary cingulate sulci
32–33	Secondary cingulate sulci, partial insular sulci
34–35	Better insular sulci, more matured secondary sulci, with or without tertiary sulci
>36	Tertiary sulci, more matured insular sulci

Table 3.10. Sulci of medial surface. (Modified from Testut and Latarjet 1948, pp 783–785)

Sulci	Eponyms
Cingulate sulcus	Scissure calloso-marginale, Scissure festonnée (Pozzi), grand sillon du lobe fronto-pariétal (Gratiolet), sillon du corps calleux (Gromier), scissure sous-frontale (Broca)
Medial parieto-occipital sulcus	Scissure perpendiculaire interne, Occipitoparietal fissure (Huxley), pars medialis sive verticalis fissuræ occipitalis perpendicularis (Ecker), scissure occipitale (Broca), fissura occipitalis (Pansch), fissura posterior (Burdach), fissura occipitalis perpendicularis interna (Bischoff)
Calcarine sulcus	Scissure calcarine, scissure des hippocampes (Gromier), partie postérieure de la scissure des hippocampes (Gratiolet), fissura occipitalis horizontalis (Henle), fissura posterior (Huschke)

Table 3.11. Sulci of inferior surface. (Modified from Testut and Latarjet 1948, pp 783–785)

Sulci	Eponyms
Olfactory sulcus	Sillon olfactif, sulcus olfactorius (Ecker), scissure olfactive (Giacomini), sillon droit ou premier sillon orbitaire (Broca)
Orbital sulci	Sillon cruciforme, sulcus orbitalis (Ecker), scissure orbitaire (Giacomini), deuxième sillon orbitaire (Broca), triradialis sulcus (Turner); the two anteroposterior branches are termed, by Weisbach, l'interne sulcus longitudinalis medius and l'externe sulcus longitudinalis externus. The transversal branch is also called the transverse sulcus by the same author.
(Lateral) occipito-temporal sulcus	Sillon temporo-occipital externe, premier sillon temporo-occipital, sulcus temporo-occipitalis (Ecker)
(Medial) occipito-temporal sulcus (Collateral sulcus)	Sillon temporo-occipital interne, deuxième sillon temporo-occipital, sulcus longitudinalis inferior (Huschke), sulcus occipito-temporalis (Pansch), fissura collateralis (Huxley), fissura collateralis sive temporalis inferior (Bischoff), sulcus occipito-temporalis inferior (Ecker), sillon collatéral

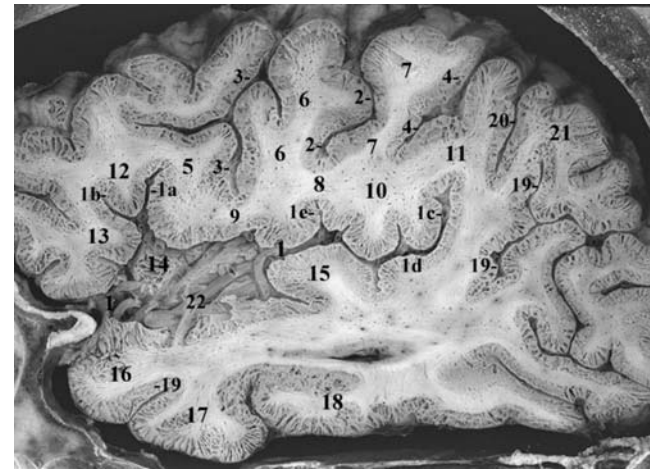

Fig. 3.16. Sagittal anatomical cut through the outer aspect of the insula showing the perisylvian region. *1*, Lateral fissure; *1a*, ascending ramus of lateral fissure; *1b*, horizontal ramus of lateral fissure; *1c,* terminal ascending tamus*, 1d,* temporal planum *2*, central sulcus; *3*, inferior precentral sulcus; *4*, inferior postcentral sulcus (ascending segment of intraparietal); *5*, inferior frontal gyrus, pars opercularis; *6*, precentral gyrus; *7*, postcentral gyrus; *8*, central operculum; *9*, frontal operculum; *10*, parietal operculum; *11*, supramarginal gyrus; *12*, inferior frontal gyrus, pars triangularis; *13*, inferior frontal gyrus, pars orbitalis; *14*, insula; *15*, transverse temporal gyrus (Heschl); *16*, superior temporal gyrus; *17*, middle temporal gyrus; *18*, inferior temporal gyrus; *19*, superior temporal (parallel) sulcus; *20*, intermediate sulcus of Jensen; *21*, angular gyrus; *22*, insular branches of middle cerebral artery

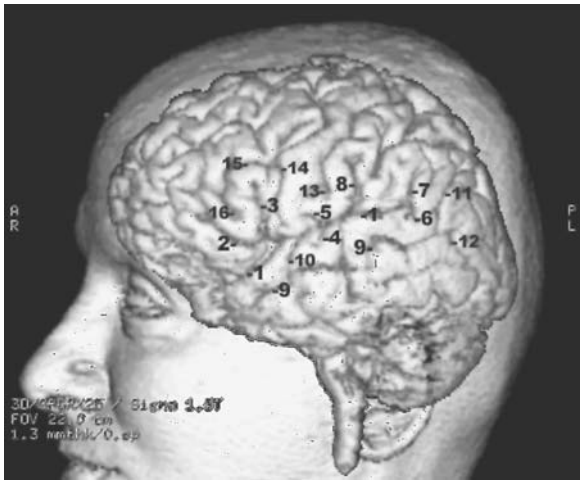

Fig. 3.14. 3D MR of the lateral aspect of the cerebral hemisphere showing the perisylvian sulci. *1*, Lateral fissure; *2*, horizontal ramus of lateral fissure; *3*, ascending ramus of lateral fissure; *4*, anterior transverse temporal sulcus; *5*, anterior subcentral sulcus; *6*, posterior transverse temporal sulcus; *7*, terminal ascending branch of lateral fissure; *8*, sulcus retrocentralis transversus (Eberstaller); *9*, superior temporal sulcus; *10*, sulcus acousticus; *11*, terminal ascending branch of temporal sulcus; *12*, descending branch of superior temporal sulcus; *13*, central sulcus; *14*, precentral sulcus; *15*, inferior central sulcus; *16*, radiate sulcus (incisura capitis)

Fi. 3.15. 3D MR of the lateral aspect of the cerebral hemisphere showing the perisylvian gyri. *1*, Superior temporal gyrus; *2*, middle temporal gyrus; *3*, inferior temporal gyrus; *4*, fronto-parietal operculum; *5*, precentral gyrus (inferior enu); *5′*, precentral gyrus (superior genu); *6*, postcentral gyrus; *7*, inferior frontal gyrus, pars opercularis; *8*, inferior frontal gyrus, pars triangularis; *9*, inferior frontal gyrus, pars orbitalis; *10*, middle frontal gyrus; *11*, inferior parietal lobule; *12*, occipital lobe

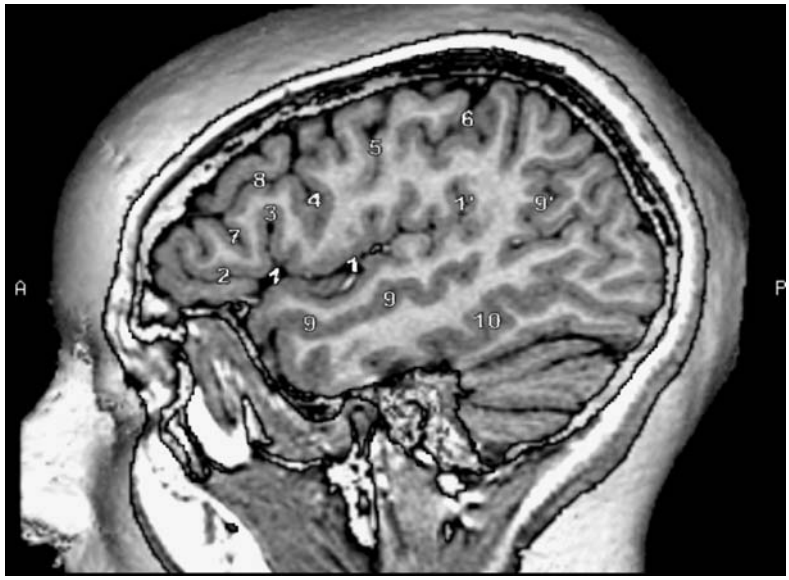

Fig. 3.17. Lateral 3D-MR view of the lateral fissure and its major rami. Sagittal cut into a 3D MR of the head showing the lateral surface of the brain. *1*, Lateral (sylvian) fissure; *1'*, ascending ramus of the lateral fissure; *2*, horizontal ramus of lateral fissure; *3*, ascending ramus of lateral fissure; *4*, inferior precentral sulcus; *5*, central (rolandic) sulcus; *6*, postcentral sulcus; *7*, radiate sulcus (incisura capitis); *8*, superior frontal sulcus; *9*, superior temporal (parallel) sulcus; *10*, inferior temporal sulcus

Fig. 3.18. Sagittal cut into a 3D MR of the head showing the lateral surface of the brain. *1*, Frontoparietal (central) operculum; *2*, precentral gyrus; *3*, postcentral gyrus; *4*, pars opercularis of inferior frontal gyrus; *5*, pars triangularis of inferior frontal gyrus; *6*, pars orbitalis of inferior frontal gyrus; *7*, superior temporal gyrus; *8*, transverse gyrus of Heschl; *9*, supramarginal gyrus; *10*, middle temporal gyrus; *11*, angular gyrus; *12*, superior occipital gyrus; *13*, middle occipital gyrus; *14*, inferior occipital gyrus; *15*, inferior temporal gyrus

length (2–3 cm) are noted in the frontal lobe: the horizontal ramus and the vertical ramus. These rami have a divergent course limiting a triangular space whose apex faces the sylvian fissure. These rami start from the sylvian fissure separately or from a common trunk (one third of cases). The terminal segment usually bifurcates at its end in about 70% of the cases forming long ascending and short descending parts. The latter is the posterior transverse temporal sulcus more frequently found on the right (70% of cases). This sulcus, which shows an anterior inferior oblique course, should not be confused with the transverse supratemporal sulcus, seen on the first temporal gyrus separating the posterior border of Heschl's gyri from the planum temporale. The cortical regions adjacent to the lateral sulcus are the frontal, parietal and temporal opercula, or lids, covering the insular lobe (Table 3.12).

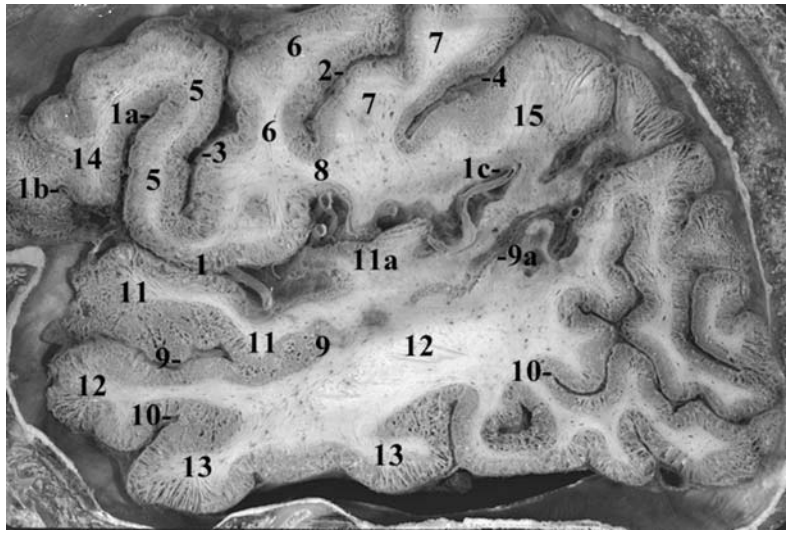

Fig. 3.19. Sagittal anatomical cut of the brain showing the lateral fissure and the perisylvian region. *1*, Lateral fissure; *1a*, ascending ramus of lateral fissure; *1b*, horizontal ramus of lateral fissure; *1c*, terminal ascending branch of lateral fissure; *2*, central sulcus; *3*, inferior precentral sulcus; *4*, inferior postcentral sulcus (ascending segment of intraparietal); *5*, inferior frontal gyrus, pars opercularis; *6*, precentral gyrus; *7*, postcentral gyrus; *8*, central operculum; *9*, superior temporal sulcus; *10*, inferior temporal sulcus; *11*, superior temporal gyrus; *11a*, transverse temporal gyri (Heschl); *12*, middle temporal gyrus; *13*, inferior temporal gyrus; *14*, inferior frontal gyrus, pars triangularis; *15*, supramarginal gyrus

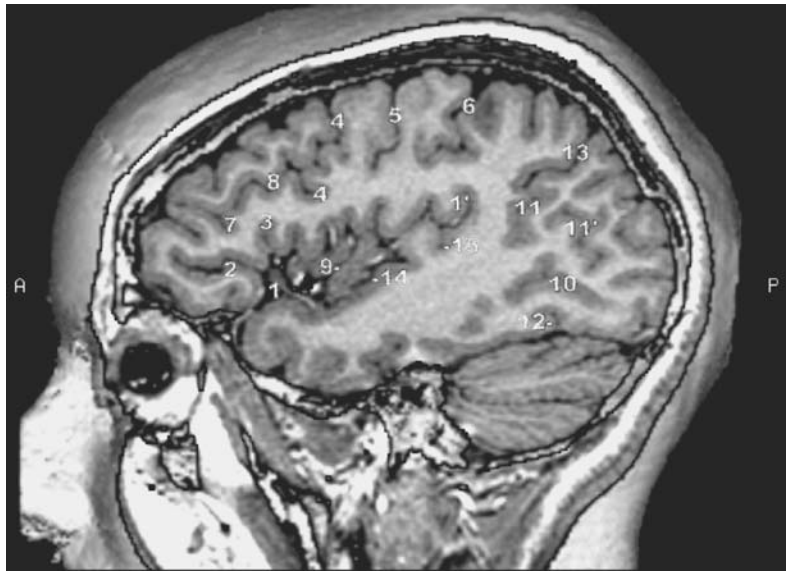

Fig. 3.20. Sagittal cut into a 3D MR of the head passing through the insular cortex and showing the main sulci. *1*, Lateral sylvian fissure; *1'*, ascending ramus of lateral fissure; *2*, horizontal ramus of lateral fissure; *3*, ascending ramus of lateral fissure; *4*, precentral sulcus; *5*, central sulcus; *6,* postcentral fissure; *7,* radiate sulcus (incisura capitis); *8,* inferior frontal sulcus; *9,* central sulcus of insula; *10*, inferior occipital sulcus; *11*, ascending ramus of parallel sulcus; *11'*, superior occipital sulcus; *12*, preoccipital incisure

2 Central Sulcus (Rolando)

Described by Rolando in 1829, the central sulcus separates the frontal from the parietal lobe (Figs. 3.22–3.31). Associated with it, Broca described three curves, a superior genu and an inferior genu. The cortex located between these genus represents the portion of the precentral gyrus innervating the arm. An increase in the depth of this sulcus is reported between the trunk and the arm motor field (Symington and Crymble 1913). The direction of this sulcus is anteriorly oblique from superior to inferior.

The rolandic sulcus is rarely interrupted and usually does not reach the sylvian fissure, resulting in most cases in a hook-like end. Anastomoses with the subcentral, precentral and postcentral sulci are fairly frequent, occurring in about 50% of cases. Extension into the sylvian fissure is found in about 20% of cases, generally as an anastomosis with the anterior or posterior subcentral sulci (Retzius 1896; Vint 1934).

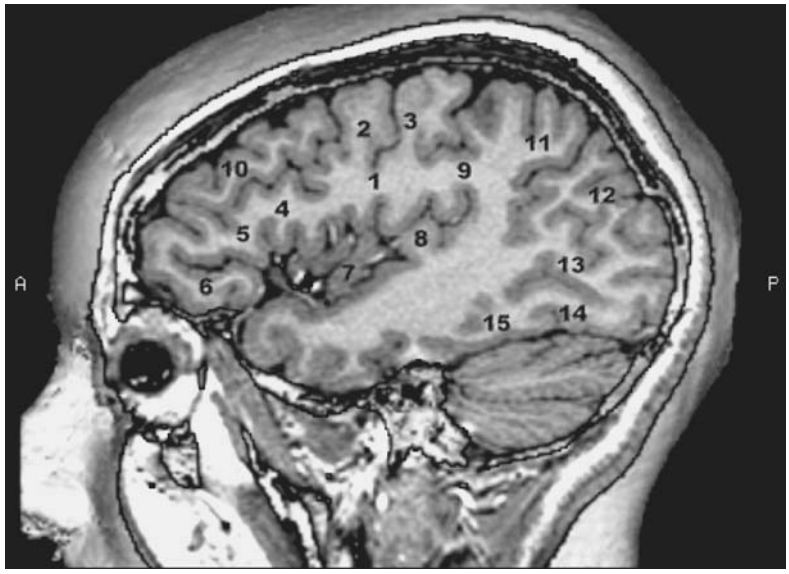

Fig. 3.21. Sagittal cut into a 3D MR of the head passing through the insular cortex and showing the main gyri. *1*, Frontoparietal operculum; *2*, precentral sulcus; *3*, postcentral sulcus; *4*, pars opercularis of inferior frontal gyrus; *5*, pars triangularis of inferior frontal gyrus; *6*, pars orbitalis of inferior frontal gyrus; *7*, insula; *8*, superior transverse gyrus of Heschl; *9*, supramarginal gyrus of inferior parietal lobule; *10*, middle frontal gyrus; *11*, angular gyrus of inferior parietal lobule; *12*, superior occipital gyrus; *13*, middle occipital gyrus; *14*, inferior occipital gyrus; *15*, inferior temporal gyrus

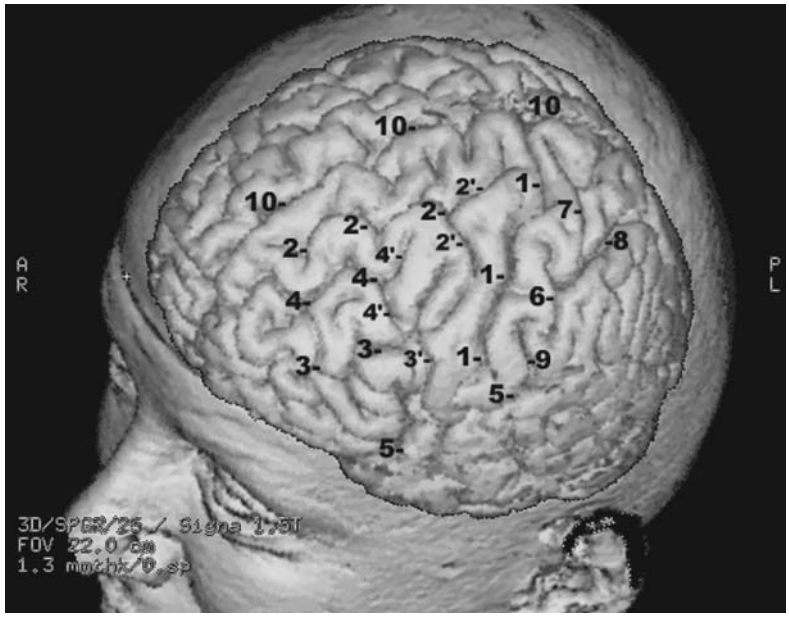

Fig. 3.22. 3D MR of the brain showing the frontal and central sulci. *1*, Central sulcus; *2*, superior frontal sulcus; *2′*, superior prefrontal sulcus; *3*, inferior frontal sulcus; *3′*, inferior precentral sulcus; *4*, intermediate frontal sulcus; *4′*, posterior Y-branching of intermediate frontal sulcus; *5*, lateral fissure; *6*, postcentral sulcus (ascending segment of intraparietal sulcus); *7*, superior postcentral sulcus; *8*, intraparietal sulcus; *9*, sulcus retrocentralis transversus; *10*, interhemispheric fissure

Table 3.12. Sylvian fissure opercula

After Ono et al. 1990	After Duvernoy et al. 1991
• Frontal operculum Pars orbitalis Pars triangularis • Frontoparietal operculum Pars opercularis Precentral gyrus Postcentral gyrus Inferior parietal lobule • Temporal operculum Superior temporal gyrus	• Frontal operculum Pars triangularis Pars opercularis • Central operculum Precentral gyrus (inferior end) Subcentral gyrus Postcentral gyrus (inferior end) • Parietal operculum: inferior parietal lobule • Temporal operculum Superior temporal gyrus

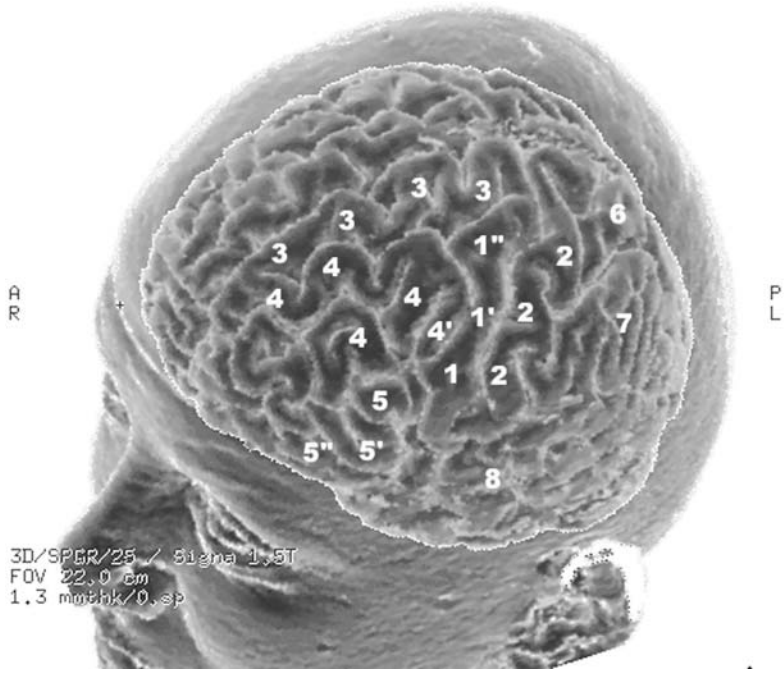

Fig. 3.23. 3D MR of the brain showing the frontal and central gyri. *1*, Central gyrus (inferior genu); *1'*, central sulcus (middle curve or genu); *1''*, central gyrus, superior genu; *2*, postcentral gyrus; *3*, superior frontal gyrus; *4*, middle frontal gyrus; *5*, inferior frontal gyrus; *5'*, inferior frontal gyrus, pars triangularis; *5''*, inferior frontal gyrus, pars opercularis; *6*, superior parietal gyrus; *7*, inferior parietal lobule; *8*, temporal lobe

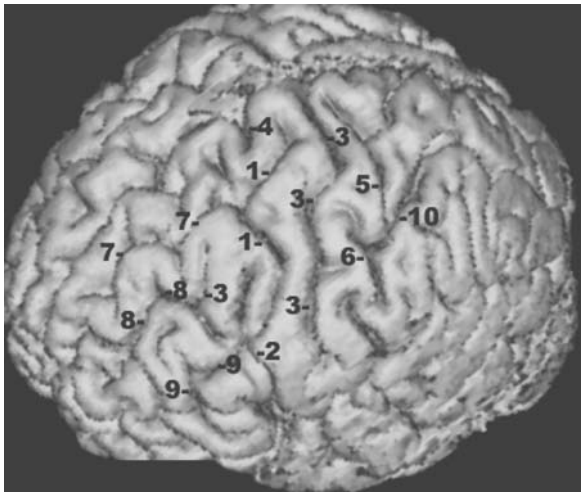

Fig. 3.24. 3D MR of the brain showing the pericentral sulci (lateral view). *1*, Precentral sulcus (superior segment); *2*, precentral sulcus (inferior segment); *3*, precentral gyrus (intermediate segment); *4*, medial precentral sulcus; *5*, postcentral sulcus, superior segment; *6*, postcentral sulcus, inferior segment; *7*, superior frontal sulcus; *8*, middle frontal sulcus; *9*, inferior frontal sulcus; *10*, intraparietal sulcus

Fig. 3.25. 3D MR of the brain showing the pericentral gyri (lateral view). *1*, Precentral gyrus; *1'*, superior genu of precentral gyrus; *1''*, inferior genu of precentral gyrus; *2*, postcentral gyrus; *3*, superior frontal gyrus; *4*, middle frontal gyrus; *5*, inferior frontal gyrus; *6*, superior parietal lobule, anterior portion; *7*, superior parietal lobule, posterior portion; *8*, supramarginal gyrus; *9,* angular gyrus; *10*, posterior parietal gyrus

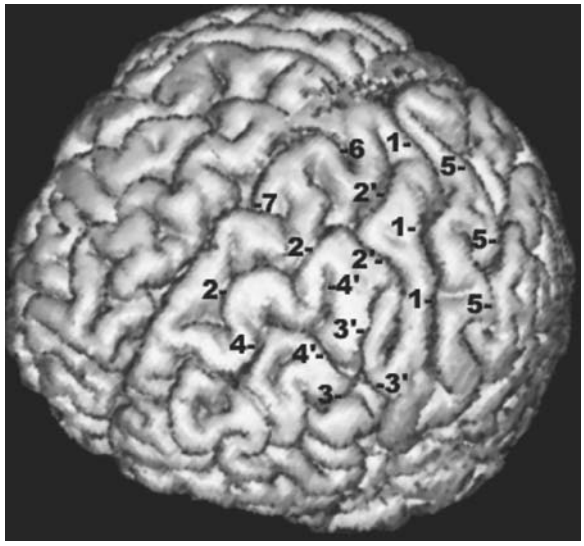

Fig. 3.26. 3D MR of the brain showing the central and frontal sulci (oblique anterior view). *1*, Precentral sulcus; *2*, superior frontal sulcus; *2'*, superior precentral sulcus; *3*, inferior frontal sulcus; *3'*, inferior precentral sulcus; *4*, intermediate frontal sulcus; *4'*, posterior branching of intermediate frontal sulcus; *5*, postcentral sulcus; *6*, medial precentral sulcus; *7*, paracentral sulcus

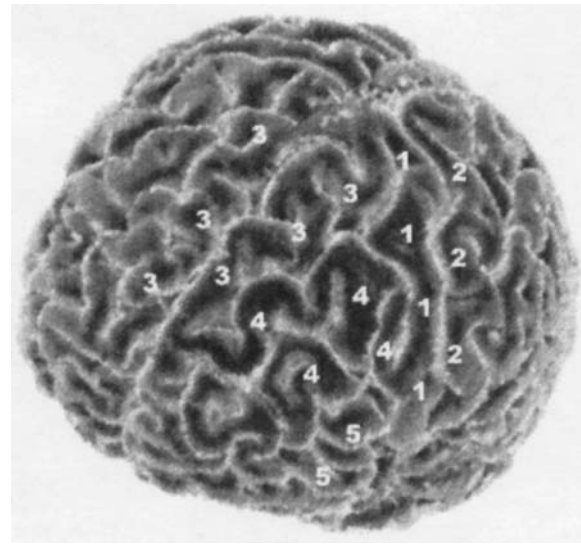

Fig. 3.27. 3D MR of the brain showing the central and frontal gyri (oblique anterior view). *1*, Precentral gyrus; *2*, postcentral gyrus; *3*, superior frontal gyrus; *4*, middle frontal gyrus; *5*, inferior frontal gyrus

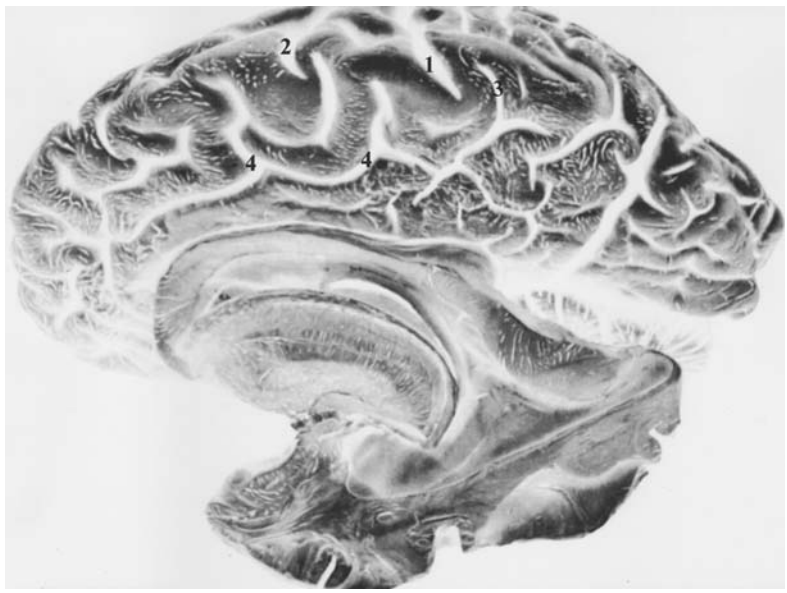

Fig. 3.28. The paracentral lobule: sulcal anatomy of the mesial aspect of the hemisphere. *1*, Central sulcus, medial extent; *2*, medial precentral sulcus; *3*, marginal ramus of cingulate; *4*, cingulate sulcus. (Brain specimen from Klingler; Ludwig and Klingler 1956)

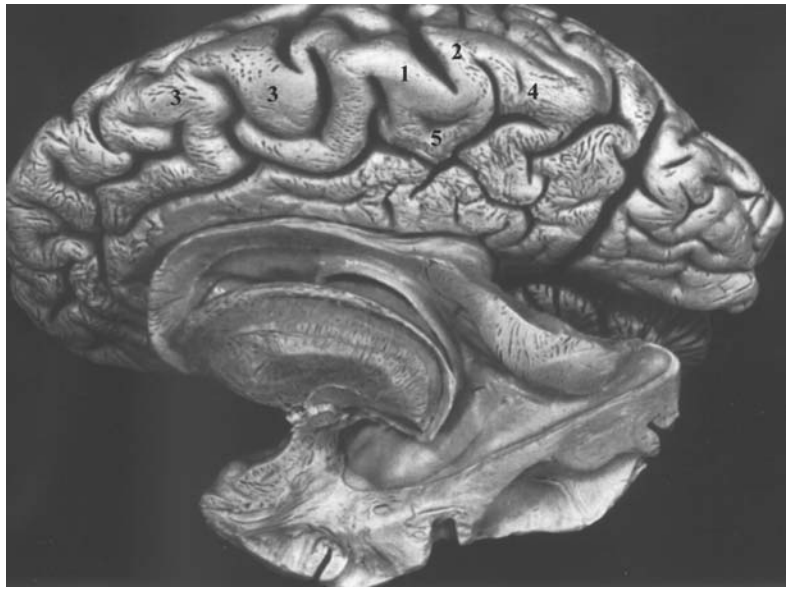

Fig. 3.29. The paracentral lobule: gyral anatomy of the mesial aspect of the hemisphere. *1*, Precentral gyrus, superior and medial extent; *2*, postcentral gyrus, superior and medial extent; *3*, medial frontal gyrus (superior frontal); *4*, precuneus; *5*, paracentral lobule. (Brain specimen from Klingler; Ludwig and Klingler 1956)

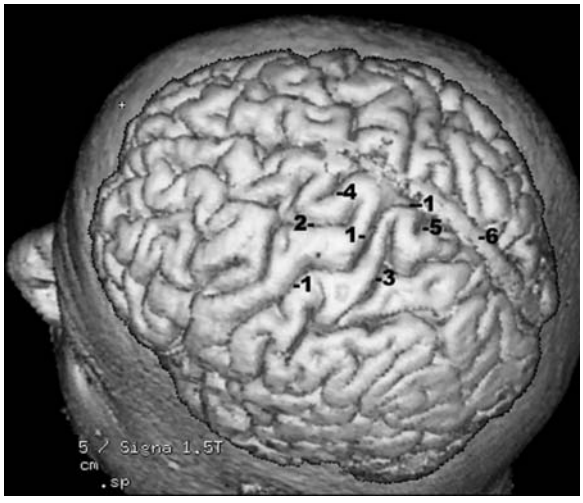

Fig. 3.30. 3D MR of the superior aspect of the brain showing the sulcation of the upper central region. *1*, Central sulcus; *2*, superior precentral sulcus; *3*, superior postcentral sulcus; *4*, medial precentral sulcus; *5*, marginal sulcus; *6*, superior sagittal sinus

Fig. 3.31. 3D MR of the superior aspect of the brain showing the gyral pattern of the central region. *1*, Precentral gyrus; *1'*, superior extent of precentral gyrus; *2*, postcentral gyrus; *2'*, superior extent of postcentral gyrus; *3*, superior frontal gyrus; *4*, superior parietal gyrus

Superiorly, the rolandic sulcus reaches the superior border of the hemisphere and may extend over the mesial aspect of the hemisphere as a small sulcus, the "crochet Rolandique" (about 80% of cases). This mesial extension is considered as being constant according to Eberstaller. It was found in 88% of the hemispheres according to Lang but was observed in only 64% of the cases as reported by Retzius.

3 Inferior Frontal Sulcus

This sulcus arises anteriorly at the level of the lateral orbital gyrus presenting an Y-shape bifurcation, and courses roughly parallel to the lateral sulcus (Figs. 3.32, 3.33). Eberstaller places its anterior extent at about the middle of the pars triangularis (1890). The inferior frontal sulcus is a deep sulcus almost reaching the insular plane and ending at the inferior precentral sulcus, where a submerged gyrus is very frequently found according to Eberstaller (1890). This "pli de passage" may come to the surface separating the inferior frontal sulcus from the inferior precentral. More developed and constant than the superior frontal sulcus, it is interrupted in about 30% of cases, usually in the middle of this sulcus by two "plis de passage". The inferior frontal sulcus is continuous in approximately 50% of cases.

4 Superior Frontal Sulcus

The superior frontal sulcus arises from the orbital margin of the hemisphere and courses parallel to the interhemispheric fissure, extending along about two thirds of the frontal lobe (Figs. 3.34, 3.35). Along its course, it gradually separates from the interhemispheric fissure. It is frequently doubled and varies from race to race. Frequently this sulcus is interrupted (26–50% of cases, according to Ono et al. 1990) and ends posteriorly at the precentral sulcus in a T-shaped branching (50% of cases). Anteriorly, the superior frontal sulcus may anastomose with the frontomarginal sulcus. According to Eberstaller this sulcus may anastomose (45% of cases) with the middle frontal sulcus.

5 Precentral Sulcus

This sulcus is usually divided into a superior and an inferior precentral sulci (75%) separated by a connection between the precentral and the middle frontal gyrus (Figs. 3.34, 3.26). It may be composed of three segments (15%), the third constituting an intermediate precentral sulcus. The precentral sulcus courses parallel to the central sulcus and is formed by the posterior bifurcations of the inferior and the superior frontal sulci. The superior end of the inferior precentral sulcus is located anteriorly to the inferior end of the superior precentral sulcus. The inferior end of the inferior precentral sulcus may connect with the sylvian fissure either directly or through the anterior subcentral or the diagonal sulcus (Eberstaller 1890; Giacomini 1878). The superior precentral sulcus is usually smaller than the inferior precentral sulcus. It generally does not reach the superior border of the hemisphere and is separated from it by an inconstant horizontal marginal precentral sulcus (Cunningham and Horsley 1892), a small dimple medial to the superior precentral sulcus. Just anterior to the latter may be found a medial precentral sulcus (Eberstaller 1890) which cuts into the dorsal margin of the hemisphere.

6 The Intraparietal Sulcus

The intraparietal sulcus is divided into three parts(Figs. 3.36–3.41), the ascending postcentral, horizontal and descending or occipital segments (Wilder 1886). The ascending segment is a vertical segment which corresponds to the inferior portion of the postcentral sulcus (Turner 1948), and may extend, mainly on the right, to the sylvian fissure. According to Cunningham (1890; Cunningham and Horsley 1892), the horizontal or true intraparietal segment has variable relationships with the inferior and superior postcentral sulci (Jefferson 1913). The most frequent pattern is represented by the type IV in which the intraparietal is continuous with both the inferior and superior postcentral sulci (40% of cases). The inferior postcentral segment is continuous with that of the superior postcentral in more than 60% of the cases. The third descending or occipital segment almost always terminates in the occipital lobe and may even reach its pole. The intraparietal sulcus is a very deep sulcus almost reaching the roof of the lateral ventricles, as identified on coronal and parasagittal cuts.

The occipital segment of the intraparietal or superior occipital sulcus, shows a T-shaped ending in about 70% of cases (Ono et al. 1990), described as the transverse occipital sulcus. The superior end of the postcentral sulcus terminates most frequently on the lateral aspect of the hemisphere without extension to the medial aspect, in a Y-shaped configuration. At this Y-shaped end, it is joined by the marginal ramus

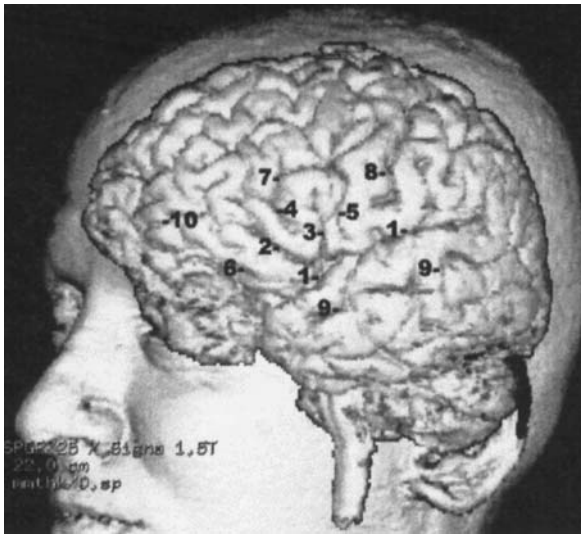

Fig. 3.32. 3D MR of the brain showing the sulcal pattern of the inferior frontal region. *1*, Lateral fissure; *2*, horizontal ramus of lateral fissure; *3*, ascending ramus of lateral fissure; *4*, radiate sulcus (incisura capitis); *5*, inferior precentral sulcus; *6*, lateral orbital sulcus; *7*, inferior frontal sulcus; *8*, central sulcus; *9*, superior temporal (parallel) sulcus; *10*, frontomarginal sulcus

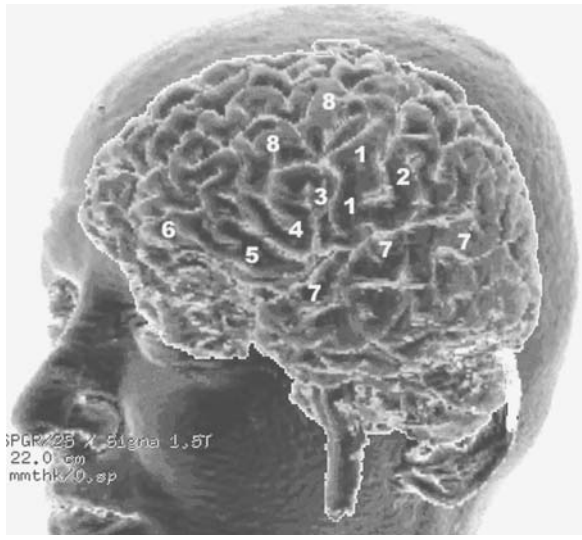

Fig. 3.33. 3D MR of the brain showing the gyral pattern of the inferior frontal region. *1*, Central gyrus; *2*, postcentral gyrus; *3*, pars opercularis of inferior frontal gyrus; *4*, pars triangularis of inferior frontal gyrus; *5*, pars orbitalis of inferior frontal gyrus; *6*, frontomarginal gyrus; *7*, superior temporal gyrus; *8*, middle frontal gyrus

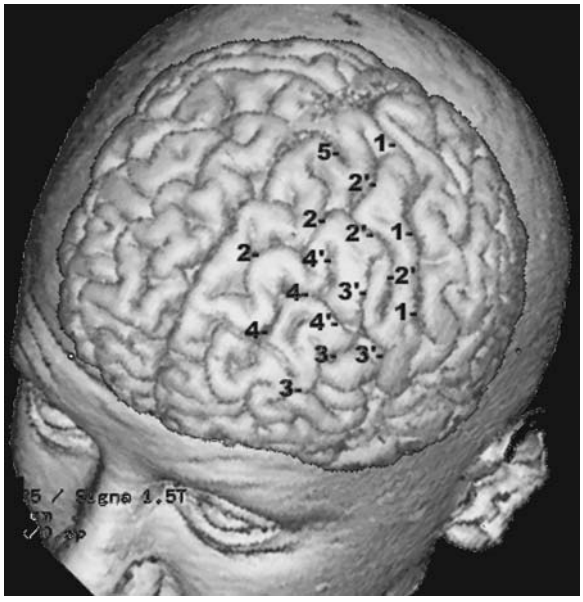

Fig. 3.34. Sulcal anatomy of the frontal lobe using 3D MR. *1*, Central sulcus; *2*, superior frontal sulcus; *2′*, superior precentral sulcus; *3*, inferior central sulcus; *3′*, inferior precentral sulcus; *4*, intermediate frontal sulcus; *4′*, posterior branching of intermediate frontal sulcus; *5*, medial precentral sulcus

Fig. 3.35. Gyral anatomy of the frontal lobe using 3D MR. *1*, Central gyrus; *2*, postcentral gyrus; *3*, superior frontal gyrus; *4*, middle frontal gyrus; *4′*, pli de passage between middle frontal gyrus and precentral gyrus; *5*, inferior frontal gyrus

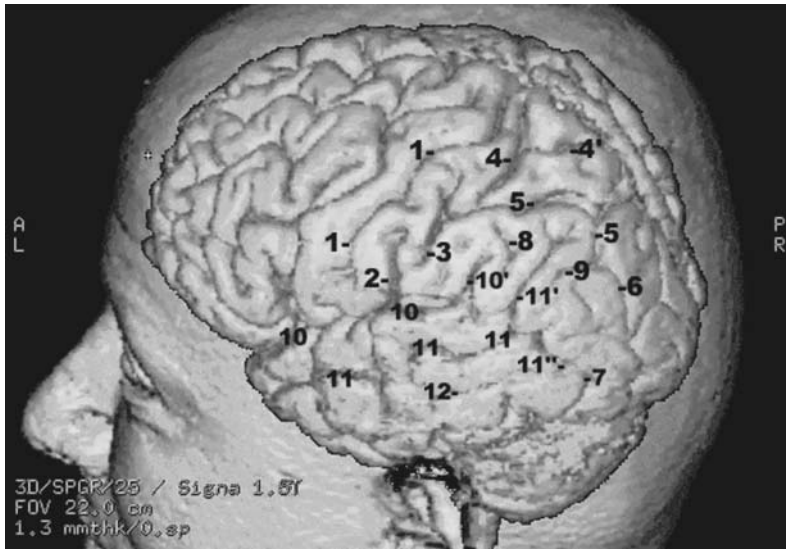

Fig. 3.36. 3D MR of the lateral aspect of the brain showing the sulcal anatomy of the temporal and parietal lobes. *1*, Central sulcus; *2*, sulcus retrocentralis transversus; *3*, inferior postcentral sulcus (ascending ramus of intraparietal sulcus); *4*, superior postcentral sulcus; *4'*, superior Y-branching of superior postcentral sulcus; *5*, intraparietal sulcus (horizontal segment); *6*, intraparietal sulcus (descending or occipital segment); *7*, preoccipital incisure; *8*, sulcus intermedius primus (Jensen); *9*, sulcus intermedius secundus (Eberstaller); *10*, lateral fissure, posterior ascending ramus; *11*, superior temporal parallel sulcus; *11'*, ascending ramus of parallel sulcus; *11"*, descending ramus of parallel sulcus; *12*, middle temporal sulcus

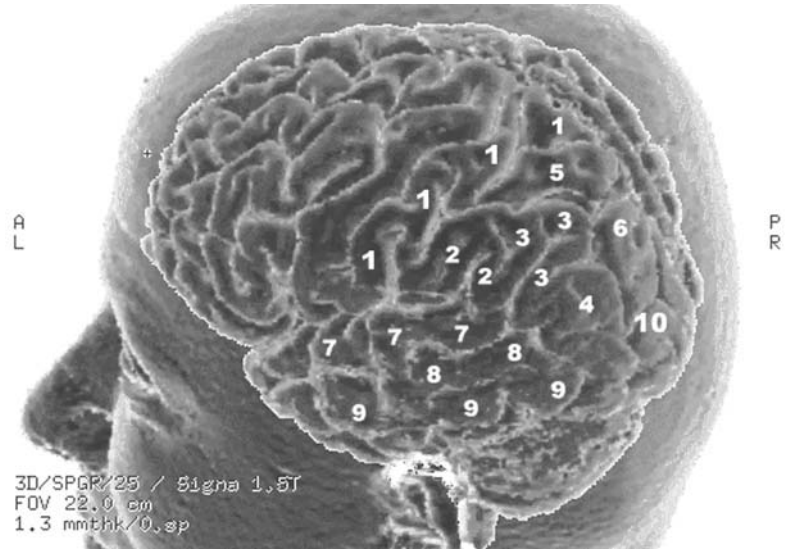

Fig. 3.37. 3D MR of the lateral aspect of the brain showing the gyral anatomy of the temporal and parietal lobes. *1*, Central gyrus; *2*, supramarginal gyrus (inferior parietal lobule); *3*, angular lobe (inferior parietal lobule); *4*, posterior parietal gyrus (inferior parietal lobule); *5*, superior parietal lobule (anterior portion); *6*, superior parietal lobule (posterior portion); *7*, superior temporal gyrus; *8*, middle temporal gyrus; *9*, inferior temporal gyrus; *10*, occipital lobe

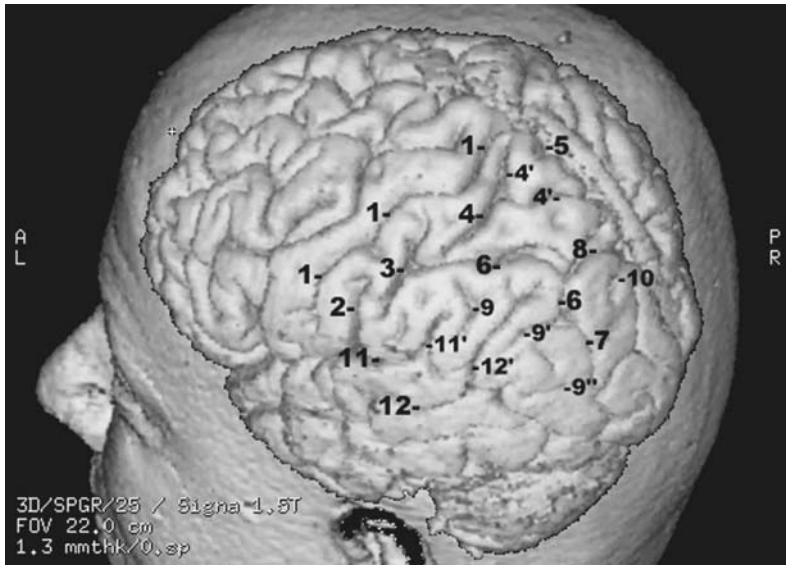

Fig. 3.38. 3D MR of the lateral aspect of the brain showing the sulcal anatomy of the inferior parietal region. *1*, Central sulcus; *2*, sulcus retrocentralis transversus (Eberstaller); *3*, inferior postcentral sulcus (ascending segment of intraparietal sulcus); *4*, superior postcentral sulcus; *4'*, end branches; *5*, marginal ramus of cingulate sulcus; *6*, intraparietal sulcus (horizontal segment); *7*, intraparietal sulcus (descending segment or superior occipital sulcus); *8*, sulcus parietalis transversus (Brissaud); *9*, sulcus intermedius primus (Jensen); *9'*, sulcus intermedius secundus (Eberstaller); *9"*, sulcus intermedius tertius (Eberstaller); *10*, lateral parieto-occipital sulcus; *11*, lateral fissure; *11'*, terminal ascending ramus of lateral fissure; *12*, superior temporal (parallel) sulcus; *12'*, ascending ramus of parallel sulcus

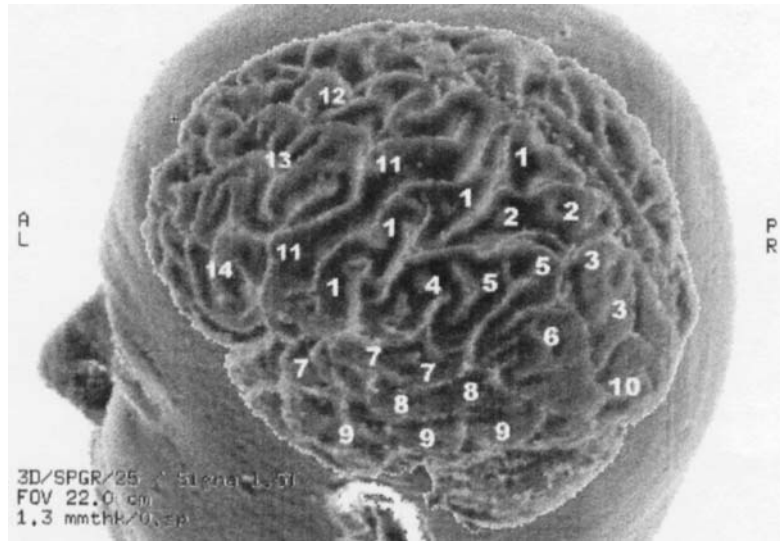

Fig. 3.39. 3D MR of the lateral aspect of the brain showing the gyral anatomy of the inferior parietal region. *1*, Postcentral gyrus; *2*, superior parietal gyrus (anterior portion); *3*, superior parietal gyrus (posterior portion); *4*, supramarginal gyrus (inferior parietal lobule); *5*, angular gyrus (inferior parietal lobule); *6*, posterior parietal gyrus; *7*, superior temporal gyrus; *8*, middle temporal gyrus; *9*, inferior temporal gyrus; *10*, occipital lobe; *11*, precentral gyrus; *12*, superior frontal gyrus; *13*, middle frontal gyrus; *14*, inferior frontal gyrus

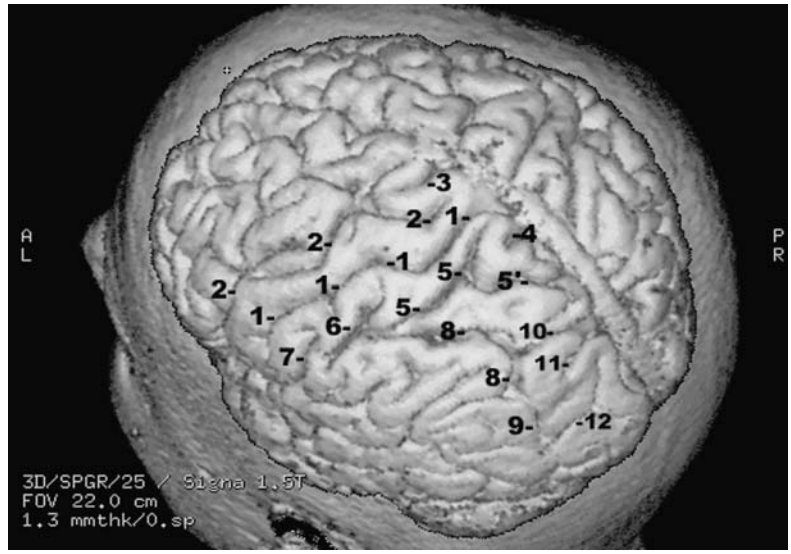

Fig. 3.40. 3D MR of the superior aspect of the brain showing the sulcal anatomy of the superior parietal region. *1*, Central sulcus; *2*, precentral sulcus; *3*, medial precentral sulcus; *4*, marginal sulcus (lateral extent); *5*, superior postcentral sulcus; *6*, inferior postcentral sulcus (ascending ramus of intraparietal sulcus); *7*, sulcus postcentralis transversus (Eberstaller); *8*, intraparietal sulcus (horizontal segment); *9*, intraparietal sulcus (descending or occipital segment); *10*, transverse parietal sulcus (Brissaud); *11*, parieto-occipital sulcus (lateral extent); *12*, transverse occipital sulcus

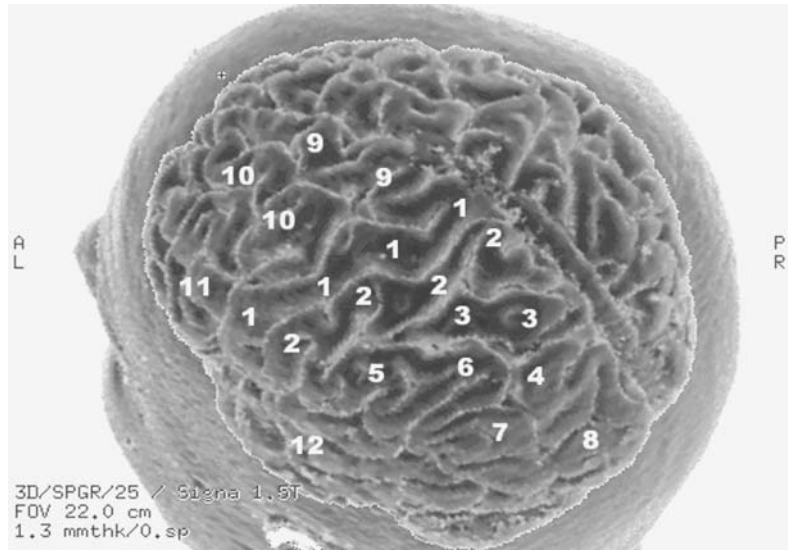

Fig. 3.41. 3D MR of the superior aspect of the brain showing the gyral anatomy of the superior parietal region. *1*, Precentral gyrus; *2*, postcentral gyrus; *3*, superior parietal gyrus; *4*, arcus parieto-occipitalis; *5*, supramarginal gyrus; *6*, angular gyrus; *7*, posterior parietal gyrus; *8*, occipital pole; *9*, superior frontal gyrus; *10*, middle frontal gyrus; *11*, inferior frontal gyrus; *12*, temporal lobe

of the cingulate sulcus terminates as it extends to the lateral aspect of the hemisphere indenting its superior border.

7 Superior Temporal Sulcus

The superior temporal sulcus is also called the parallel sulcus because it follows closely the course of the sylvian fissure. This sulcus is one of the oldest of the primate brain. It is a deep sulcus (2.5–3 cm) almost reaching the level of the inferior border of the insula, coursing roughly parallel to the opercular surface of the superior temporal gyrus as shown on the coronal cuts(Figs. 3.42–3.45). It is a rarely interrupted sulcus (32% of cases) divided into anterior and posterior parts. The posterior part is the angular sulcus which penetrates into the inferior parietal lobule and usually divides into three rami within the angular gyrus.

Its most consistent interruption point is below the inferior end of the central sulcus and its anterior extremity never extends into the temporal tip. This explains the apparent extension of the superior temporal gyrus to form the temporal pole. The superior temporal sulcus limits the superior temporal gyrus inferiorly. At the level of the central sulcus, this gyrus may show an inconstant sulcus acousticus which originates from the parallel sulcus and courses towards the lateral fissure, limiting the anterior extent of Heschl gyri.

8 Frontomarginal Sulcus

Described by Wernicke (1876), the frontomarginal sulcus is fairly constant and deep and is found at the frontal pole. It courses parallel to the orbital margin (Figs. 3.32, 3.33, 3.46). It corresponds to the frontomarginal sulcus found in the orangutan. It is connected posteriorly with the middle frontal sulcus more frequently than with the superior frontal sulcus, and is deeper than the latter, from which it seems to arise. This sulcus separates the transverse frontopolar gyri from the frontomarginal gyrus inferiorly.

C Gyri of the Lateral Surface of the Cerebral Hemisphere

The convolutions on the lateral aspect of the cerebral hemisphere determined by these primary fissures are the inferior, middle and superior frontal gyri, the pre- and postcentral gyri, and the inferior and superior parietal convolutions, in the suprasylvian region anteroposteriorly, and the superior, middle and inferior temporal gyri, in the infrasylvian region. The gyri of the parietal and the temporal lobes merge posteriorly with the variable occipital gyri, and are generally delimited by a superior occipital, a lateral occipital and an inferior occipital sulci.

1 The Frontal Lobe

The frontal lobe is the largest of the hemisphere, occupying about one third of its surface. It comprises four gyri extending from the lateral to the medial and basal aspects of the hemisphere. Medially, this lobe consists of a hook-like gyrus bounded inferiorly by the cingulate sulcus, and anteriorly corresponds to the orbital region. The gyri on the lateral aspect are the inferior frontal, the middle frontal and the superior frontal gyri. They follow a roughly parallel direction as compared to the lateral fissure and the superior border of the hemisphere. The fourth gyrus, the precentral gyrus, parallels the central sulcus and is almost perpendicular to the others.

a Inferior Frontal Gyrus

The inferior frontal gyrus is the smallest one and is situated between the lateral fissure and the inferior frontal sulcus, in relation with the horizontal and vertical rami of the lateral fissure (Figs. 3.15, 3.17, 3.19, 3.32, 3.33). These rami divide the gyrus into three parts: the pars orbitalis, the pars triangularis and the pars opercularis. The orbital part passes into the basal orbital aspect of the hemisphere and the opercular part continues with the lower extension of the precentral gyrus, constituting the frontal operculum. This gyrus is more developed on the left side in right-handed subjects, particularly in its triangular and opercular parts. It is called Broca's convolution and is regarded as the motor speech area.

The pars opercularis is frequently traversed (70% of cases) by the diagonal sulcus (Eberstaller 1890) arising from the precentral or the inferior frontal sulci, but not involving the circular sulcus of the insula, and ending at or about the sylvian fissure. According to Turner (1948) this sulcus would be a characteristic furrow of the human brain. Nevertheless, it remains inconstant.

The pars triangularis is traversed in more than one third of the cases by the radiate sulcus (Fig. 3.44) or incisura capitis (Eberstaller).

b Middle Frontal Gyrus

The middle frontal gyrus is located between the inferior and the superior frontal sulci and is separated from the precentral gyrus posteriorly by the branch-

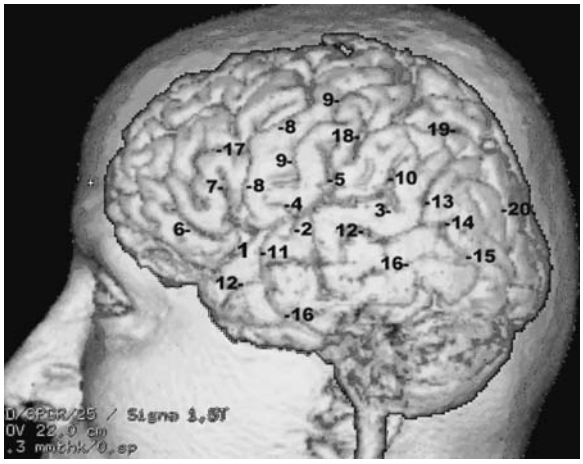

Fig. 3.42. Sulcal anatomy of the lateral surface of the cerebral hemisphere using 3D MR. *1*, Lateral fissure; *2*, transverse supratemporal sulcus; *3*, posterior transverse temporal sulcus; *4*, anterior subcentral sulcus; *5*, sulcus retrocentralis transversus; *6*, horizontal ramus of lateral fissure; *7*, ascending ramus of lateral fissure; *8*, precentral sulcus; *9*, central sulcus; *10*, ascending ramus of lateral fissure; *11*, sulcus acousticus; *12*, superior temporal (parallel) sulcus; *13*, ascending ramus of superior temporal sulcus; *14*, horizontal or descending ramus of parallel sulcus; *15*, lateral occipital sulcus; *16*, inferior temporal sulcus; *17*, inferior frontal sulcus; *18*, central sulcus (ascending ramus of intraparietal sulcus); *19*, intraparietal sulcus, horizontal segment; *20*, intraparietal sulcus (descending or occipital segment)

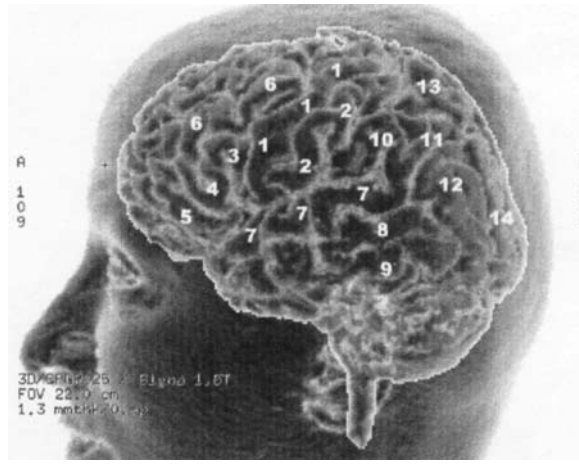

Fig. 3.43. Gyral anatomy of the lateral surface of the cerebral hemisphere using 3D MR. *1*, Central gyrus; *2*, postcentral gyrus; *3*, pars opercularis of inferior frontal gyrus; *4*, pars triangularis of inferior frontal gyrus; *5*, pars orbitalis of inferior frontal gyrus; *6*, middle frontal gyrus; *7*, superior temporal gyrus; *8*, middle temporal gyrus; *9*, inferior temporal gyrus; *10*, supramarginal gyrus; *11*, angular gyrus; *12*, posterior parietal gyrus; *13*, superior parietal gyrus; *14*, superior occipital gyrus

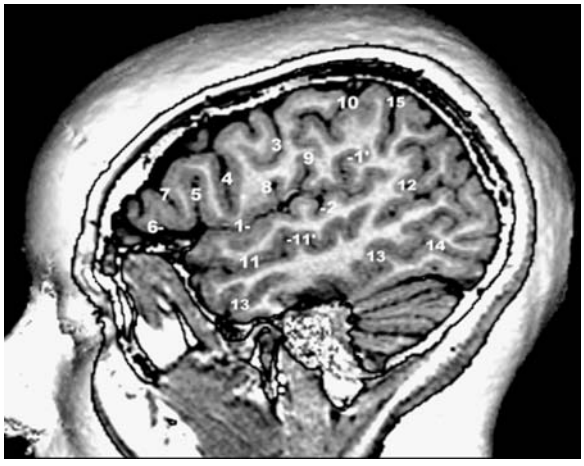

Fig. 3.44. Sulcal anatomy of the lateral surface of the cerebral hemisphere based on a sagittal lateral MR cut. *1*, Lateral sylvian fissure; *1'*, ascending ramus of lateral fissure; *2*, transverse temporal sulcus; *3*, central sulcus; *4*, inferior precentral sulcus; *5*, ascending ramus of lateral fissure; *6*, horizontal ramus of lateral fissure; *7*, radiate sulcus (incisura capitis); *8*, anterior subcentral sulcus; *9*, posterior subcentral sulcus; *10*, postcentral sulcus; *11*, superior temporal (parallel) sulcus; *11'*, sulcus acousticus; *12*, ascending ramus of parallel sulcus; *13*, middle temporal sulcus; *14*, inferior occipital sulcus; *15*, intraparietal sulcus

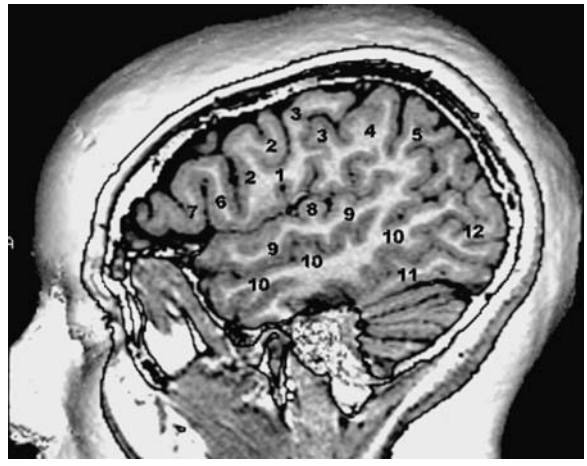

Fig. 3.45. Gyral anatomy of the lateral surface of the cerebral hemisphere based on a sagittal lateral MR cut. *1*, Frontoparietal operculum; *2*, precentral gyrus; *3*, postcentral gyrus; *4*, supramarginal gyrus; *5*, angular gyrus; *6*, pars opercularis of inferior frontal gyrus; *7*, pars triangularis of inferior frontal gyrus; *8*, superior transverse gyrus; *9*, superior temporal gyrus; *10*, middle temporal gyrus; *11*, inferior temporal gyrus; *12*, middle occipital gyrus

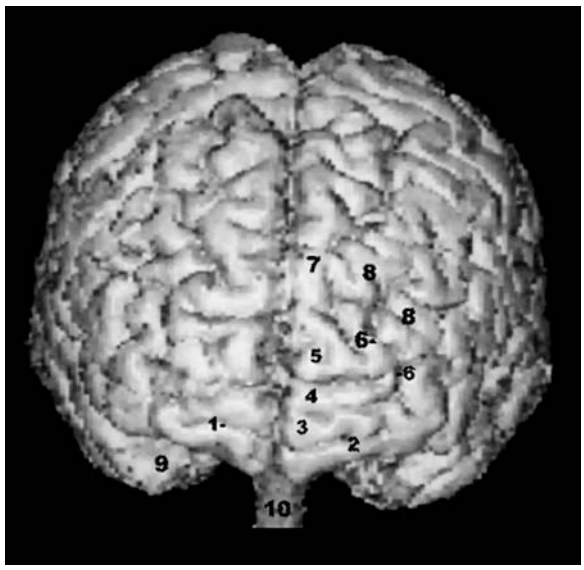

Fig. 3.46. 3D MR anatomy of the frontal pole (anterior view). *1*, Frontomarginal sulcus; *2*, frontomarginal gyrus; *3*, inferior transverse frontopolar gyrus; *4*, middle transverse frontopolar gyrus; *5*, superior transverse frontopolar gyrus; *6*, intermediate frontal sulcus; *7*, superior frontal gyrus; *8*, middle frontal gyrus; *9*, temporal pole; *10*, spinal cord

es of the precentral sulci (Figs. 3.22, 3.23, 3.26, 3.27). It is connected to the precentral gyrus by a deep annectent gyrus. The middle frontal gyrus is traversed by an inconstant intermediate or middle frontal sulcus which courses parallel to the inferior and superior frontal sulci, and shows a great variability in length. It originates about halfway between the precentral gyrus and the orbital margin, and usually ends in a bifurcation at the orbitodorsal margin as a part of the frontomarginal sulcus.

c Superior Frontal Gyrus

The superior frontal gyrus is situated between the superior frontal sulcus and the dorsal margin of the hemisphere and is therefore longer than the other frontal parallel gyri (Figs. 3.34, 3.35). It continues on the medial aspect of the hemisphere as the medial frontal gyrus and is connected posteriorly to the central gyrus.

d Precentral Gyrus

Also called the ascending frontal gyrus (circonvolution frontale ascendante), the precentral gyrus is located posteriorly between the central sulcus and between the inferior and superior frontal sulci anteriorly (Figs. 3.22–3.25, 3.30). Its is limited inferiorly by the lateral fissure and extends superiorly to reach the superior border of the hemisphere where it is continuous with the paracentral lobule on the medial aspect of the hemisphere. Its lower end may be traversed by the anterior subcentral sulcus, a sulcus of variable length arising from the upper bank of the lateral fissure and ending in the precentral gyrus behind the inferior precentral sulcus with which it may anastomose.

2 The Parietal Lobe

The parietal lobe is located superior to the lateral fissure and behind the central sulcus, extending posteriorly to an arbitrary line connecting the lateral extent of the parieto-occipital sulcus to the preoccipital notch. It extends to the medial aspect of the hemisphere as the precuneus gyrus and to the medial postcentral gyrus anteriorly. Its largest portion is on the lateral surface of the hemisphere where it is divided into three gyri by the intraparietal sulcus: the inferior parietal, the superior parietal and the postcentral gyri. The inferior parietal gyrus is usually further subdivided into three small gyri.

a Postcentral Gyrus

Also called the ascending postcentral gyrus, it is found posterior to the central sulcus, bounded caudally by the inferior and superior postcentral sulci (Figs. 3.24, 3.25, 3.40, 3.41). Its lower end is connected to the inferior precentral gyrus and may be traversed by a posterior subcentral sulcus (Marchand 1895) arising from the lateral fissure and ending as a small indentation in the parietal operculum.

b Inferior Parietal Gyri

The inferior parietal gyri lobule is situated between the lateral fissure inferiorly, the horizontal segment of the intraparietal sulcus superiorly, and the ascending postcentral segment of the intraparietal sulcus anteriorly (Figs. 3.36, 3.37). It is composed from front to back as the supramarginal gyrus arching over the terminal ascending ramus of the lateral fissure, the angular gyrus arching over the extremity of the upturned branch of the parallel sulcus, and the last corresponding to the posterior parietal gyrus which may cap the posterior end of the inferior temporal sulcus. The supramarginal and the angular arched convolutions are separated by a short sulcus, the primary intermediate sulcus of Jensen (1870) which is usually fused with the intraparietal but may anastomose with the lateral fissure. The angular gyrus may be separated from the posterior parietal gyrus by another secondary intermediate sulcus (Eberstaller 1884) which may anastomose with the parallel sulcus.

c Superior Parietal Gyrus

Located dorsal to the inferior parietal lobule, the superior parietal gyrus is limited inferiorly by the intraparietal sulcus, anteriorly by the superior postcentral sulcus, and extends posteriorly to the lateral extremity of the parieto-occipital sulcus, beyond which it passes into the occipital lobe forming the arcus parieto-occipitalis (Figs. 3.38, 3.39). The superior parietal gyrus may be divided into an anterior and a posterior portion by the transverse parietal sulcus (Brissaud 1893) originating on the medial side and extending to the lateral side of the superior aspect of the hemisphere where it is found between the postcentral sulcus and the parieto-occipital sulcus. The superior parietal gyrus extends posteriorly along the superior lateral aspect of the hemisphere to the lateral occipital lobe, arching over the lateral extent of the parieto-occipital sulcus to form the superior parieto-occipital "pli de passage" of Gratiolet (1854).

3 The Temporal Lobe

Somewhat pyramidal in shape, the temporal lobe has lateral, basal and dorsal aspects and an anterior apex or pole. The lateral aspect is bounded superiorly by the lateral fissure which separates it from the frontoparietal lobes. Caudally, it is continuous with the inferior parietal lobule superiorly, and with the occipital lobe, inferiorly. Ventrally the temporal lobe extends to the collateral sulcus at the basal aspect of the hemisphere, which separates it from the limbic lobe. The lateral convolutions of the temporal lobe are three in number, oriented anteroposteriorly and roughly parallel to the lateral fissure. From superior to inferior these are: the superior, middle and inferior temporal gyri.

a Superior Temporal Gyrus

The superior temporal gyrus is located between the lateral fissure above and the parallel sulcus below (Figs. 3.15, 3.42, 3.43, 3.45). Its anterior extent participates in the formation of the temporal pole and its posterior extremity merges with the supramarginal gyrus. At its caudal extremity, this gyrus is continuous with the supramarginal gyrus. The dorsal surface of this gyrus which forms the lower boundary of the sylvian fissure, called the operculo-insular surface, extends over 9 cm from anterior to posterior. It is divided into an opercular and an insular segment. The former is located in relation to the frontal and parietal opercula and the latter is related to the insula. One or two transverse temporal gyri, the Heschl gyri (Heschl 1878), cross the dorsal aspect of the superior temporal gyrus, obliquely forward, at the depth of the lateral fissure. More frequently doubled on the right side (Pfeifer 1936), these gyri are separated at least partly by an intermediate transverse temporal sulcus. These gyri are posteriorly separated from the planum temporale, by the transverse supratemporal sulcus (Holl 1908) originating from the lateral fissure and are frequently noticed on the lateral aspect of the superior temporal gyrus. Even the intermediate temporal sulcus may cut into the lateral surface of the first temporal gyrus. The frontal boundary of the Heschl gyri is marked by the anterior limiting sulcus of Holl. The anterior extent of the of these gyri is demarcated by the sulcus acousticus, originating from the parallel sulcus and cutting into the lateral aspect of the first temporal gyrus.

b Middle Temporal Gyrus

The middle temporal gyrus is almost parallel to the superior gyrus and is separated from the superior temporal gyrus by the superior temporal or parallel sulcus and bounded inferiorly by the inferior temporal sulcus which is a regularly interrupted sulcus (Figs. 3.15, 3.17, 3.37, 3.45). This gyrus is continuous at its posterior extremity with the angular gyrus superiorly, and with the occipital lobe inferiorly, following the inferior branching of the inferior temporal sulcus, namely the anterior occipital sulcus. This gyrus is more flexuose and larger than the superior temporal gyrus.

c Inferior Temporal Gyrus

The inferior temporal gyrus is bounded superiorly by the inferior temporal sulcus and extends inferiorly over the basolateral border of the cerebral hemisphere, to the inferior surface, limited at this level by the occipitotemporal sulcus (Fig. 3.15). It is largely discontinuous (70% of cases), mainly posteriorly, extending like the occipitotemporal gyrus close to the preoccipital notch. At this level, it is continuous posteriorly and inferiorly with the inferior occipital gyrus.

4 The Occipital Lobe

The occipital lobe is the smallest of all hemispheric lobes occupying the posterior aspect of the hemisphere and lying on the tentorium cerebelli (Figs. 3.18, 3.47A–C). It is limited anteriorly in apes by the lateral parieto-occipital sulcus which in humans is reduced to a notch on the superior border of the hemisphere due to the characteristic presence of two

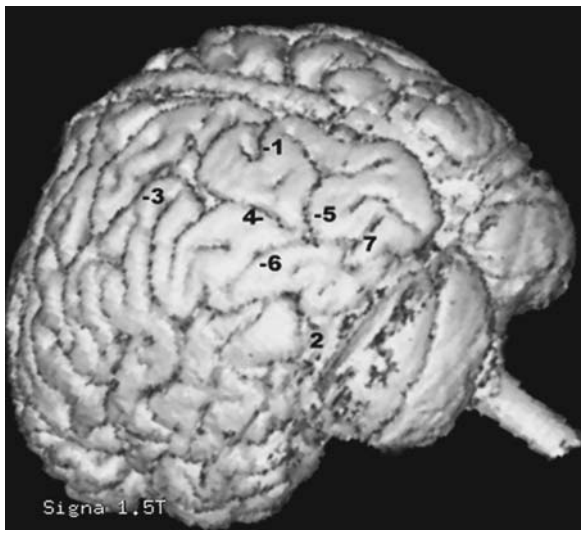

A

B

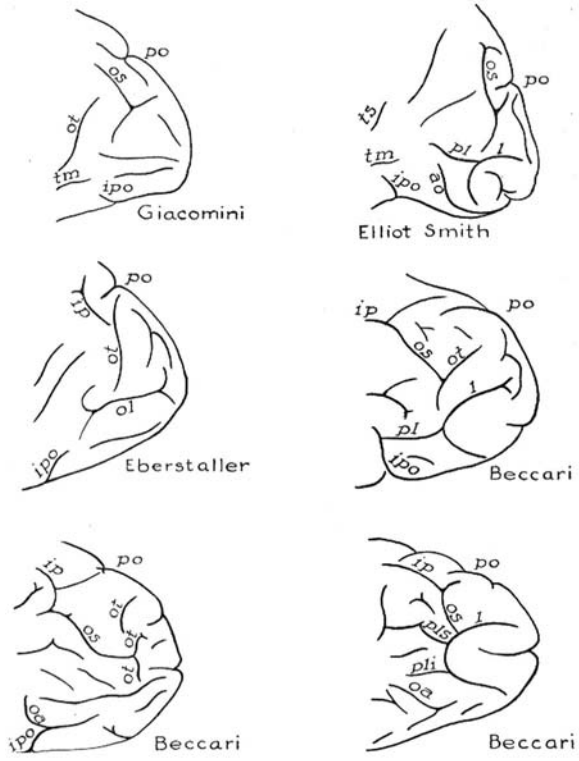

C

Fig. 3.47. A 3D MR sulcal anatomy of the occipital lobe (posterior lateral view). *1*, Lateral parieto-occipital sulcus; *2*, preoccipital incisure; *3*, intraparietal sulcus; *4*, superior occipital sulcus (occipital segment of intraparietal); *5*, transverse occipital sulcus; *6*, lateral occipital (middle) sulcus; *7*, lunate sulcus. **B** 3D MR gyral anatomy of the occipital lobe (posterior lateral view). *1*, Superior parietal gyrus; *2*, superior occipital gyrus (arcus parieto-occipitalis or 1st pli de passage parieto-occipital of Gratiolet); *3*, middle occipital gyrus (2nd pli de passage parieto-occipital of Gratiolet); *4*, inferior occipital gyrus; *5*, posterior parietal gyrus; *6*, angular gyrus; *7*, superior temporal gyrus; *8*, middle temporal gyrus. **C** Variations of the fissural pattern of the lateral aspect of the occipital lobe. *Left*, vertical type; *right*, horizontal type (from Bailey and von Bonin 1951)

longitudinal parieto-occipital "plis de passage" of Gratiolet. The first occupies the superior aspect of the hemisphere, paralleling the superior border of the hemisphere and joining the superior parietal gyrus to the superior, or first occipital, gyrus, limited laterally by the occipital segment of the intraparietal sulcus. This segment is therefore also called the superior occipital sulcus which may be crossed at its end by the transverse occipital sulcus. The latter shows variable length across the lateral aspect of the occipital lobe and may correspond to the end branching of the pars occipitalis of the intraparietal sulcus (Wilder's paroccipital sulcus). The other parieto-occipital "pli de passage" joins the angular gyrus to the middle or second occipital gyrus. This middle or lateral occipital gyrus is the largest of the lateral aspects of the occipital lobe and may be subdivided into superior and inferior portions by the middle occipital or lateral sulcus which may anastomose anteriorly with the parallel sulcus. Its posterior end

joins the inconstant concave lunate sulcus posteriorly the existence of which, in humans, remains controversial. The middle occipital gyrus is bounded superiorly by the superior occipital sulcus and inferiorly by the inferior occipital sulcus. Two other temporal occipital "plis de passage", which are separated by an inconstant inferior occipital sulcus that may correspond to a side branch of the inferior temporal sulcus, occupy the inferior lateral aspect of the occipital lobe. These flexuose plis de passage are found in all primates. The inferior occipital sulcus medially limits the inferior occipital gyrus, or third occipital gyrus, extending posteriorly just anterior to the occipital pole. The anterior extent of the inferior occipital gyrus is ill-defined and found at the level of the preoccipital incisure (inferior preoccipital sulcus of Meynert, 1877), a sulcus indenting the inferior lateral border of the hemisphere. It is continuous anteriorly with the inferior temporal gyrus.

The sulcal and gyral configuration of the inferior temporal-occipital region shows wide unsettled morphological variations which explain the lack of consensus between authors. The sulci are shallow and may show numerous variable ramifications which has lead to the divergent descriptions (Testut and Latarjet 1948; Paturet 1964; Duvernoy et al. 1991).

5 The Insula of Reil

The insula of Reil is the smallest of the cerebral lobes found in the depth of the lateral fissure (Figs. 3.48, 3.49, 3.50, 3.51). It is best shown after excision of the lateral fissure opercula. It is triangular in shape with an apex directed anteriorly and inferiorly, called the monticulus. The latter is connected to the anterior perforated substance through the limen insulae. The insula is separated from the frontoparietal and the temporal opercula by the circular sulcus.

The insular cortex is constituted of convergent gyri presenting a fan-like arrangement, usually separated into three short and one or two long convolutions by the central sulcus of the insula, the deeper of all insular furrows always reaching the circular sulcus. The two insular lobules separated by the central sulcus, are connected with the third frontal gyrus and the superior temporal gyrus by two "plis de passages", fronto-insular and temporo-insular.

D The Mesial Surface of the Cerebral Hemisphere

The development of the specific gyral pattern characteristic of the interhemispheric area is influenced by the development of the callosal connections. Absence of the corpus callosum will lead to vertically oriented sulci and absence of the cingulate sulcus (Fig. 3.52). Sulci and gyri of the mesial aspect of the hemisphere are evident on the sagittal and parasagittal cuts of the brain (Fig. 3.53).

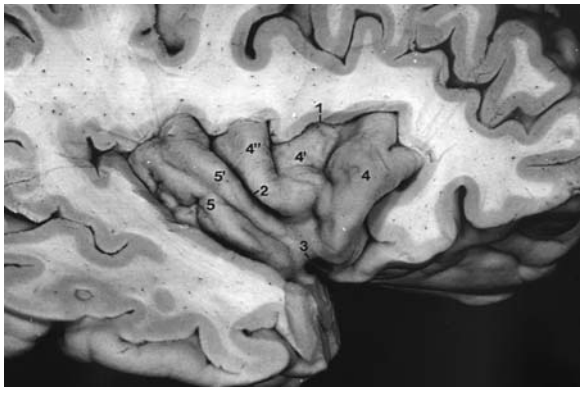

A

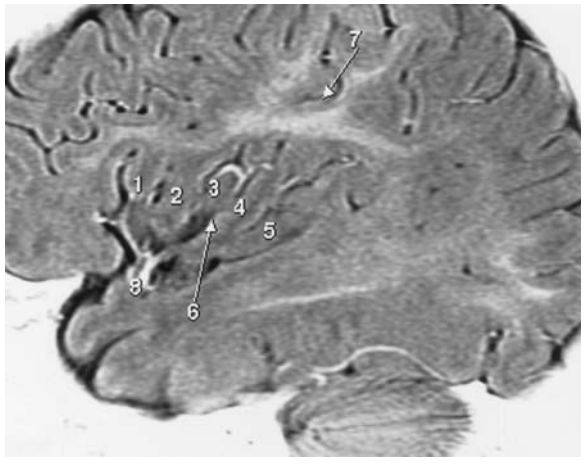

B

Fig. 3.48. A The insular cortex, anatomic dissection. *1*, Circular sulcus of insula; *2*, central sulcus of insula; *3*, falciform sulcus; *4*, *4'*, *4''*, short insular gyri; *5*, *5'*, long insular gyri. (from Duvernoy et al. 1991) **B** MR correlation in the sagittal plane, using STIR pulse sequence with inverse video display. *1*, *2*, *3*, Short insular gyri (anterior lobe of insula); *4*, *5*, long insular gyri; *6*, central sulcus of insula; *7*, central sulcus, inferior end; *8*, sylvian artery and its insular branches

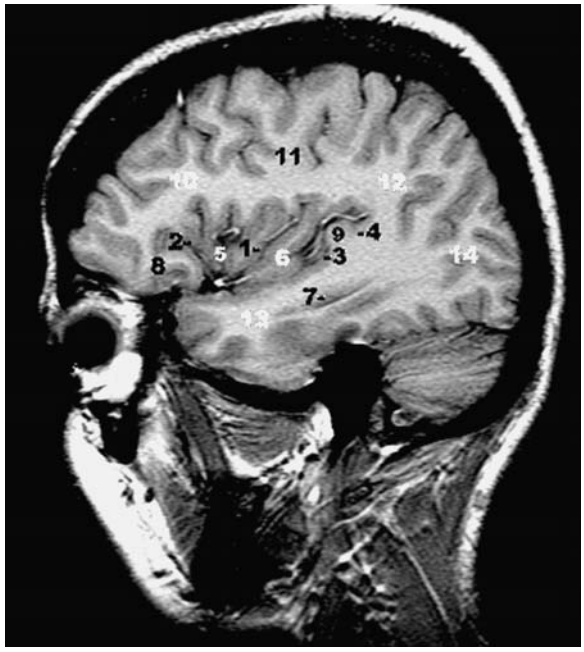

Fig. 3.49. Sagittal MR cut through the insula. *1*, Central insular sulcus; *2*, circular sulcus of insula; *3*, anterior transverse supratemporal sulcus (anterior limiting sulcus of Holl); *4*, posterior transverse supratemporal sulcus; *5*, short insular gyri; *6*, long insular gyri; *7*, inferior horn of lateral ventricle; *8*, lateral orbital gyrus; *9*, transverse temporal gyrus; *10*, inferior frontal gyrus; *11*, central operculum; *12*, inferior parietal lobule; *13*, temporal lobe; *14*, occipital lobe

Fig. 3.51. Parasagittal MR cut showing the insular branches of the middle cerebral artery

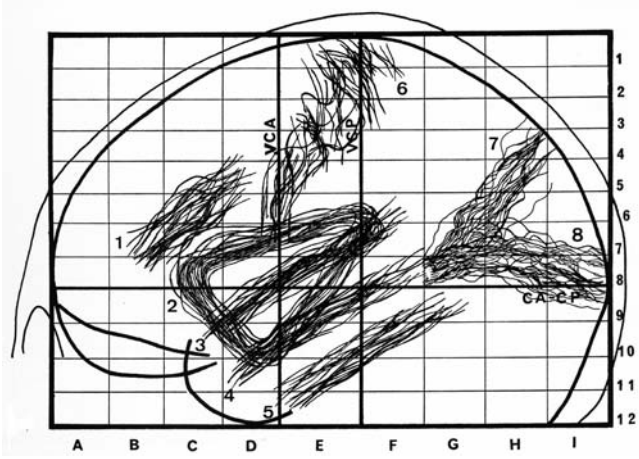

Fig. 3.50. Constant localization of the insula on the proportional grid. *1*, Superior frontal sulcus; *2*, insula; *3*, lateral fissure; *4*, superior temporal or parallel sulcus; *5*, inferior temporal sulcus; *6*, central sulcus; *7*, parieto-occipital sulcus; *8*, calcarine sulcus. Note the approximate parallelism of the frontal (excluding the central) and temporal sulci to the lateral fissure. (According to Szikla et al. 1977)

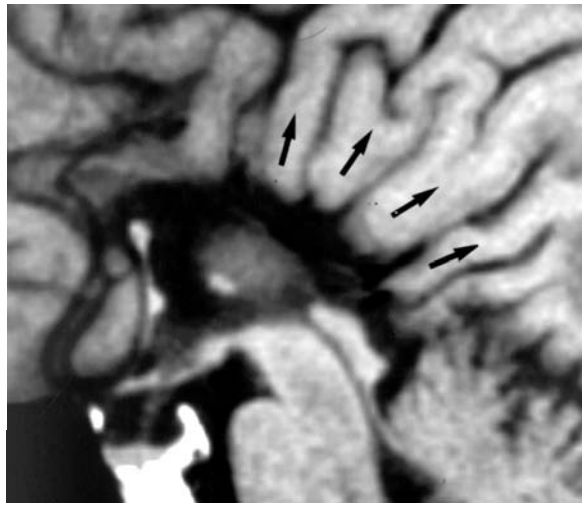

Fig. 3.52. Midsagittal MR cut showing the characteristic abnormal radiate pattern of the brain convolutions (*arrows*)

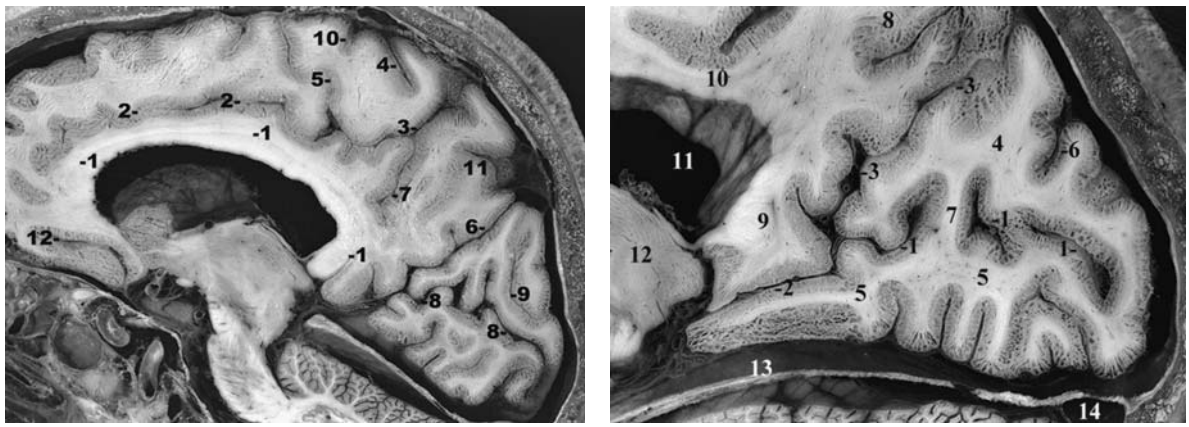

Fig. 3.53. A Anatomic parasagittal cut of the brain, showing the main sulci of the medial aspect of the hemisphere. *1*, Callosal sulcus; *2*, cingulate sulcus; *3*, marginal ramus of cingulate sulcus; *4*, central sulcus; *5*, paracentral sulcus; *6*, parieto-occipital sulcus; *7*, subparietal sulcus; *8*, calcarine sulcus; *9*, dorsal paracalcarine sulcus; *10*, medial precentral sulcus; *11*, transverse parietal sulcus; *12*, superior rostral sulcus. **B** The calcarine and parieto-occipital sulci: medial parasagittal anatomical cut. *1*, Calcarine sulcus, posterior segment; *2*, calcarine sulcus, anterior segment; *3*, parieto-occipital sulcus; *4*, cuneus; *5*, lingual gyrus; *6*, sulcus cunei; *7*, anterior cuneolingual gyrus; *8*, precuneus; *9*, isthmus; *10*, cingulate gyrus; *11*, lateral ventricle body; *12*, thalamus; *13*, tentorium cerebelli; *14*, transverse sinus

1 Cingulate Sulcus

Also called the callosomarginal sulcus (Huxley 1861) or scissure limbique (Broca 1878), the cingulate sulcus begins below the rostrum of the corpus callosum, in the subcallosal region before it sweeps around the genu paralleling the corpus callosum (Figs. 3.54, 3.55). This sulcus separates the medial frontal gyrus from the cingulate gyrus posteriorly, ending as a marginal ramus in the parietal lobe, and separating the precuneus from the paracentral lobule. The marginal ramus has a fairly constant relationship to the central sulcus, ending about 10 mm (range 8–12 mm) posterior to it in 96% of examined hemispheres. The cingulate sulcus is duplicated in 24% of examined hemispheres, mainly in its anterior segment, giving rise to an accessory intralimbic sulcus. Doubling of the anterior cingulate sulcus occurs twice as frequently in the left hemisphere according to Weinberg (1905). Up to three interruptions are frequently (40%) noted along its course. These interruptions lead to invaginations of the mesial frontal gyrus into the cingulate gyrus, corresponding to the "plis de passage fronto-limbiques" of Broca.

Fig. 3.54. : Parasagittal MR cut showing the sulcal anatomy of the mesial aspect of the cerebral hemisphere. *1*, Callosal sulcus; *2*, cingulate sulcus; *3*, marginal sulcus; *4*, central sulcus; *5*, paracentral sulcus; *6*, parieto-occipital sulcus; *7*, subparietal sulcus; *8*, calcarine sulcus; *9*, dorsal paracalcarine sulcus; *10*, ventral paracalcarine sulcus; *11*, superior rostral sulcus; *12*, inferior (accessory) rostral sulcus; *13*, transverse parietal sulcus; *14*, medial precentral sulcus

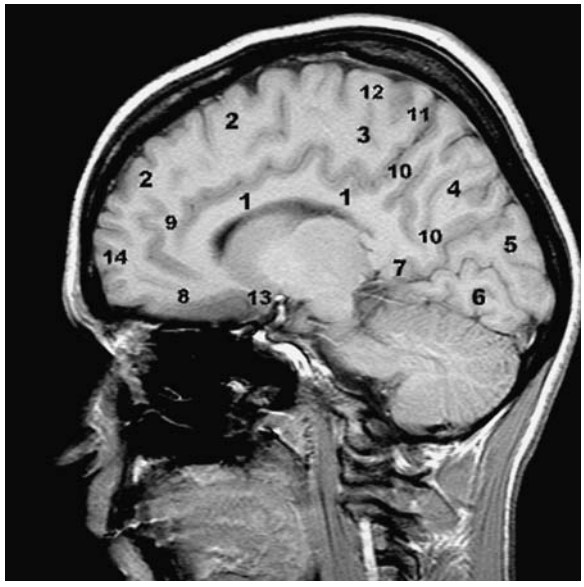

Fig. 3.55. Parasagittal MR cut showing the gyral anatomy of the mesial aspect of the cerebral hemisphere. *1*, Cingulate gyrus; *2*, medial frontal gyrus; *3*, paracentral lobule; *4*, precuneus; *5*, cuneus; *6*, lingual gyrus; *7*, isthmus; *8*, medial orbital gyrus; *9*, frontolimbic "pli de passage"; *10*, parietolimbic "pli de passage"; *11*, postcentral gyrus; *12*, precentral gyrus; *13*, subcallosal gyrus; *14*, fronto-orbital gyri

2 Parieto-occipital Sulcus

First analyzed by Gratiolet (1854), the parieto-occipital sulcus is deep (2–2.5 mm), constant and characteristic of the primate brain. Situated principally on the posterior mesial aspect of the hemisphere, it extends downward from the dorsal margin of the hemisphere forward to the caudal aspect of the splenium where it joins the stem of the calcarine fissure (Figs. 3.54, 3.55, 3.56). At this level it forms a Y-shaped sulcus. Actually, this sulcus is frequently separated from the calcarine by the cuneolimbic gyrus connecting the apex of the cuneus to the isthmus and shows a number of folds connecting the cuneus to the precuneus in its depths. The parieto-occipital sulcus continues as the external incisure on the lateral aspect of the hemisphere for a short distance of about 10–12 mm, cutting deeply into its edge. Close to the dorsal margin this sulcus may diverge into the sulcus limitans precunei which connects in 25% of the cases with the intraparietal sulcus. A line connecting the parieto-occipital incisure to the preoccipital notch draws the arbitrary boundary on the lateral surface separating the occipital lobe from the temporal and parietal lobes.

3 Calcarine Sulcus

The calcarine sulcus arises behind and just below the splenium of the corpus callosum and proceeds backward toward the occipital pole where it ends in a bifurcation, but it may encroach, most frequently by its superior ramus, on the lateral aspect of the hemisphere (Figs. 3.54, 3.55, 3.56). This deep sulcus (2.5–3 cm) is divided into two segments at the point of its junction with the parieto-occipital sulcus. The first, cephalad to this junction, having its counterpart in the calcar avis, is the anterior calcarine sulcus and the other caudal division is the posterior calcarine sulcus. The posterior calcarine sulcus ends posteriorly in a bifurcation found in half the cases on the medial aspect of the hemisphere. The superior branch extends more frequently to the lateral aspect of the occipital lobe (Zuckerkandl 1906). The course and bend of the posterior calcarine sulcus is variable. Its variations in relation with the cephalic index remain unclear.

One or two submerged gyri, the anterior and the posterior cuneolingual folds of Déjerine, may be found within the posterior calcarine segment. Exceptionally, one of these anastomotic folds may become superficial and interrupt the calcarine sulcus. The upper and the lower lips of the posterior calcarine sulcus and the lower lip only of the anterior calcarine correspond to the striate cortex (area 17).

4 Rostral Sulci

The superior rostral sulcus of Eberstaller (1884) or "incisure susorbitaire" of Broca courses anteroposteriorly around the rostrum of the corpus callosum, originating near the "carrefour olfactif " of Broca, and ends closely behind the frontal pole (Fig. 3.57). It is independent and roughly parallel to the anterior cingulate sulcus in two thirds of the cases according to Beccari (1911) and is very frequently doubled by the inferior shallower rostral sulcus, also named the accessory rostral sulcus.

5 Gyri of the Mesial Surface of the Cerebral Hemisphere

Seven gyri constitute the mesial hemisphere (Comair et al. 1996a). These are described as follows, from anterior to posterior.

a The Gyrus Rectus

The gyrus rectus is limited anteriorly by the floor of the anterior cranial fossa, laterally by the olfactory

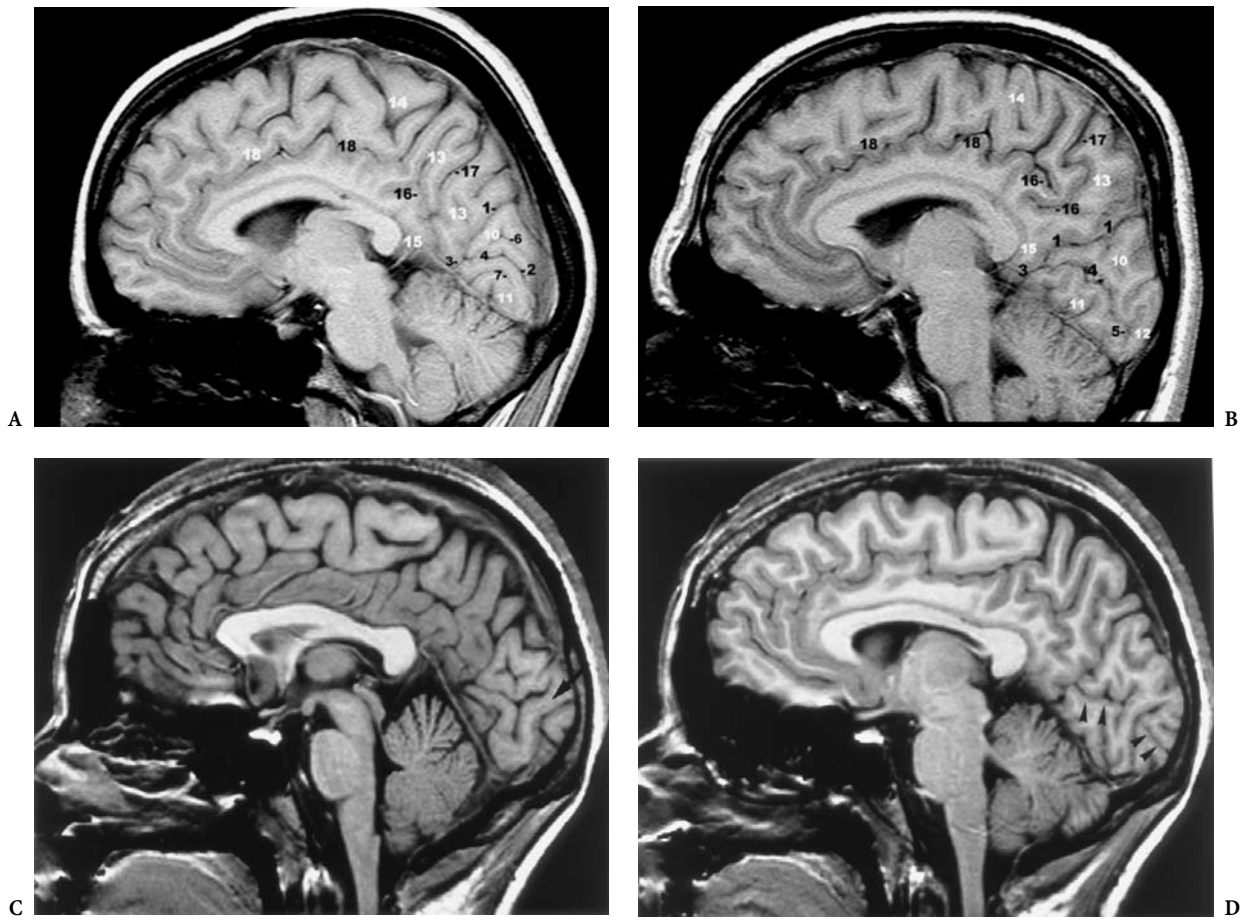

Fig. 3.56. A,B The mesial occipital lobe: MR correlations. *1*, Parieto-occipital sulcus; *2*, calcarine sulcus; *3*, anterior calcarine sulcus; *4*, posterior calcarine sulcus; *5*, retrocalcarine sulcus; *6*, paracalcarine sulcus (dorsal); *7*, paracalcarine sulcus (ventral); *8*, pli de passage, anterior cuneolimbic; *9*, pli de passage, posterior cuneolimbic; *10*, cuneus; *11*, lingual gyrus; *12*, gyrus descendens of Ecker; *13*, precuneus; *14*, paracentral lobule; *15*, isthmus cinguli; *16*, subparietal sulcus; *17*, transverse parietal sulcus; *18*, cingulate sulcus. **C,D** Cuneolingual gyrus (*arrow*) connecting the cuneus to the lingual gyrus through the calcarine sulcus (*arrowheads*) and showing a fairly unusual pattern

sulcus and superiorly by the superior rostral sulcus. A transverse rostral sulcus separates the gyrus rectus from the carrefour olfactif or subcallosal gyrus (Figs. 3.58–3.64). This latter was observed in about 60% of cases by Beccari.

b The Cingulate Gyrus

The cingulate gyrus is limited ventrally by the callosal sulcus, ventrally and anteriorly by the anterior paraolfactory sulcus, superiorly by the cingulate sulcus, superiorly and posteriorly by the subparietal sulcus, and posteriorly and inferiorly by the anterior calcarine sulcus (Figs. 3.53, 3.54, 3.55). It is continuous with the parahippocampal gyrus through the isthmus, a "pli de passage temporo-limbique". This arched convolution may be subdivided into three portions: the anterior located beneath the rostrum and in front of the genu of the corpus callosum, the intermediate middle portion roughly horizontal and parallel to the superior aspect of the body of the corpus callosum, and the last portion which is concave anteriorly, sweeps around the splenium and continues inferiorly and forward with the isthmus. The latter links the posterior cingulate gyrus with the parahippocampal gyrus. The anterior cingulate is followed in the subcallosal region, where it abuts the subcallosal gyrus, which is limited anteriorly by the anterior subcallosal sulcus (or transverse rostral sulcus of Beccari) and bounded posteriorly by the posterior subcallosal, the latter limiting anteriorly the paraterminal gyrus. The cingulate gyrus forms with the subcallosal, the isthmus hippocampi and the parahippocampal gyri, the limbic lobe.

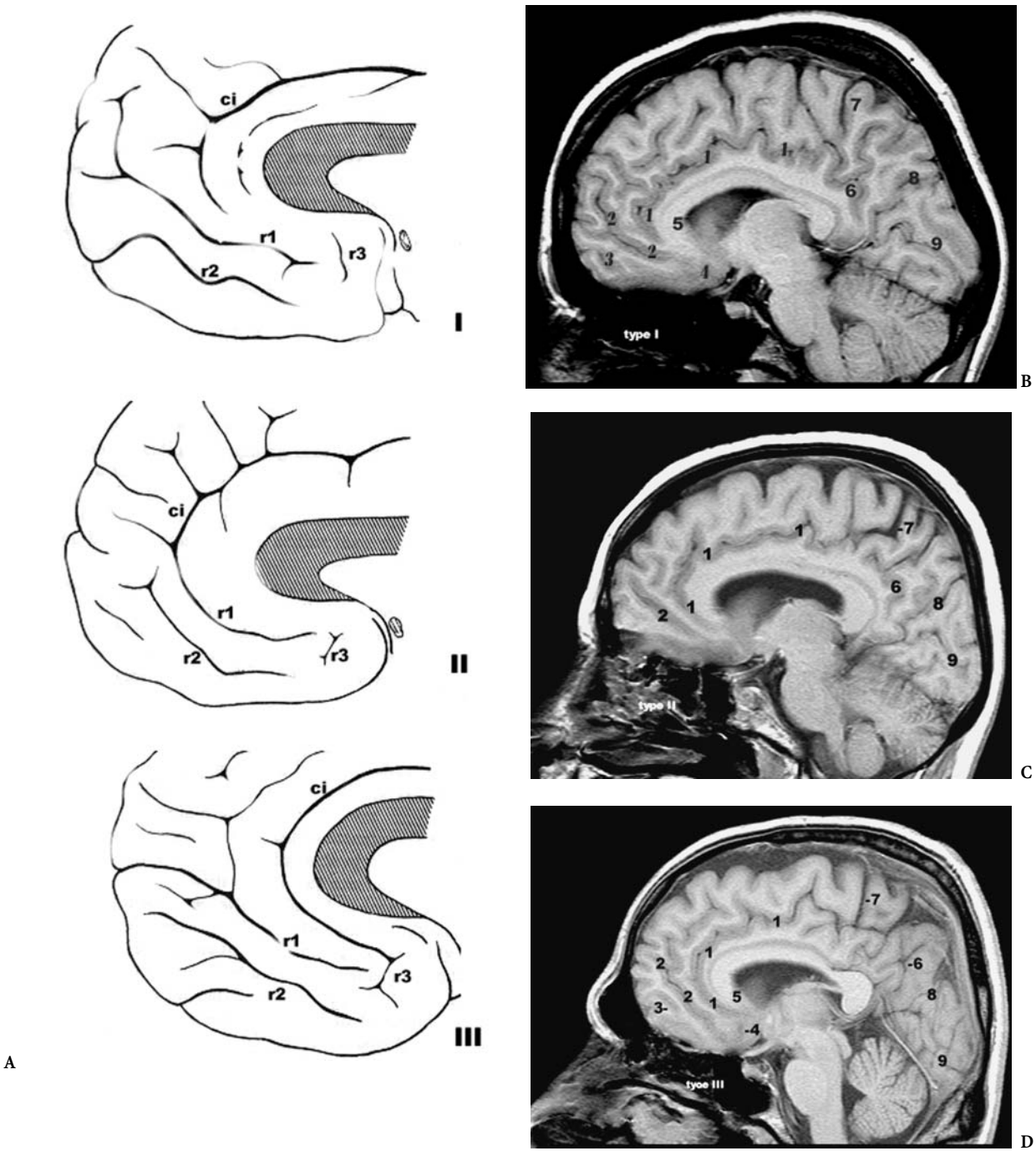

Fig. 3.57A–D. The rostral sulci with MR correlations. **A** Three major configurations are noted: type I (23%), type II (25%), type III (52%). *r1*, Superior rostral sulcus; *r2*, inferior rostral sulcus or accessory rostral sulcus; *r3*, transverse rostral sulcus; *ci*, cingulate sulcus. **B–D** *1*, Cingulate sulcus; *2*, superior rostral sulcus; *3*, inferior rostral sulcus; *4*, parolfactory sulcus; *5*, corpus callosum, genu and rostrum; *6*, subparietal sulcus; *7*, marginal ramus of cingulate sulcus; *8*, parieto-occipital sulcus; *9*, calcarine sulcus. (After Beccari 1911)

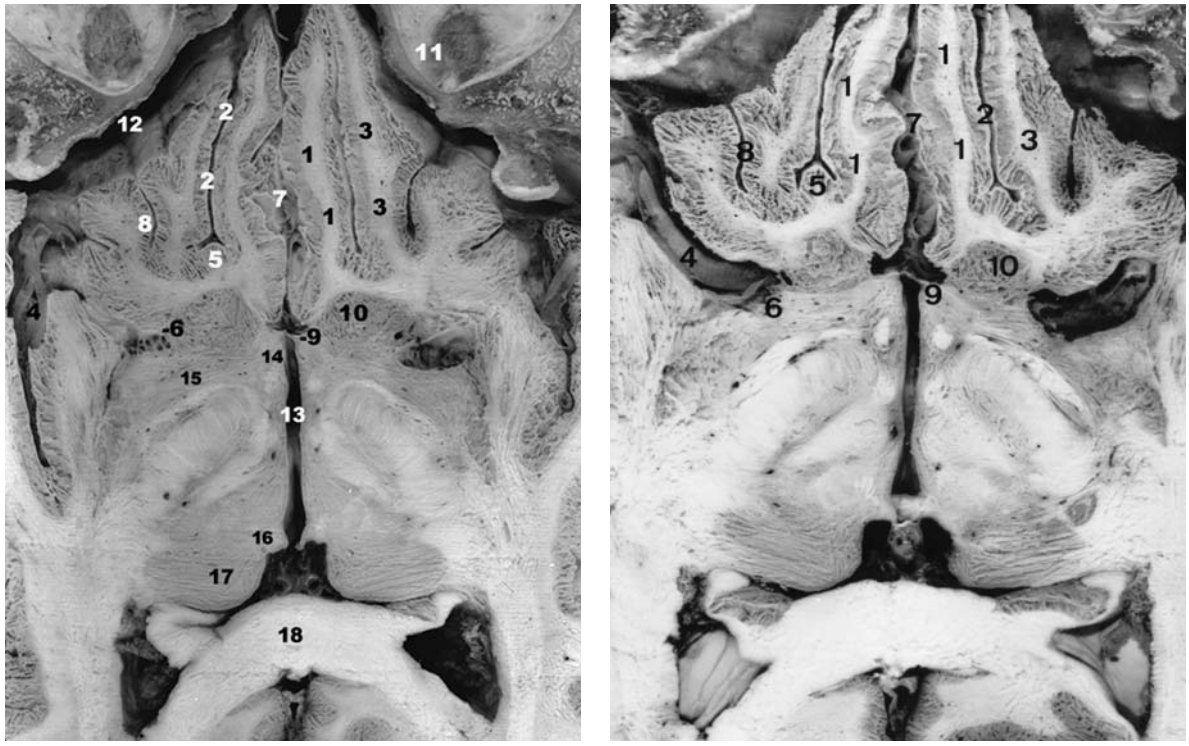

Fig. 3.58A,B. Horizontal cut of the brain showing the fronto-orbital sulci and gyri. *1*, Gyrus rectus; *2*, olfactory sulcus; *3*, medial orbital gyrus; *4*, lateral fissure; *5*, branching of olfactory sulcus; *6*, anterior perforated substance; *7,* interhemispheric fissure; *8*, medial fronto-orbital sulcus; *9*, lamina terminalis; *10*, ventral striatum; *11*, roof of the orbit; *12*, anterior cranial fossa; *13*, third ventricle; *14*, hypothalamus; *15*, innominate substance; *16*, habenula; *17*, pulvinar thalami; *18*, splenium of corpus callosum

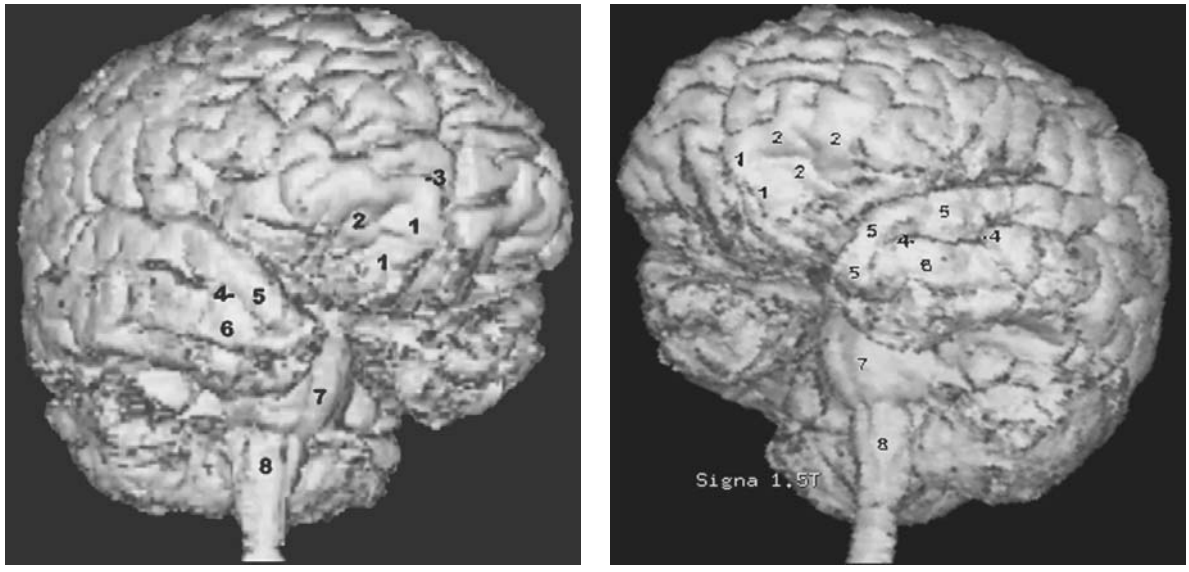

Fig. 3.59. 3D MR of the temporal pole and fronto-orbital region. *1*, Gyrus rectus; *2*, fronto-orbital gyri; *3*, supramarginal sulcus; *4*, superior temporal sulcus; *5*, superior temporal gyrus; *6*, middle temporal gyrus; *7*, pons; *8*, medulla oblongata

Fig. 3.60. 3D MR of the brain showing the frontal and temporal polar regions. *1*, Gyrus rectus; *2*, fronto-orbital gyri; *4*, superior temporal sulcus; *5*, superior temporal gyrus; *6*, middle temporal gyrus; *7*, pons; *8*, medulla oblongata

Fig. 3.61. Coronal anatomical cut showing the sulcal and gyral anatomy of the fronto-orbital lobe. *1*, Olfactory sulcus; *2*, medial orbital sulcus; *3*, lateral orbital sulcus; *4*, gyrus rectus; *5*, medial orbital gyrus; *6*, lateral orbital gyrus; *7*, anterior orbital gyrus; *8*, cingulate sulcus; *9*, cingulate gyrus; *10*, superior frontal sulcus; *11*, superior frontal gyrus; *12*, middle frontal gyrus; *13*, superior rostral sulcus; *14*, arcuate orbital sulcus; *15*, interhemispheric fissure

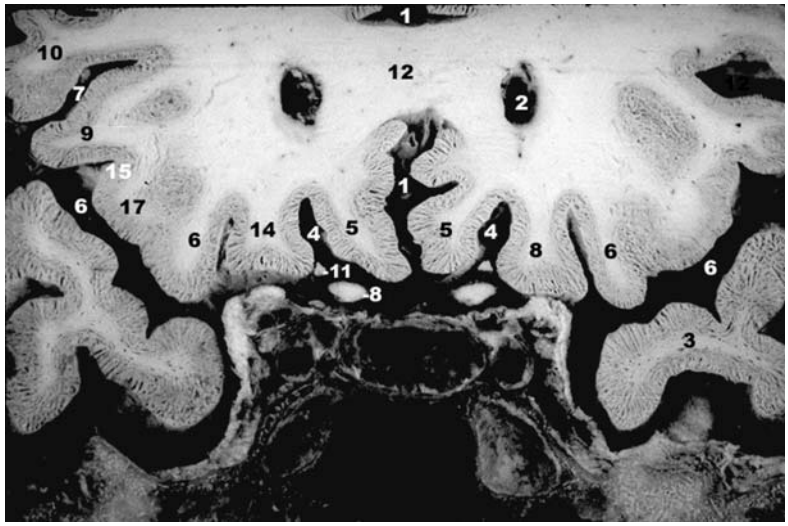

Fig. 3.62. Coronal anatomical cut of the fronto-orbital gyri. *1*, Interhemispheric fissure; *2*, tip of frontal horn; *3*, temporal pole; *4*, olfactory sulcus; *5*, gyrus rectus; *6*, posterior orbital gyrus; *7*, horizontal ramus of lateral fissure; *8*, cisternal optic nerve; *9*, inferior frontal gyrus, pars orbitalis; *10*, inferior frontal gyrus, pars triangularis; *11*, olfactory tract; *12*, corpus callosum, genu; *13*, inferior frontal sulcus; *14*, medial orbital gyrus; *15*, lateral orbital sulcus; *16*, cingulate sulcus; *17*, lateral orbital gyrus

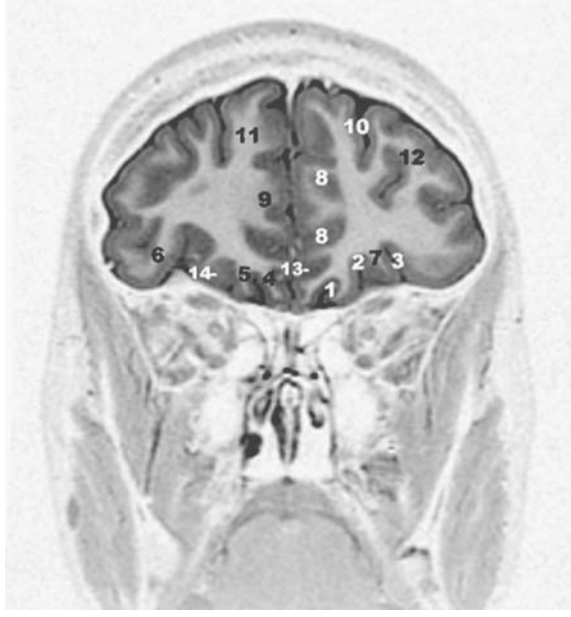

Fig. 3.63. MR coronal cut of the brain through the orbitofrontal lobes, parallel to PC-OB. *1*, Olfactory sulcus; *2*, medial orbital sulcus; *3*, lateral orbital sulcus; *4*, gyrus rectus; *5*, medial orbital gyrus; *6*, lateral orbital gyrus; *7*, anterior orbital gyrus; *8*, cingulate sulcus; *9*, cingulate gyrus; *10*, superior frontal sulcus; *11*, superior frontal gyrus; *12*, middle frontal gyrus; *13*, superior rostral sulcus; *14*, arcuate orbital sulcus

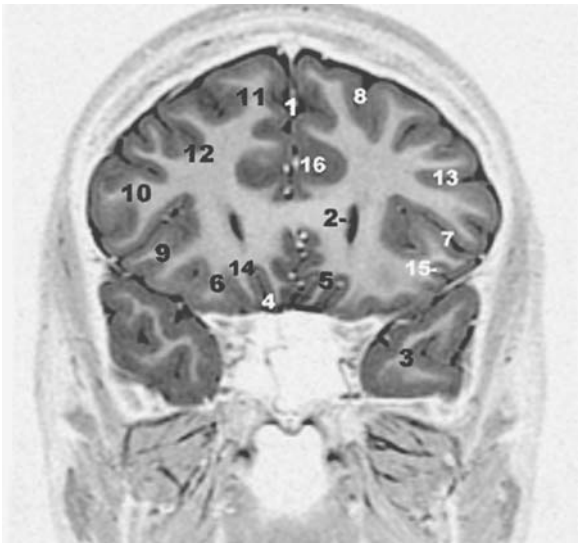

Fig. 3.64. Coronal anatomical cut of the brain passing through the genu of corpus callosum and the tip of the frontal ventricular horns. *1*, Interhemispheric fissure; *2*, tip of frontal horn; *3*, temporal pole; *4*, olfactory sulcus; *5*, gyrus rectus; *6*, posterior orbital gyrus; *7*, horizontal ramus of lateral fissure; *8*, superior frontal sulcus; *9*, inferior frontal gyrus, pars orbitalis; *10*, inferior frontal gyrus, pars triangularis; *11*, superior frontal gyrus; *12*, middle frontal gyrus; *13*, inferior frontal sulcus; *14*, medial orbital gyrus; *15*, lateral orbital sulcus; *16*, cingulate sulcus

c The Medial Frontal Gyrus

The medial frontal gyrus is limited ventrally and anteriorly by the gyrus rectus (Figs. 3.53, 3.62, 3.64). Superiorly it constitutes the superior border of the hemisphere and posteriorly it is limited by the paracentral sulcus, a well-demarcated sulcus that has its most constant portion in contact with the cingulate sulcus. This sulcus occasionally extends throughout the mesial surface and abuts the superior part of the hemisphere, being situated anterior to the medial precentral sulcus. Because of the interruptions of the cingulate sulcus, the medial frontal gyrus can invaginate into the cingulum.

d The Paracentral Lobule

The paracentral lobule is limited superiorly by the superior border of the hemisphere and anteriorly by the paracentral sulcus (Figs. 3.52, 3.53, 3.65). When the paracentral sulcus is only visible in contact with the cingulate sulcus its extension up to the medial border marks the anterior limit of the lobule. Posteriorly, the paracentral lobule is limited by the marginal ramus, an extension of the cingulate sulcus. The marginal ramus ends at the hemispheric border and in 80% of examined hemispheres it extends to the lateral surface. Two sulci are most frequently noted. The central sulcus extends into the paracentral lobule in 65% of examined hemispheres and assumes a characteristic shape, being oriented sharply posteriorly. More anteriorly, the medial precentral sulcus constitutes the most superior extent of the interrupted precentral sulcus, marking the anatomic limit of the primary motor area. The paracentral lobule proper usually extends anterior to the precentral sulcus.

Despite numerous reported stimulation studies, the relationship of the marginal ramus to the central area has not been adequately assessed. Anatomically, the marginal ramus has a relatively constant relationship with the central sulcus and ends posterior to the central sulcus in 97% of examined hemispheres. The precentral sulcus on the lateral border of the hemisphere has an extremely complex anatomy. It is frequently an interrupted sulcus, arising inferolaterally in contact with the sylvian fissure as the inferior precentral sulcus and delineating the anterior border of the ascending frontal gyrus (frontale ascendante). The posterior superior limit of the first frontal convolution is complex and is constituted by the marginal precentral and the medial precentral sulci, respectively. The latter extends over the mesial hemisphere. The paracentral sulcus is frequently anterior to the medial precentral sulcus. Since the medial precentral sulcus is usually shallow and does not extend down to the cingulate, the anterior limit of the primary motor area over the mesial hemisphere tends to be unclear. The postcentral sulcus extends to the mesial surface in 20% to 40% of examined hemispheres. Most commonly, it is posterior to the marginal ramus. Thus the primary sensory leg/foot area appears to extend anatomically beyond the limits of the paracentral lobule.

e The Precuneus

The precuneus is limited anteriorly by the marginal ramus, superiorly by the superior border of the hemisphere, posteriorly by the parieto-occipital sulcus and inferiorly by the subparietal sulcus (Figs. 3.53, 3.65). The superior parietal sulcus extends to the medial aspect and cuts into the precuneus. The parieto-occipital sulcus is a deep constant sulcus which demarcates the precuneus from the cuneus of the occipital lobe. The subparietal sulcus is a variable sulcus which may show various branching (H-shaped or "split H") or may appear as a posterior branching of the cingulate sulcus. It is frequently traversed by one or two "plis de passages" parietal limbic. Inferior to the subparietal sulcus, the cingulate gyrus becomes wide and then tapers sharply at the level of the splenium of the corpus callosum.

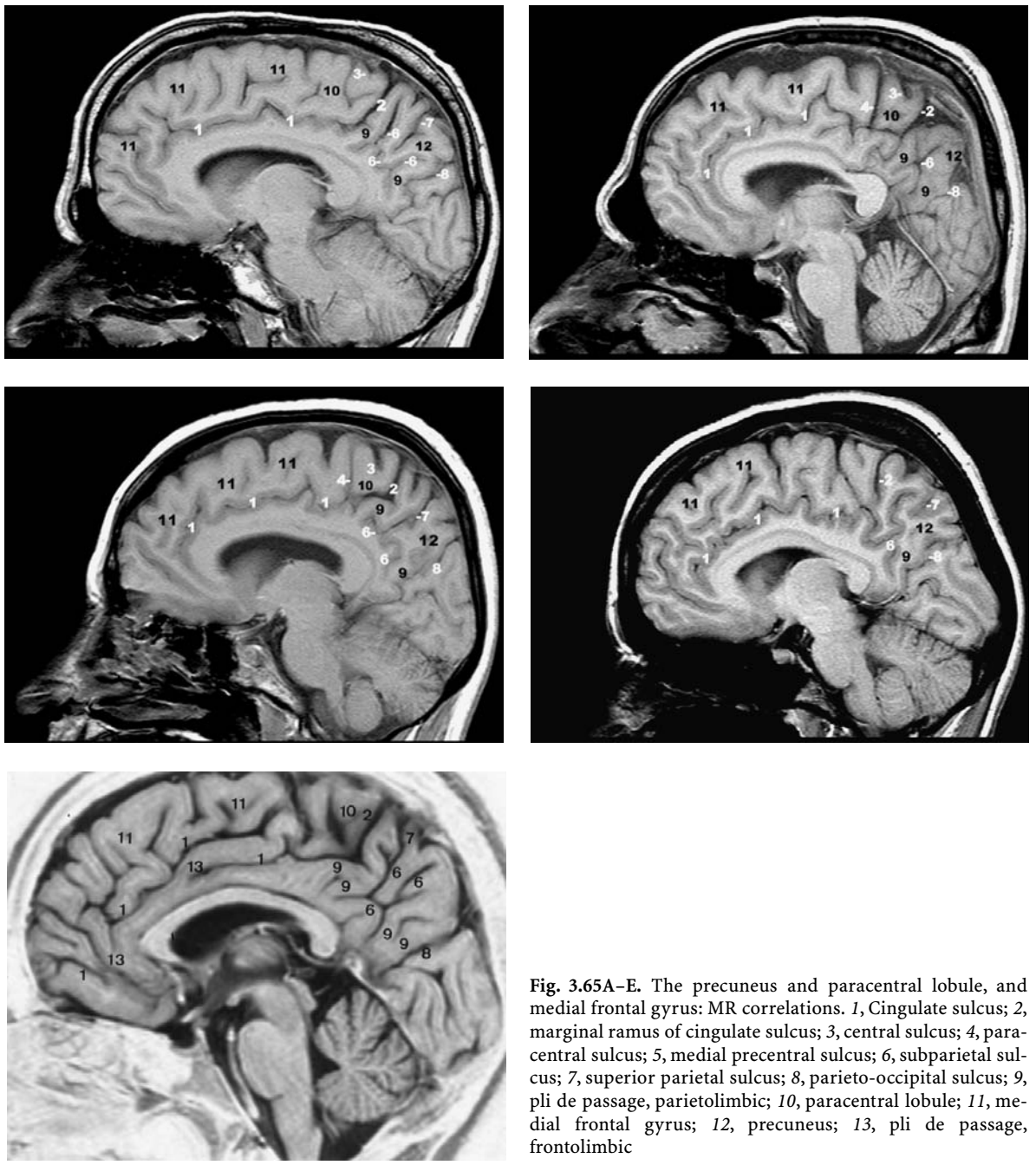

Fig. 3.65A–E. The precuneus and paracentral lobule, and medial frontal gyrus: MR correlations. *1*, Cingulate sulcus; *2*, marginal ramus of cingulate sulcus; *3*, central sulcus; *4*, paracentral sulcus; *5*, medial precentral sulcus; *6*, subparietal sulcus; *7*, superior parietal sulcus; *8*, parieto-occipital sulcus; *9*, pli de passage, parietolimbic; *10*, paracentral lobule; *11*, medial frontal gyrus; *12*, precuneus; *13*, pli de passage, frontolimbic

f The Cuneus

Triangular in shape, the cuneus is the only occipital gyrus to be well delimited. It is in fact bounded anteriorly by the parieto-occipital sulcus, superiorly by the superior and posterior borders of the hemisphere and inferiorly by the posterior calcarine sulcus (Figs. 3.55, 3.56). It is continuous with the lateral surface. The calcarine sulcus extends anteriorly and stops at the most posterior extent of the collateral sulcus, where the isthmus of the cingulate gyrus extends into the parahippocampal gyrus. The cuneus is connected to the posterior aspect of the adjacent cingulate gyrus by the deeply situated cuneolimbic pli de passage of Broca. In all primates except the gibbon, this gyrus is superficial and separates the parieto-occipital from the calcarine sulci. At the oc-

cipital pole, the calcarine sulcus terminates as the vertical retrocalcarine sulcus behind which is found the gyrus descendens of Ecker (1869). The latter may sometimes be located on the lateral aspect of the hemisphere, or bounded posteriorly by an occipital polar sulcus limiting the striate area.

g The Lingual Gyrus

The lingual gyrus constitutes the inferior and mesial aspect of the occipital lobe and is bordered superiorly by the calcarine sulcus (Figs. 3.55, 3.56). It is connected to the cuneus through the retrocalcarine sulcus by one or two cuneolingual gyri, "plis de passage cuneo-limbiques of Broca" (Déjerine 1895). It is continuous anteriorly with the parahippocampal gyrus. An inconstant lingual sulcus may further subdivide the lingual gyrus into superior and inferior parts, both connected anteriorly to the parahippocampal gyrus.

E The Basal Surface of the Cerebral Hemisphere

Sulci and gyri of the basal aspect of the frontotemporal lobes are best imaged and analyzed on coronal cuts as performed parallel to the commissural-obex brain reference line (Tamraz et al. 1990, 1991). Coronal anatomic correlations are available in previous works (Tamraz 1983; Cabanis et al. 1988). In the following sections we will separate the basal surface into the anterior basal orbitofrontal lobe and the posterior basal temporal lobe.

1 The Frontal Orbital Lobe

The orbital surface of the frontal lobe presents a primary sulcus, the olfactory sulcus and a secondary composite sulcus showing great individual variations and named the orbital sulci (Figs. 3.58–3.64, 3.66).

a Olfactory Sulcus and Gyrus Rectus

The olfactory sulcus originates at the anterior border of the anterior perforated substance in two rami, of which the longer lateral branch may anastomose with the lateral fissure or, less frequently, with the arcuate orbital sulcus. It courses from back to front roughly parallel to the anterior interhemispheric fissure, to end about 15 mm behind the frontal pole, relatively close to the interhemispheric fissure. It is related to the olfactory tract.

This sulcus separates the gyrus rectus medially from the orbital gyri laterally. The gyrus rectus is easily distinguished as the narrow strip of cortex of about 1 cm width, mesial to the olfactory sulcus and is a part of the longitudinal arciform region corresponding to the orbital portion of the superior frontal convolution.

b Orbital or Orbitofrontal Sulci and Gyri

The orbital or orbitofrontal sulci show numerous variations (Kanai 1938) consisting of two longitudinal sulci connected by a transverse furrow. These sulci are arranged in the shape of "H" (incisure en H of Broca), an "X" or a "K" (Figs. 3.66, 3.67). The longitudinal sulci are the medial and the lateral orbital sulci, which divide the orbital surface into medial and lateral orbital gyri and an intermediate orbital cortex. This is subdivided transversely into anterior and posterior middle orbital gyri by the arcuate orbital sulcus, which is situated near the frontal pole with a convex border directed toward the pole. Such subdivisions are not independent but are parts of the superior and inferior frontal gyri of the lateral aspect of the hemisphere. The lateral orbital sulcus limits the orbitofrontal lobe from the lateral aspect of the inferior frontal gyrus.

2 The Temporal Basal Lobe

The ventral surface of the temporal lobe extends laterally from the inferior and lateral border of the hemisphere to the mesial temporal border at the lateral wing of the transverse fissure (Figs. 3.68–3.71). It extends from the temporal pole to the inferior occipital lobe without definite anatomic demarcation other than the preoccipital notch. An arbitrary line joining this notch to the isthmus behind the splenium posteriorly limits the ventral temporal gyri. From mesial to lateral, two longitudinal sulci, the collateral sulcus and the occipitotemporal sulcus divide the inferior temporal lobe into three longitudinal gyri, the parahippocampal gyrus, the fusiform gyrus and the inferior temporal gyrus at the junction between the lateral and the inferior aspects of the hemisphere.

a Collateral Sulcus and Parahippocampal Gyrus

The collateral sulcus, a primary sulcus also called the medial occipitotemporal sulcus, is a constant, elongated S-shaped sulcus of the basal aspect of the temporal lobe. According to Landau (1911) it is interrupted in about half the cases but according to Ono

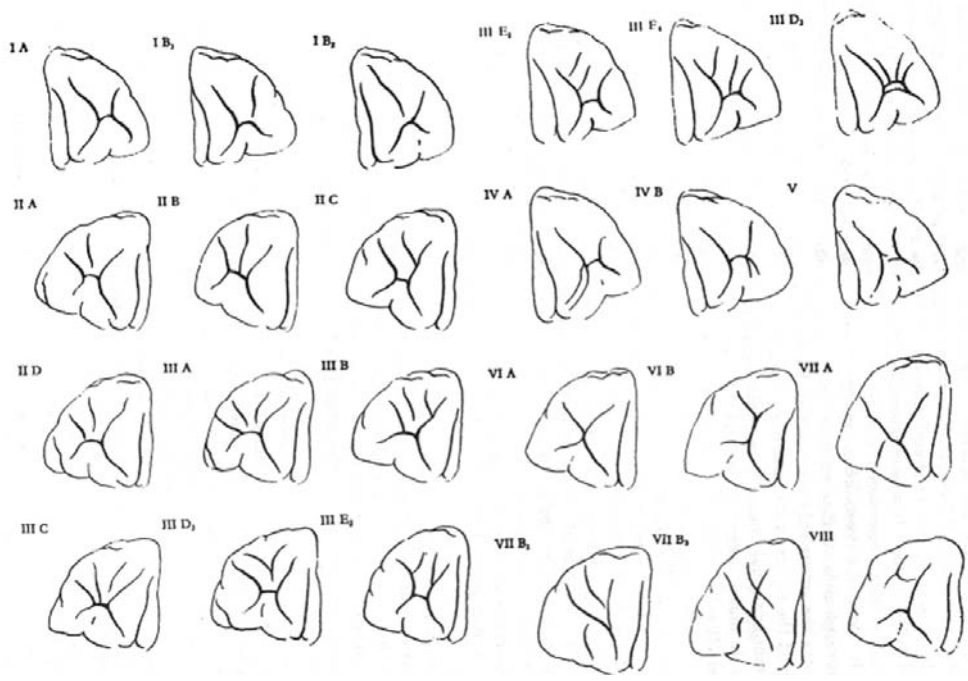

Fig. 3.66. Fissural patterns of the fronto-orbital region. (After Kanai 1938)

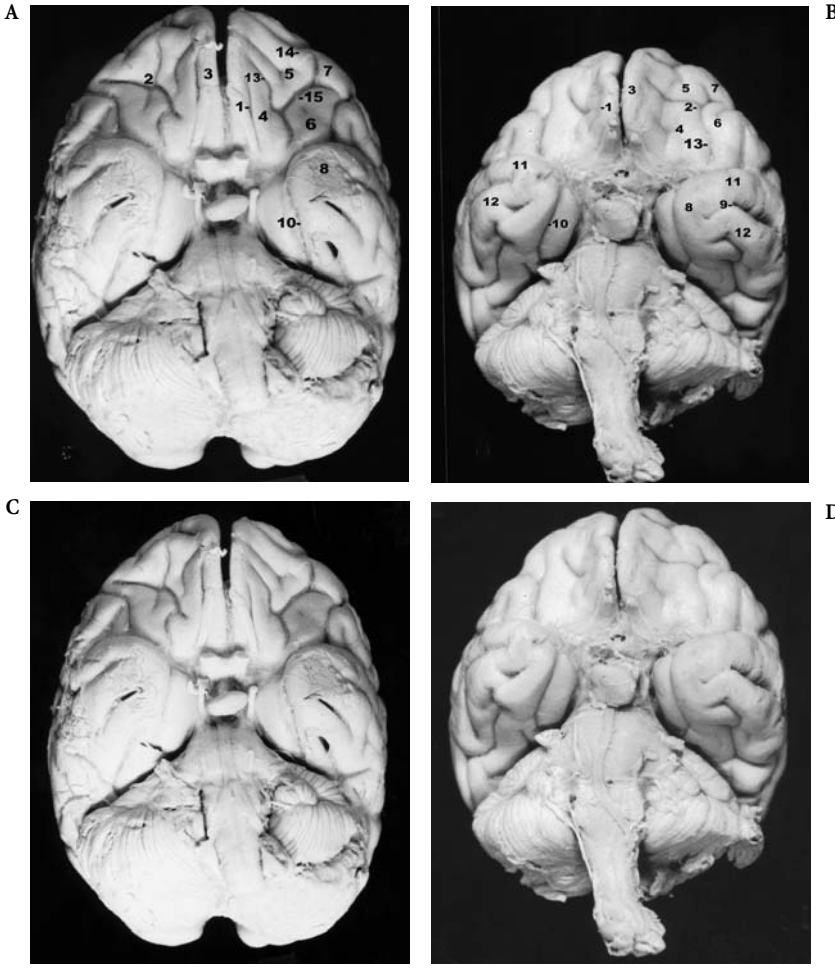

Fig. 3.67A–D. Inferior aspect of the brain showing the fissural pattern of the fronto-orbital lobe and the temporal poles, in anthropoids. **A,C** Gorilla, **B,D** orangutan. *1*, Olfactory sulcus; *2*, fronto-orbital "H-shape" sulci (cruciform); *3*, gyrus rectus; *4*, medial orbital gyrus; *5*, anterior orbital gyrus; *6*, posterior orbital gyrus; *7*, lateral orbital gyrus; *8*, temporal pole; *9*, parallel sulcus; *10*, rhinal sulcus; *11*, superior temporal gyrus; *12*, middle temporal gyrus; *13*, medial orbital sulcus; *14*, lateral orbital sulcus; *15*, arcuate sulcus

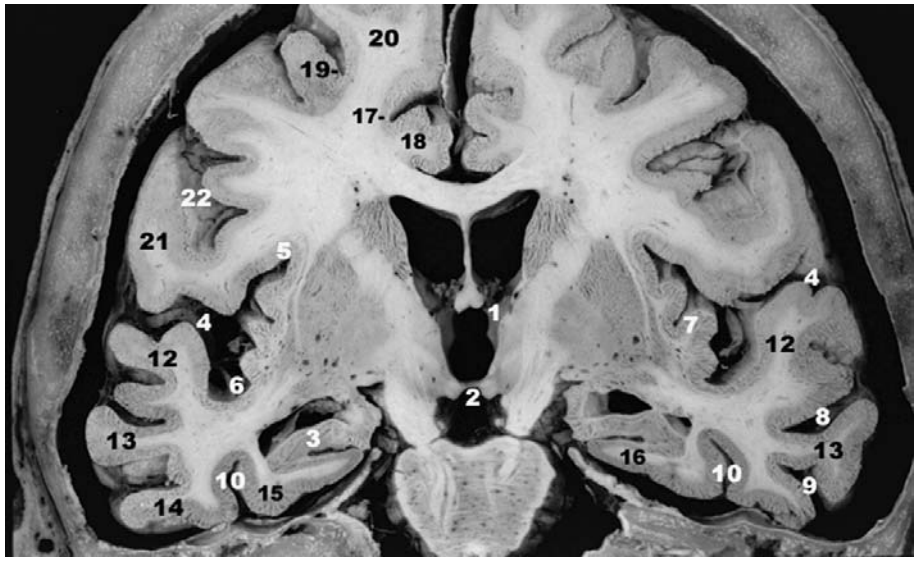

Fig. 3.68. Coronal anatomical cut of the brain through the interventricular foramina and the mamillary bodies. *1*, Interventricular foramen; *2*, mamillary body; *3*, hippocampal head; *4*, lateral fissure; *5*, superior circular sulcus; *6*, inferior circular sulcus; *7*, insula; *8*, superior temporal (parallel) sulcus; *9*, inferior temporal sulcus; *10*, occipitotemporal sulcus; *11*, collateral sulcus; *12*, superior temporal gyrus; *13*, middle temporal gyrus; *14*, inferior temporal gyrus; *15*, fusiform gyrus; *16*, parahippocampal gyrus; *17*, cingulate sulcus; *18*, cingulate gyrus; *19*, superior frontal sulcus; *20*, superior frontal gyrus; *21*, precentral gyrus; *22*, central sulcus.

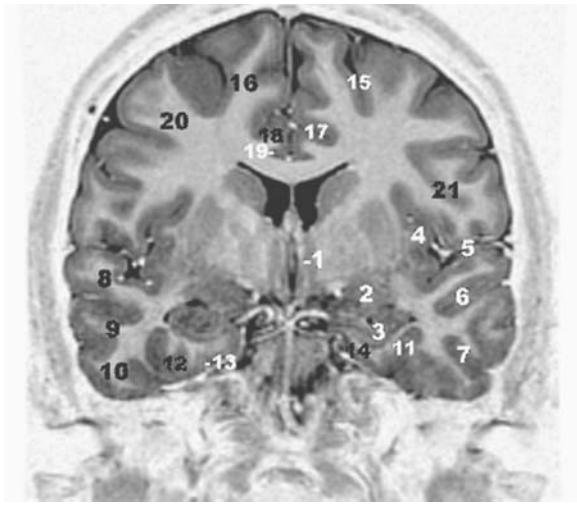

Fig. 3.69. MR coronal cut of the brain through the anterior columns of the fornix and the mamillary bodies, parallel to PC-OB.*1*, Anterior columns of fornix; *2*, amygdala; *3*, hippocampal head; *4*, insula; *5*, lateral fissure; *6*, superior temporal (parallel) sulcus; *7*, inferior temporal sulcus; *8*, superior temporal gyrus; *9*, middle temporal gyrus; *10*, inferior temporal gyrus; *11*, occipitotemporal sulcus; *12*, fusiform gyrus; *13*, collateral sulcus; *14*, parahypocampal gyrus; *15*, superior frontal sulcus; *16*, superior frontal gyrus; *17*, cingulate sulcus; *18*, cingulate gyrus; *19*, callosal sulcus; *20*, middle frontal gyrus; *21*, precentral gyrus

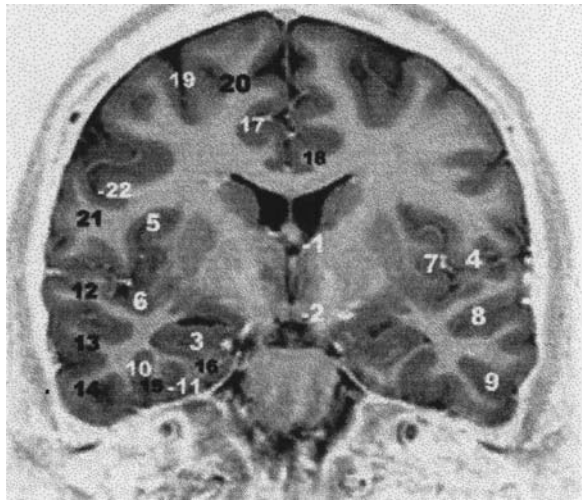

Fig. 3.70. MR coronal cut of the brain through the interventricular foramina and the mamillary bodies, parallel to PC-OB. *1*, Interventricular foramen; *2*, mamillary body; *3*, hippocampal head; *4*, lateral fissure; *5*, superior circular sulcus; *6*, inferior circular sulcus; *7*, insula; *8*, superior temporal (parallel) sulcus; *9*, inferior temporal sulcus; *10*, occipito-temporal sulcus; *11*, collateral sulcus; *12*, superior temporal gyrus; *13*, middle temporal gyrus; *14*, inferior temporal gyrus; *15*, fusiform gyrus; *16*, parahippocampal gyrus; *17*, cingulate sulcus; *18*, cingulate gyrus; *19*, superior frontal sulcus; *20*, superior frontal gyrus; *21*, precentral gyrus; *22*, central sulcus

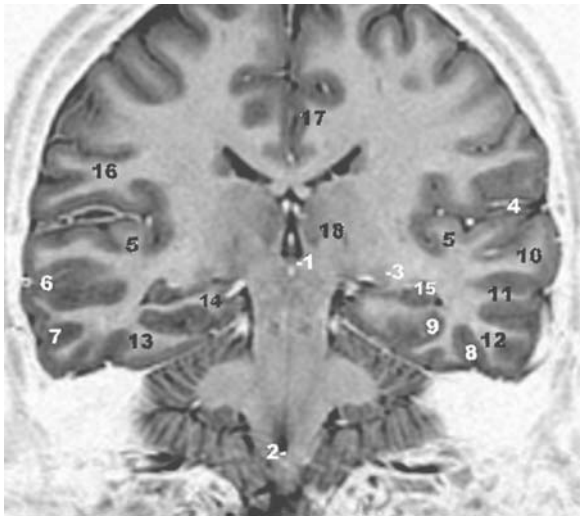

Fig. 3.71. MR coronal cut of the brain passing through the posterior commissure and the obex, according to the PC-OB orientation. *1*, Posterior commissure; *2*, obex; *3*, lateral geniculate body; *4*, lateral fissure; *5*, transverse gyrus of Heschl; *6*, superior temporal sulcus; *7*, inferior temporal sulcus; *8*, occipitotemporal sulcus; *9*, collateral sulcus; *10*, superior temporal gyrus; *11*, middle temporal gyrus; *12*, inferior temporal gyrus; *13*, fusiform gyrus; *14*, parahippocampal gyrus; *15*, hippocampus; *16*, supramarginal gyrus; *17*, cingulate gyrus; *18*, thalamus

et al. (1990), it is uninterrupted. It usually originates in a transverse collateral sulcus, near the temporal pole and ends in another transverse occipitotemporal sulcus which may show one (sulcus sagittalis gyri fusiformis of Retzius) or several small oblique connections with the inferior temporal sulcus. At this end, the collateral sulcus may fuse with the calcarine sulcus. The collateral sulcus laterally separates the parahippocampal gyrus and the lingual gyrus from the fusiform gyrus. Its depth impresses the inferior wall of the atrium and the temporal horn of the lateral ventricle, as observed on coronal cuts.

b Occipitotemporal Sulcus and Fusiform Gyrus

The lateral occipitotemporal sulcus is a secondary sulcus coursing lateral to the collateral sulcus, near the inferolateral margin of the hemisphere and ending close to the preoccipital notch in about two thirds of the cases. It shows frequent interruptions, being continuous in less than 40% of the cases according to Ono et al. (1990). It constitutes the outer boundary of the occipitotemporal or fusiform gyrus, and is limited medially by the collateral sulcus or medial occipitotemporal sulcus. This gyrus does not reach the temporal pole anteriorly. Its width increases from the pole to its posterior extremity before it decreases again to merge with the inferior occipital lobe.

F White Matter Core and Major Association Tracts

Raymond Vieussens, well known for his labeling of "centrum semi-ovale", first reported that the hemispheric white matter consists of fiber bundles. Baillarger (1840) emphasized that the gray and white matter are intimately linked. Meynert (1877) made a major contribution with a classification of the myelinated fibers into three major groups: (1) the association fibers, which interconnect different cortical regions and consist of most of the white matter substance; (2) the commissural fibers which link both hemispheres and cross through the corpus callosum, the anterior commissure and the fornix; (3) the projection fibers between the cortex and the subcortical centers, which contribute to the formation of the corona radiata (Fig. 3.72).

We will focus on the long association fibers which may be routinely clearly identified on MR (particularly in coronal cuts) using proton density, T2 or STIR pulse sequences (Fig. 3.73). Diffusion-weighted imaging sequences are more powerful for disclosing such bundles and will certainly modify the microsurgical approach to resections of brain tumors.

The medullary white matter with the very long association fibers bundles is found deep inside the white matter core on the medial or the lateral sides of the corona radiata. These fiber systems are at present

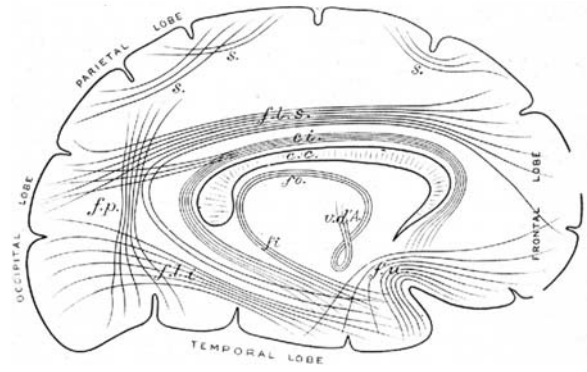

Fig. 3.72. The intrahemispheric association fibers. *s*, short association fibers between adjacent gyri; *f.l.s.*, superior longitudinal fasciculus; *ci.*, Cingulate fasciculus; *f.l.i.*, inferior longitudinal fasciculus; *f.u.*, uncinate fasciculus; *f.p.*, perpendicular fasciculus; *f.i.*, fimbria; *f.o.*, fornix; *v.d' A.*, thalamic fasciculus of Vicq d'Azyr; *c.c.*, corpus callosum. (After Meynert 1877)

best recognized from the macroscopic dissections as described in the major contributions of Meynert (1877), Déjerine (1895) and Klingler (1935) (Fig. 3.74). For MR correlations we will use the anatomical dissections as performed by Ludwig and Klingler (1956) at the Basel Institute of Anatomy.

Seven association fiber systems may be disclosed in the cerebral hemisphere: (1) the cingulum; (2) the superior fronto-occipital; (3) the superior longitudinal; (4) the arcuate; (5) the inferior fronto-occipital; (6) the uncinate; and (7) the inferior longitudinal fasciculus.

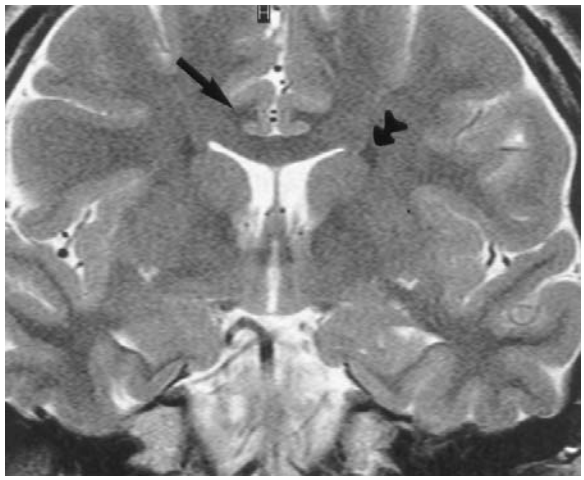

A

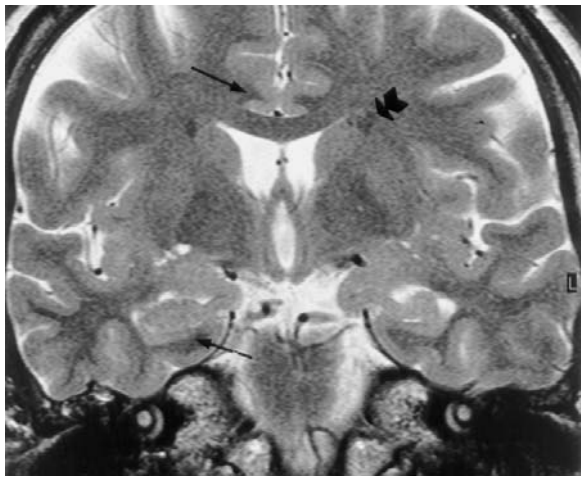

B

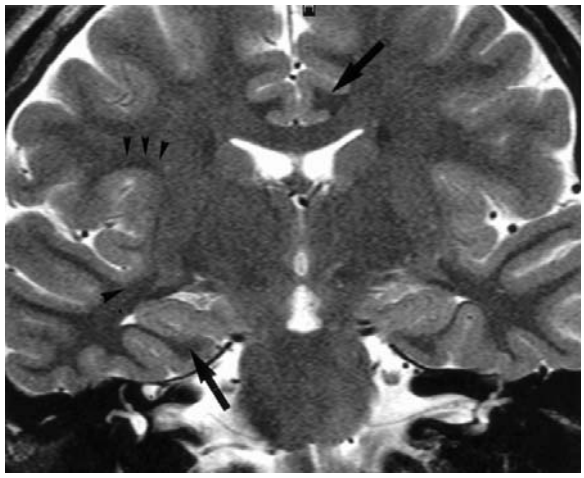

C

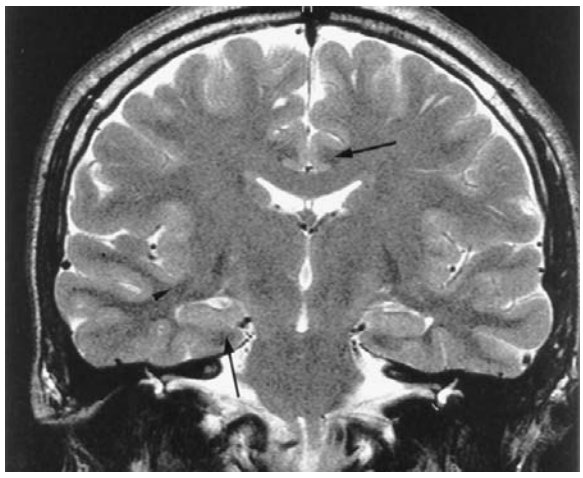

D

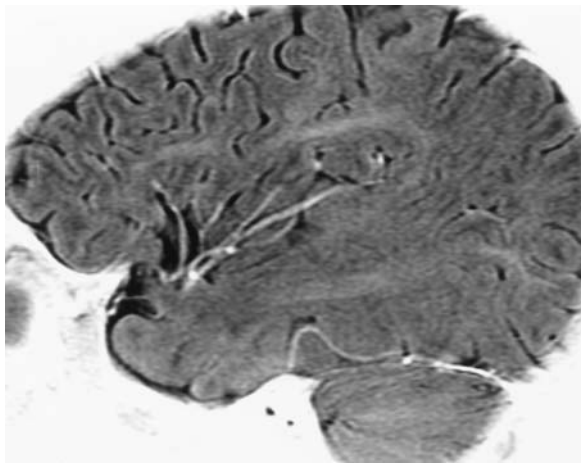

E

Fig. 3.73A–E. Brain long association fiber bundles as visualized by coronal FSE-T2 weighted MR. **A,B** Cut through the anterior columns of the fornix; **C,D** cut through the anterior brainstem at the fundus of the interpeduncular cistern. Both cuts are parallel to the PC-OB reference line. These cuts show the cingulum (*long arrow*) in the gyral white matter of the cingulate gyrus; the parahippocampal gyrus; the superior fronto-occipital fasciculus (*short arrow*) at the angle between the corpus callosum and the superolateral border of the lateral ventricle; the superior longitudinal fasciculus (*triple arrowheads*) dorsal to the upper border of the insula; and the inferior fronto-occipital fasciculus (*single arrowhead*) in the floor of the lateral fissure, beneath the claustrum and the external capsule. **E** Parasagittal MR cut in an infant showing the early myelinated arcuate fasciculus.

1. The cingulum is a bundle of long association fibers easily depicted on frontal MR cuts in the gyral white matter of the cingulate and the parahippocampal gyri. It is found above the corpus callosum, below the cingulate sulcus. It may be divided into an anterior part around the genu of the corpus callosum, a horizontal part relative to the body and a posterior part sweeping around the splenium and extending towards the parahippocampal gyrus. Its fibers link the cortex of the frontal, parietal, temporal and occipital lobes (neocerebrum) with the limbic lobe. The precuneus receives a consistent amount of these fibers (Elze 1929) (Fig. 3.75).
2. The superior fronto-occipital fasciculus is found in the angle between the corpus callosum and the superolateral border of the lateral ventricle and the adjacent caudate nucleus. It was described by Déjerine (1895) and was presumed to be homologous to the bulky fiber bundles observed in cases of agenesis of the corpus callosum (Onufrowicz 1887; Kaufman 1887) (Fig. 3.76). It interconnects the frontal to the occipital cortices (Chusid et al. 1948). Both the identity and the role of this bundle are still debated. It is lesioned after frontal lobotomy (McLardy 1950).
3. The superior longitudinal fasciculus, is a long association tract situated dorsal to the upper border of the insula. It conveys impulses posteriorly from the frontal lobe to the associative regions of the parietal and occipital lobes. Lesions in the dominant hemisphere of the superior longitudinal fasciculus impair the capability to identify objects or to understand spoken or written sentences (Figs. 3.77, 3.78, 3.79).
4. The arcuate fasciculus is found dorsal to the insula around which it sweeps, interconnecting portions of the frontal to the temporal lobes. Zenker (1985) reported that the associative fibers interconnect the middle and inferior gyri of the frontal lobe with the middle and inferior gyri of the temporal lobe. This could represent a component of the superior longitudinal fasciculus.
5. The inferior fronto-occipital fasciculus, located more deeply than the uncinate fasciculus, is presumed to interconnect parts of the frontal and occipital lobes (Figs. 3.78–3.79).
6. The uncinate fasciculus interconnects the fronto-orbital lobe and parts of the middle and inferior frontal gyri, with the anterior temporal lobe and pole, coursing along the floor of the sylvian fissure. This fasciculus is found coursing through the anterior inferior border of the external capsule and the inferior aspect of the claustrum (Schnopfhagen 1890). It may also pass through the extreme capsule according to Landau (1919) (Figs. 3.77–3.79).
7. The inferior longitudinal fasciculus of Burdach is a long association fiber bundle situated contiguous to the lateral aspect of the inferior horn of the lateral ventricle, in the temporo-occipital lobe. It extends from the occipital to the temporal pole.

Fig. 3.74A–G. Dissection of the brain showing the subgyral medullary white matter and the short association fibers. **A**,**B** Lateral aspect. *1*, Sulcus intraparietalis; *2*, sulcus postcentralis; *3*, sulcus lateralis; *4*, sulcus postcentralis; *5*, sulcus centralis; *6*, sulcus praecentralis; *7*, sulcus centralis; *8*, sulcus praecentralis; *9*, sulcus frontalis inferior; *10*, sulcus frontalis medius; *11*, sulcus frontalis superior; *12*, sulcus lateralis, ramus anterior; *13*, sulcus lateralis, ramus ascendens; *14*, sulcus temporalis medius; *15*, sulcus temporalis superior; *16*, sulcus temporalis medius. **C**,**D** Superior aspect. *1*, Gyrus frontalis inferior; *2*, gyrus frontalis superior; *3*, gyrus frontalis medius; *4*, gyrus praecentralis; *5*, sulcus centralis; *6*, gyrus postcentralis; *7*, sulcus intraparietalis; *8*, lobulus parietalis superior. **E**,**F** Mesial aspect. *1*, Gyrus frontalis superior; *2*, gyrus cinguli; *3*, septum pellucidum; *4*, fornix; *5*, corpus callosum; *6*, stria medullaris thalami; *7*, lobulus paracentralis; *8*, ramus marginalis sulci cinguli; *9*, praecunens; *10*, sulcus parieto-occipitalis; *11*, cuneus; *12*, Sulcus calcarinus; *13*, Isthmus gyri cinguli; *14*, corpus pineale; *15*, gyrus parahippocampalis; *16*, aquaeductus cerebri; *17*, uncus; *18*, corpus mamillare; *19*, adhaesio interthalamica; *20*, commissura anterior; *21*, foramen interventriculare. **G**,**H** Inferior aspect. *1*, bulbus olfactorius; *2*, tractus olfactorius; *3*, gyrus rectus; *4*, trigonium olfactorium; *5*, nervus opticus; *6*, substantia perforata; *7*, chiasma opticum; *8*, tractus opticus; *9*, corpus mamillare; *10*, crus cerebri; *11*, substantia nigra; *12*, tectum mesencephali; *13*, aquaeductus cerebri; *14*, pulvinar; *15*, splenium corporis callosi; *16*, Isthmus gyri cinguli; *17*, pars communis sulcorium parieto-occipitalis, calcarini; *18*, sulcus temporalis inferior; *19*, sulcus collateralis; *20*, gyrus occipitotemporalis lateralis; *21*, gyrus parahippocampalis; *22*, sulcus rhinicus; *23*, polas temporalis; *24*, gyri orbitales; *25*, sulcus olfactorius. (By Klingler. From Ludwig and Klingler 1956, Tables 1–4) ▷

A

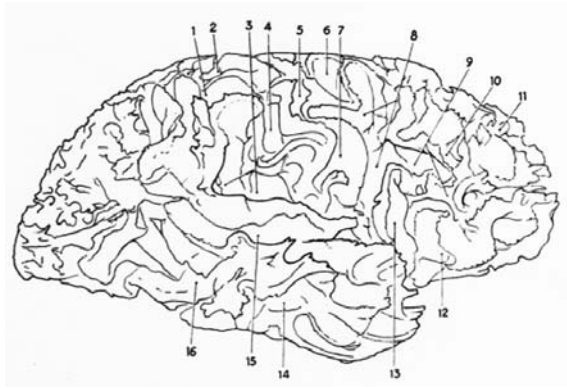
1 2 3 4 5 6 7 8 9 10 11 12 13 14 15 16

B

C

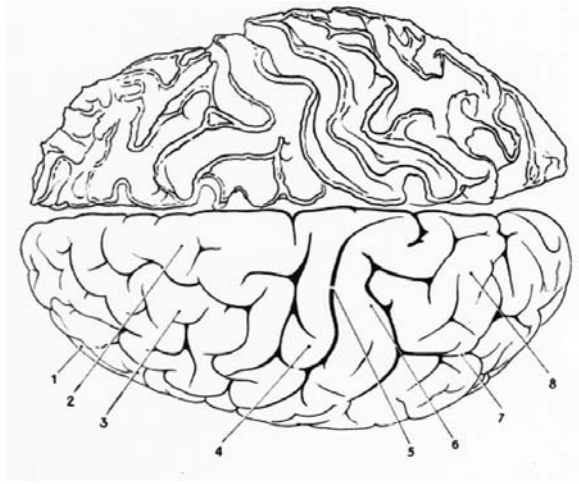
1 2 3 4 5 6 7 8

D

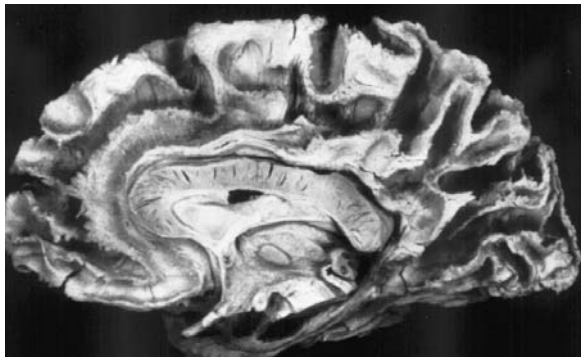

E

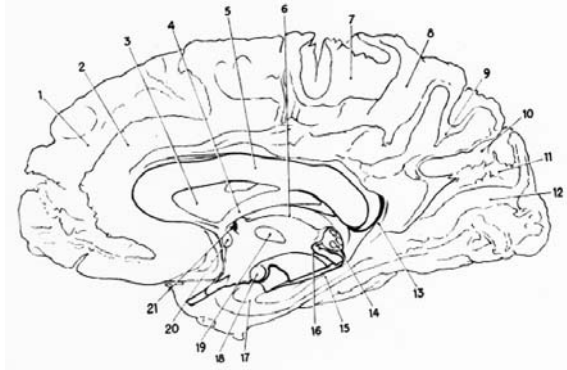
1 2 3 4 5 6 7 8 9 10 11 12 13 14 15 16 17 18 19 20 21

F

G

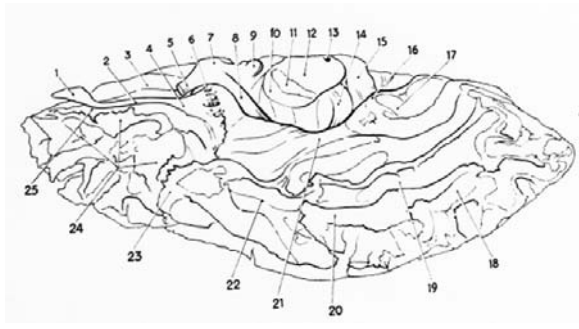
1 2 3 4 5 6 7 8 9 10 11 12 13 14 15 16 17 18 19 20 21 22 23 24 25

H

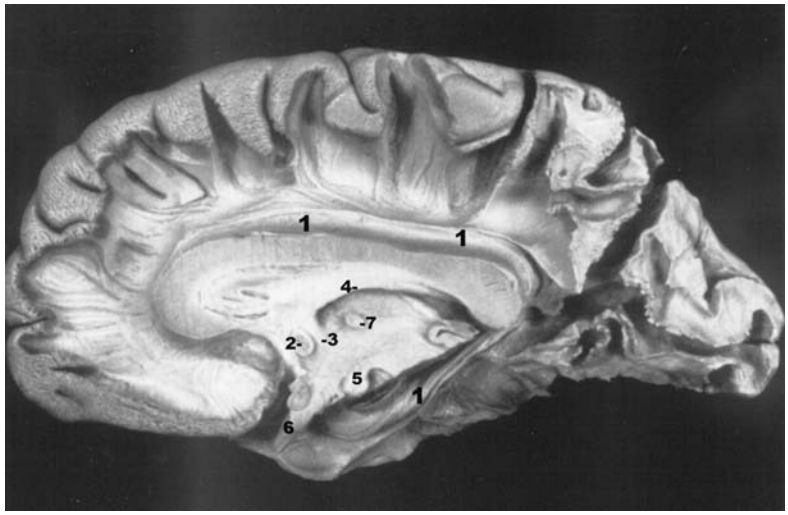

Fig. 3.75. Dissection of the brain disclosing the major association fiber bundles and showing the cingulum. *1*, Cingulum; *2*, anterior commissure; *3*, anterior column of the fornix; *4*, body of the fornix; *5*, mamillary body; *6*, optic chiasm; *7*, interthalamic adhesion. (By Klingler. From Ludwig and Klingler 1956, Table 9)

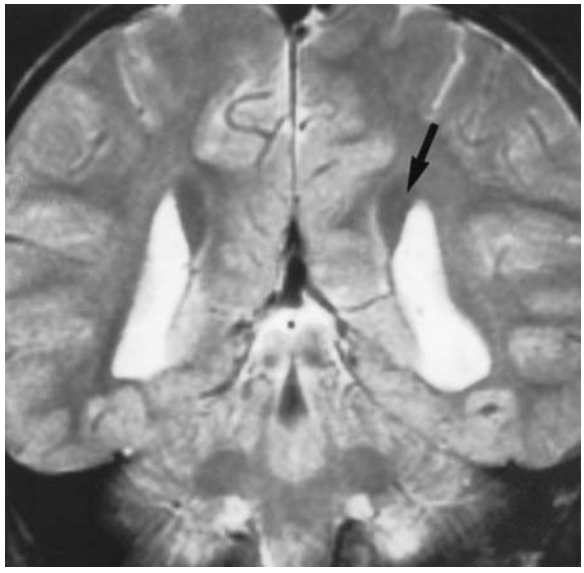

Fig. 3.76. Coronal MR cut (T2-ω) showing the Probst bundles (*arrow*) in a case of agenesis of the corpus callosum

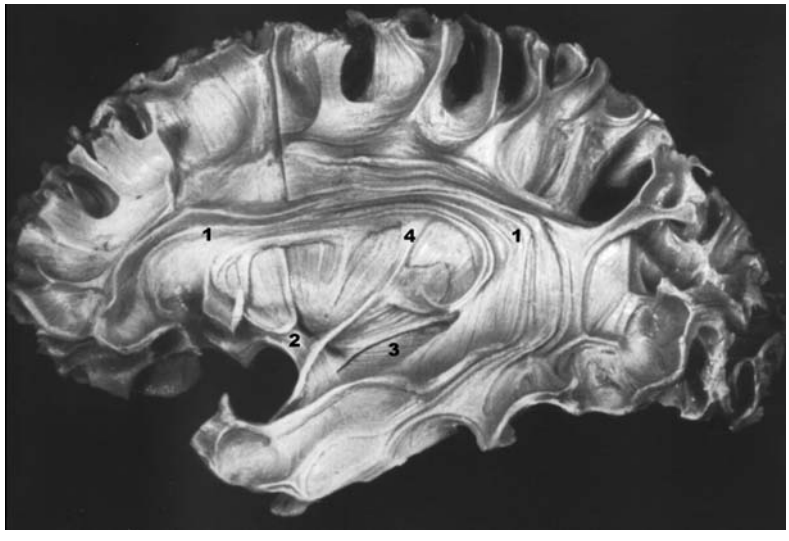

Fig. 3.77. Dissection of the brain disclosing the major association fiber bundles, showing the superior longitudinal fasciculus. *1*, Superior longitudinal fasciculus; *2*, uncinate fasciculus; *3*, inferior longitudinal fasciculus; *4*, medullary substance of the insula. (By Klingler. From Ludwig and Klingler 1956, Table 6)

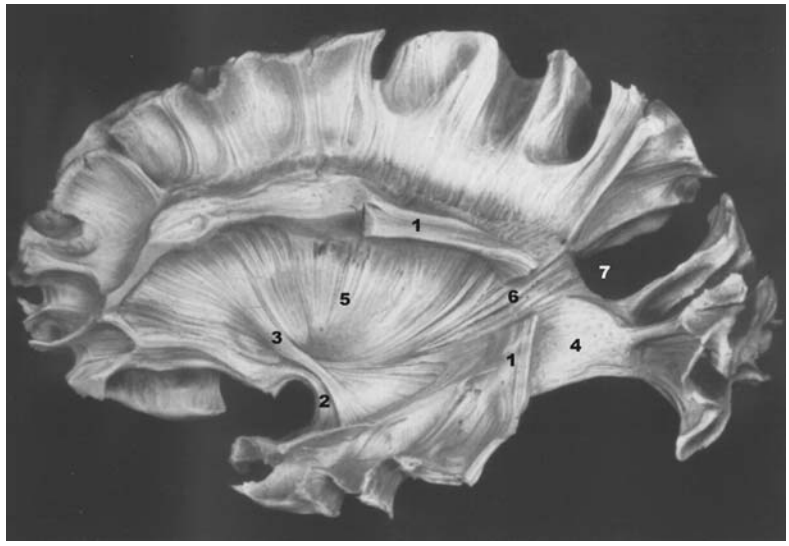

Fig. 3.78. Dissection of the brain disclosing the major association fiber bundles, showing the uncinate fasciculus and the external capsule. *1*, Superior longitudinal fasciculus; *2*, uncinate fasciculus; *3*, inferior fronto-occipital fasciculus; *4*, sagittal stratum; *5*, external capsule; *6*, splenium fibers; 7, parieto-occipital sulcus. (By Klingler. From Ludwig and Klingler 1956, Table 8)

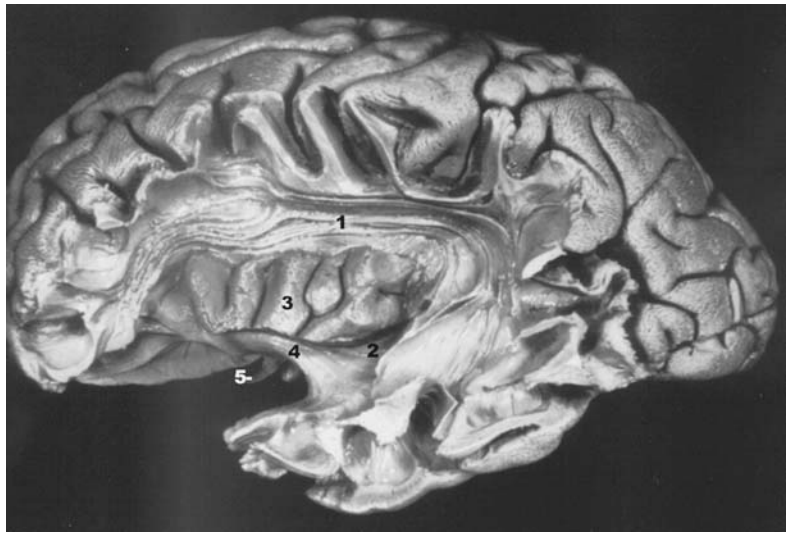

Fig. 3.79. Dissection of the brain disclosing the major association fiber bundles at the level of the insula. *1*, Superior longitudinal fasciculus; *2*, inferior fronto-occipital fasciculus; *3*, insula; *4*, uncinate fasciculus; *5*, optic chiasm. (By Klingler. From Ludwig and Klingler 1956, Table 5)

III Vascular Supply of the Brain

A The Arterial Supply of the Brain

The brain is supplied by the internal carotid arteries and the vertebral arteries (Fig. 3.80). The common carotid artery arises on the left side directly from the aortic arch. On the right side it arises from the bifurcation of the brachiocephalic artery (innominate artery). The common carotid arteries bifurcate at the upper level of the thyroid cartilage corresponding to the upper margin of the fourth cervical vertebra to form the internal and external carotid arteries. The vertebral artery originates in the neck as the third branch of the subclavian artery on each side. The vertebral arteries enter the transverse foramen of the C6 cervical vertebra and ascend in the transverse foramina until they reach the C2. At this level the vertebral arteries proceed laterally, penetrating the transverse foramen of the atlas. The arteries then proceed upward and medially, and pierce the atlanto-occipital membrane and dura as they enter the foramen magnum. The left and right vertebral arteries unite to constitute the basilar artery, usually at the lower border of the pons (Fig. 3.81).

1 The Internal Carotid Artery

The internal carotid artery may be divided into four segments: the cervical, intrapetrosal, intracavernous

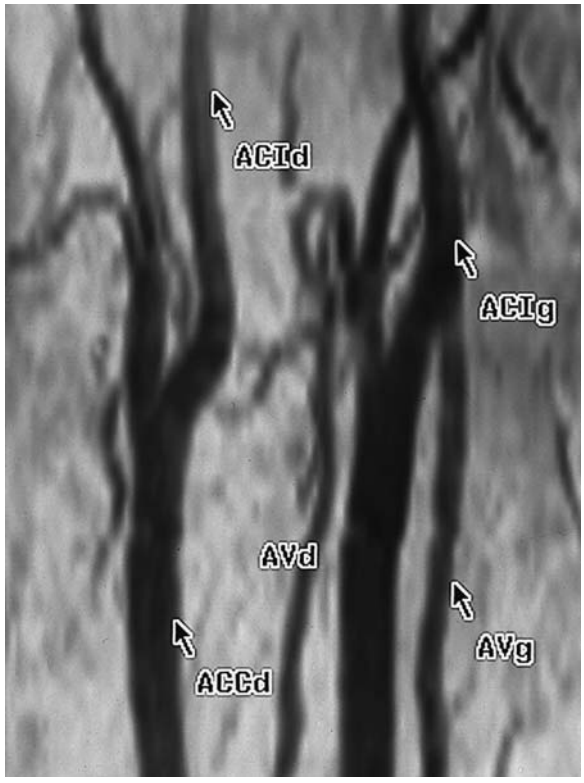

Fig. 3.80. MR angiography of the carotid and vertebral vessels, using 2D time of flight pulse sequence and a neck surface coil. *ACId*, Right internal carotid artery; *ACIg*, left internal carotid artery; *ACCd*, right common carotid artery; *AVd*, right vertebral artery; *AVg*, left vertebral artery

Fig. 3.81. The vertebral basilar system and major branches using FSE T2 weighted MR in the coronal plane. *1*, Posterior cerebral artery; *2*, superior cerebellar artery; *3*, middle cerebellary artery; *4*, posterior inferior cerebellar artery; *5*, vertebral artery. *F*, fornix; *CM*, Mammillary body (corpus mamillare)

and supraclinoid. The intracavernous and the supraclinoid segments are referred to as the "carotid siphon" because of their characteristic shape.

The cervical segment arises from the bifurcation of the common carotid, has no branches and ends as the artery enters the carotid canal in the petrous bone. This segment of the artery corresponds to the intrapetrosal portion where the carotid artery is contained for a short distance in a canal surrounded extradurally by areolar tissue. The intracavernous segment contained within the cavernous sinus lies near its the medial wall. Note that as it enters the cavernous sinus, the artery may show a circular constriction which should not be confused with abnormal narrowing on MR angiographs. In the cavernous sinus, the carotid artery courses roughly horizontally, at the level or just above the floor of the sella turcica. Important relationships to the cranial nerves III, IV, VI and V2, which are located along the wall of the sinus, can be identified. The abducens nerve (VI) is located within the cavernous sinus adjacent to the carotid artery. The supraclinoid segment begins as the artery emerges from the cavernous sinus and projects medially to the anterior clinoid process, becoming intradural, extending upward and backward to its bifurcation and giving rise to all its major branches.

The major branches of the internal carotid artery are the ophthalmic artery, the posterior communicating artery, the anterior choroidal artery, the anterior cerebral artery and the middle cerebral artery (Fig. 3.82).

a The Ophthalmic Artery

The ophthalmic artery arises from the carotid artery immediately after the latter leaves the cavernous sinus. It enters the orbit through the optic foramen, ventral and lateral to the optic nerve (II), then turns upward and medially to pass over the nerve in the orbital cavity. The ophthalmic artery yields several branches, including the lacrimal, supraorbital, ethmoidal and palpebral branches as well as the central retinal artery. It may originate from the middle meningeal artery. The branches of the ophthalmic artery anastomose profusely with those of the external carotid artery.

b The Posterior Communicating Artery

The posterior communicating artery originates from the dorsal aspect of the carotid siphon proceeding medially and posteriorly to join the posterior cerebral artery approximately 10 mm distal to the bifurcation of the basilar artery (Fig. 3.82). At its junction

with the carotid siphon a slight dilatation may be observed which should not be confused with an ectasia. The posterior communicating artery may be continuous with the parieto-occipital branch of the posterior cerebral artery, the posterior temporal branch arising from the carotid siphon.

c The Anterior Choroidal Artery

The anterior choroidal artery arises distal to the origin of the posterior communicating artery in 75% of cases, and passes backward across the cisternal space and the optic tract. It then extends laterally to reach the medial surface of the temporal lobe before entering through the choroidal fissure in the temporal horn to supply the choroid plexus. The anterior choroidal artery also supplies the hippocampal formation and part of the basal ganglia. Its usual length is about 30 mm.

d The Anterior Cerebral Artery

The anterior cerebral artery arises at the bifurcation of the internal carotid artery, lateral to the optic chiasm, as one of the two terminal branches of the internal carotid artery(Fig. 3.83). It is subdivided into a horizontal and a vertical segment. The horizontal (A1) portion runs medially and forward above the cisternal optic nerve to the anterior communicating artery. At this level, the artery bends sharply and the vertical segment (A2) ascends along the interhemispheric fissure. At the junction between the rostrum and the genu of the corpus callosum, the anterior cerebral artery turns dorsally forming a so-called arterial "knee" (A3), then continues backward above and along the corpus callosum (A4 and A5). The anterior cerebral artery gives rise to the medial striate artery or recurrent artery of Hubner, an orbital artery, a frontopolar artery, a callosomarginal artery and a pericallosal artery.

The medial striate artery arises usually distal (80% of cases) to the anterior communicating artery but may also arise proximal to it or even at the same level. This recurrent artery courses caudally and laterally and branches many times before entering the anterior perforated substance to partially supply the striatum and internal capsule. It may give rise to branches supplying the inferior aspect of the frontal lobe (Perlmutter and Rhoton 1976).

The orbital artery, consisting sometimes of two or three branches, arises from the ascending portion of the anterior cerebral artery. It extends forward and downward to supply the orbital and medial surfaces of the frontal lobe.

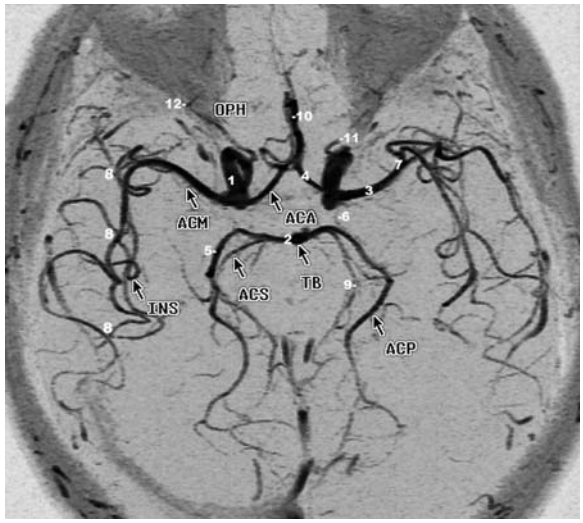

Fig. 3.82. The circle of Willis (MR angiography using 3D time of flight pulse sequence). *1*, Internal carotid artery; *2*, basilar artery; *3*, proximal segment of middle cerebral artery; *4*, proximal segment of anterior cerebral artery; *5*, proximal segment of posterior cerebral artery; *6*, posterior communicating artery; *7*, bifurcation of middle cerebral artery; *8*, insular branches of middle cerebral artery; *9*, perimesencephalic segment of superior cerebellar artery; *10*, pericallosal artery; *11*, ophthalmic artery; *12*, perioptic loop of ophthalmic artery; *OPH*, ophthalmic artery; *ACA*, anterior cerebral artery; *ACM*, middle cerebral artery; *INS*, insular branches of middle cerebral artery; *TB*, basilar artery; *ACP*, posterior cerebral artery; *ACS*, superior cerebellar artery

The callosomarginal artery is the major branch of the anterior cerebral artery. It arises from the knee of the anterior cerebral artery, distal to the origin of the frontopolar artery, around the genu of the corpus callosum. It gives an anterior, a middle and a posterior internal frontal branch, and may terminate as a paracentral branch. When the internal frontal and the paracentral branches reach the upper margin of the cerebral hemisphere, they anastomose with the pre- and postcentral branches of the middle cerebral artery. The branches of this artery supply the paracentral lobule and parts of the cingulate gyrus (Lazorthes et al. 1976).

The pericallosal artery, also called the terminal branch of the anterior cerebral artery, is usually located close to the upper surface of the corpus callosum giving rise to the paracentral branch, which may alternatively arise from the callosomarginal artery. It terminates as the precuneal branch which supplies the medial surface of the parietal lobe, including the precuneus. A posterior callosal branch supplies the corpus callosum and anastomoses with

A

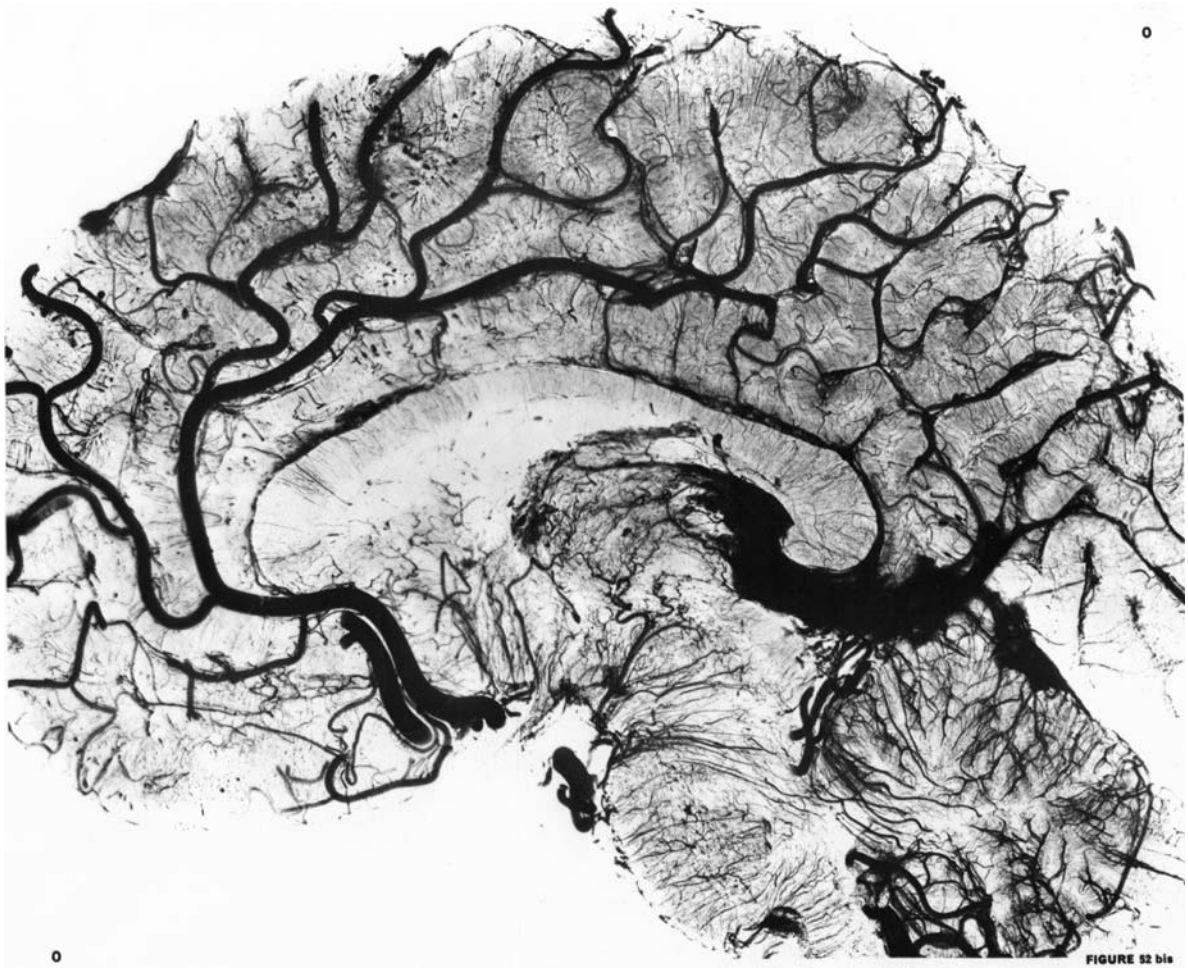

B

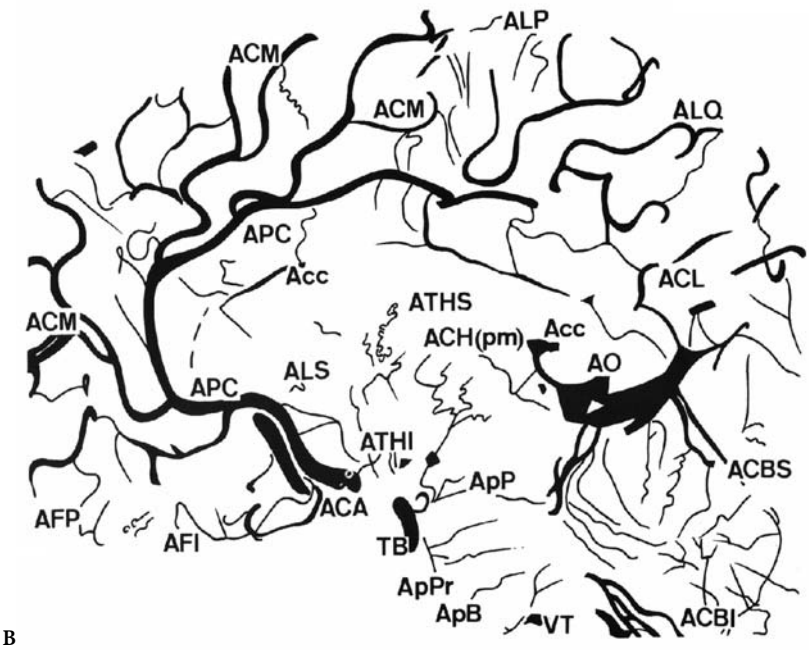

Fig. 3.83A,B. The anterior cerebral artery (*ACA*) and its cortical branches. **A** Macroscopic cut and corresponding diagram (**B**) of a brain specimen showing the disposition of the arterial branches. *ACA*, Anterior cerebral artery; *ACBI*, posterior inferior cerebellar artery; *ACBS*, superior cerebellar artery; *Acc*, arteries of the corpus callosum; *ACH*, medial posterior choroidal arteries; *ACL*, calcarine artery; *ACM*, callosomarginal artery; *AFI*, orbitofrontal artery; *AFP*, frontopolar artery; *ALQ*, artery of the precuneus; *ALP*, artery of the paracentral lobule; *ALS*, lenticulostriate arteries; *AO*, occipital artery; *ApB*, perforating medullary arteries; *APC*, pericallosal artery; *ApP*, peduncular branches; *ApPr*, pontine arteries; *ATHI*, inferior thalamic arteries; *ATHS*, superior thalamic arteries; *TB*, basilar trunk; *VT*, vertebral artery. (From Salamon 1971)

a branch of the posterior cerebral artery. Anatomic variants of the anterior cerebral artery occur in about 25% of brains including a hypoplastic horizontal portion or, more rarely, a total absence of this segment.

e The Middle Cerebral Artery

The middle cerebral artery is larger than the anterior artery and is regarded as the direct continuation of the internal carotid artery or its main branch. It is normally never absent. The proximal portion of the middle cerebral artery is nearly horizontal (M1) coursing laterally over the anterior perforated substance to enter the lateral cerebral fossa between the temporal lobe and the lower aspect of the insula (Figs. 3.84, 3.85). Turning around the lower part of the insula, the middle cerebral artery passes upward and backward in the deepest portion of the lateral fissure forming a number of large branches. Variations of two or three, in the number of branches formed at the end of M1 segment, are the rule (Figs. 3.84, 3.85).

In the insular area, the middle cerebral artery gives rise to five to eight branches. The most posterior branch emerging from the lateral fissure corresponds to the sylvian point. The branches of the middle cerebral artery emerge from the lateral fissure and are distributed over the lateral aspect of the cerebral hemisphere (Fig. 3.86).

Before giving rise to the cortical branches, the horizontal segment of the middle cerebral artery forms the striate arteries, represented by two groups of three to six small arteries named the medial and lateral striate arteries, which penetrate the brain through the anterior perforated substance. These small perforating arteries tend to rise at nearly right angles from the main vessels (Fig. 3.87).

Before describing the cortical branches, it is important to consider the anatomy of these middle cerebral arterial branches as they course through the sylvian fissure and form the so-called "sylvian triangle" (Schlesinger 1953). The inferior side of the sylvian triangle, as shown on a lateral cut or projection, is formed by the line starting at the posterior point of the lateral fissure, called the angiographic sylvian point, and extending to the anterior extremity of the middle cerebral artery. The anterior superior aspect of the triangle corresponds to the top of the first identifiable opercular branch. The actual position of the sylvian or lateral fissure may be placed on lateral angiograms as the line joining the points where the opercular vessels turn to leave the lateral fissure after having descended. On frontal views the sylvian point, which corresponds to the most medial extent of the last branch of the middle cerebral artery before it emerges from the fissure, is centered between the roof of the orbit and the horizontal line tangential to the inner table of the skull vertex (Vlahovitch et al. 1964, 1965, 1970).

The orbitofrontal artery found on the orbitofrontal cortex may anastomose with the frontopolar branch of the anterior cerebral artery. The remaining branches of the cerebral artery are ascending on the lateral aspect of the frontoparietal lobe including the precentral branches, a central or rolandic artery, a postcentral artery and a posterior parietal branch. A posterior temporal branch supplies the lateral aspect of the occipital lobe. The angular artery, or angular branches, form the terminal segment of the middle cerebral artery supplying the angular gyrus. The middle cerebral artery, which is the major artery of the lateral aspect of the cerebral hemisphere, supplies an extensive and functionally important region of the cerebral cortex including the central and motor areas, the somesthetic and the auditory areas, as well as large regions of the associative cortex (Figs. 3.86, 3.88).

2 The Arterial Circle of Willis

Described by Willis (1664), this anastomotic arterial circle is a constant anatomic structure located at the basal surface of the brain in the chiasmal cistern encircling the optic chiasm, the tuber cinereum and the interpeduncular fossa (Fig. 3.82). It is formed by anastomotic branches of the internal carotid artery and the basilar artery, as well as by the anterior and posterior communicating arteries and the proximal segments of the anterior, middle and posterior cerebral arteries. Several variants are observed and it is common to find asymmetrical development of the various components. A symmetrical circle is observed in about 20% of cases.

From the arterial circle of Willis and the main cerebral arteries arise the central and cortical branches. The small central arteries arise from the circle of Willis and the proximal segments of the anterior, middle and posterior cerebral arteries. These arteries penetrate perpendicularly into the basal brain substance to supply the basal ganglia, the internal capsule and the diencephalon. The cortical or circumferential arteries, branches of the three major cerebral arteries, course on the lateral and medial aspects of the cerebral hemispheres. From these cortical branches arise smaller terminal arteries which penetrate the brain substance at right angles, some

A

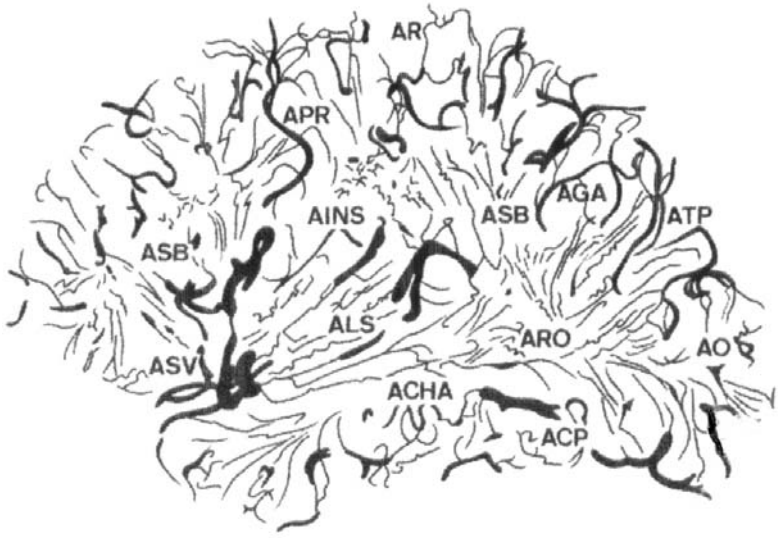

B

Fig. 3.84A,B. The insular branches of the middle cerebral artery (*MCA*) and the cortical branches. **A** Macroscopic cut and corresponding diagram (**B**) of a brain specimen showing the disposition of the arterial branches. *ACHA*, Anterior choroidal artery; *ACP*, posterior cerebral artery; *AGA*, artery of the angular gyrus; *AINS*, insular artery; *ALS*, lenticulostriate arteries; *AO,* occipital artery; *APR*, prerolandic artery; *AR*, rolandic artery; *ARO*, arteries of the optic radiation; *ASB*, arteries of the white matter; *ASV*, sylvian artery; *ATP*, posterior temporal artery. (From Salamon 1971)

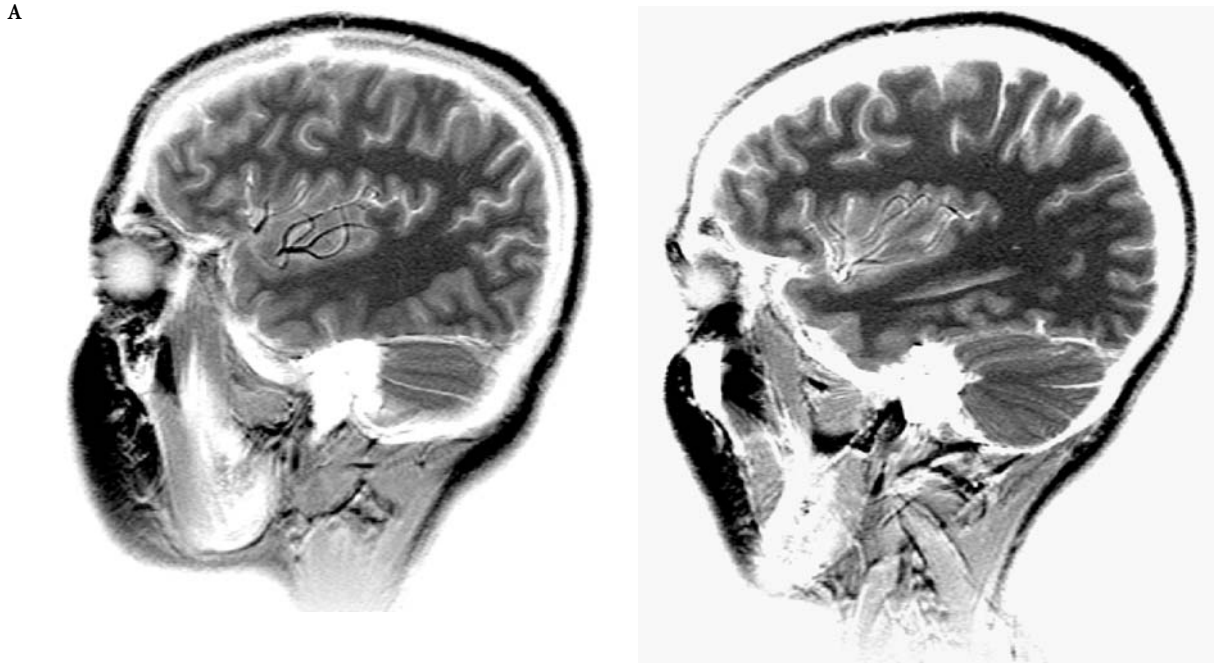

Fig. 3.85A,B. Parasagittal MR cuts showing the variable branching of the insular branches of the middle cerebral artery

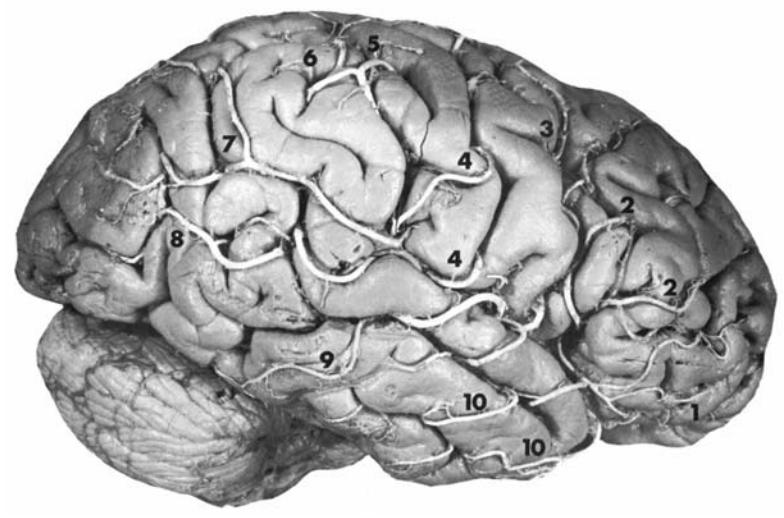

Fig. 3.86. Anatomic arrangement of the cortical branches of the middle cerebral artery on the lateral aspect of a right hemisphere. *1*, Orbitofrontal artery; *2*, prefrontal artery; *3*, precentral artery; *4*, central artery; *5*, anterior parietal artery; *6*, posterior parietal artery; *7*, angular gyrus artery; *8*, posterior temporal artery; *9*, middle temporal artery; *10*, anterior temporal artery. (From Salamon 1971)

A

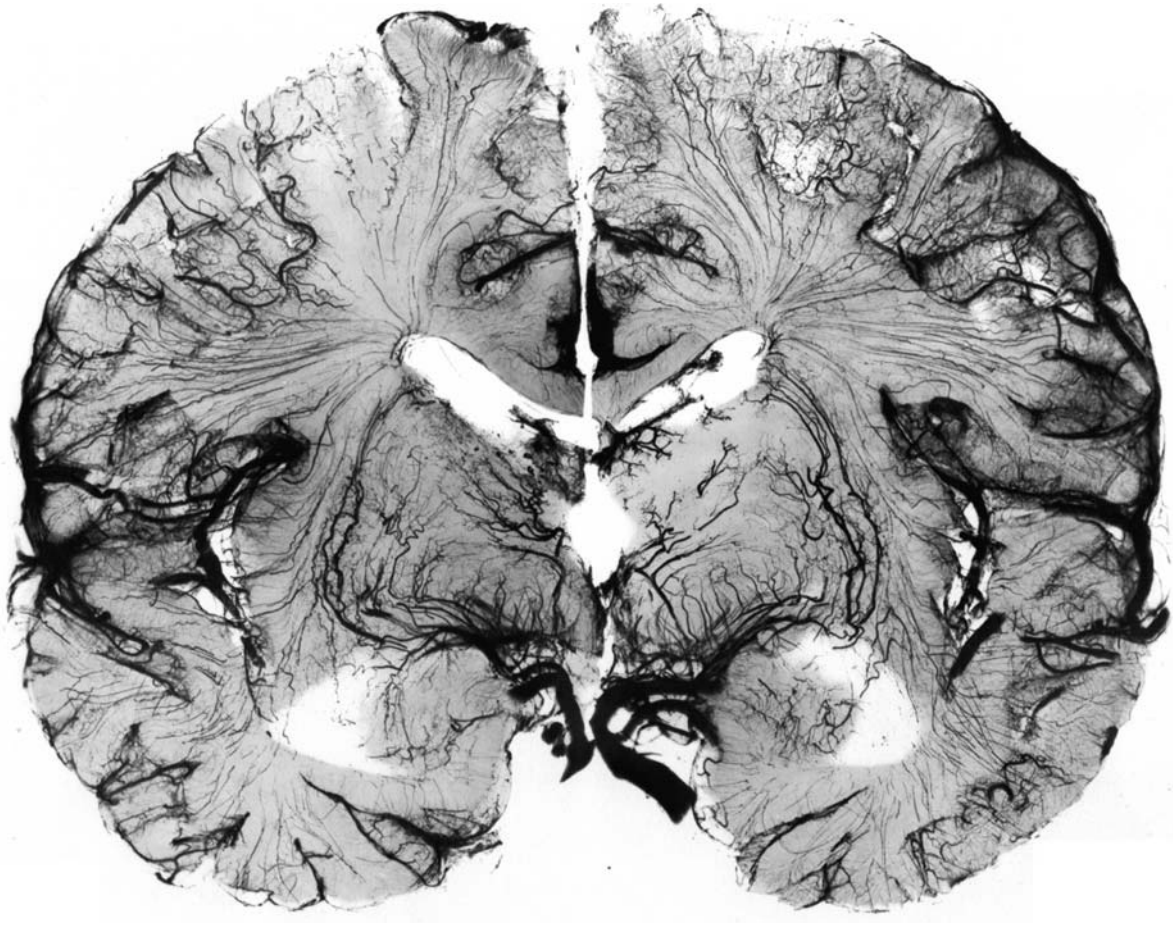

B

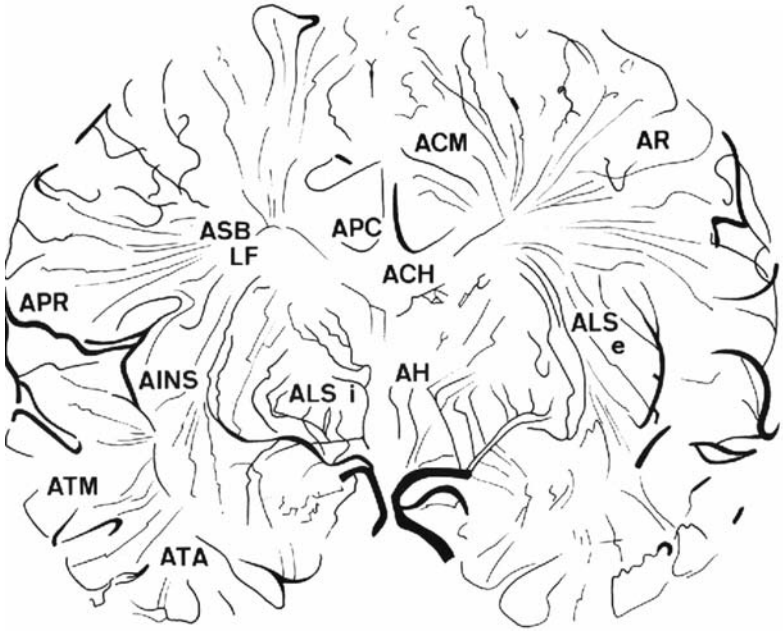

Fig. 3.87A,B. The striate arteries of the interbrain structures. **A** Macroscopic section and corresponding diagram (**B**) of a brain specimen and correlated angiogram. *ACH*, choroidal arteries (superior group); *ACM*, callosomarginal artery; *AH*, artery of Heubner; *AINS*, insular arteries; *ALS*, lenticulostriate arteries; *e*, external striate; *i*, internal striate; *APC*, pericallosal artery; *APR*, prerolandic artery; *AR*, rolandic artery; *ASB*, arteries of the white matter (*LF*) of the frontal lobe; *AYA*, anterior temporal artery; *ATM*, middle temporal artery. (From Salamon 1971)

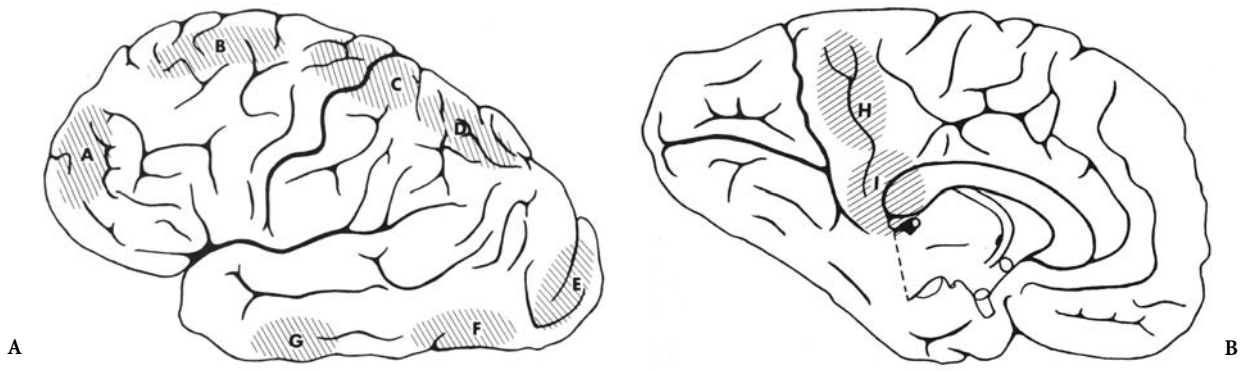

Fig. 3.88. A Areas of anastomoses (*hatched*) between the terminal branches of the major cerebral arteries (lateral aspect of the hemisphere). *A*, Orbital branches of ACA and MCA; *B*, callosomarginal (ACA) and operculofrontal (MCA) branches; *C*, central (MCA) and pericentral (ACA) branches; *D*, posterior parietal branches (MCA) and PCA; *E*, posterior temporal branches (MCA) and calcarine (PCA); *F*, posterior temporal branches (MCA) and posterior cerebral branches (PCA); *G*, anterior temporal branches (MCA and PCA). **B** Areas of anastomoses (*hatched*) between the terminal branches of the major cerebral arteries (mesial aspect of the hemisphere). *H*, Precuneal branches (ACA) and parieto-occipital (PCA); *I*, pericallosal branch (ACA) and posterior callosal ramus of PCA. (From Gillilan 1974)

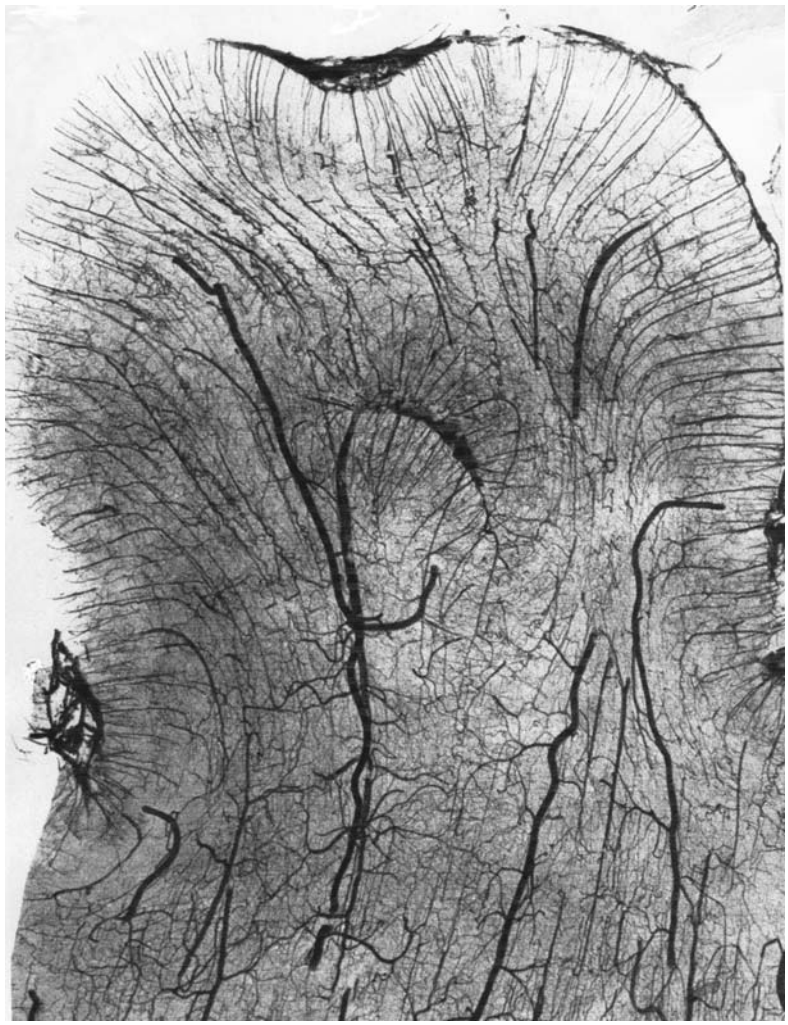

Fig. 3.89. Perforating arteries of the central cortex of the cerebral hemisphere, corresponding to the smaller terminal arteries penetrating the brain substance at right angles which supply the cortical mantle and the subcortical white matter. (From Salamon 1971) +100

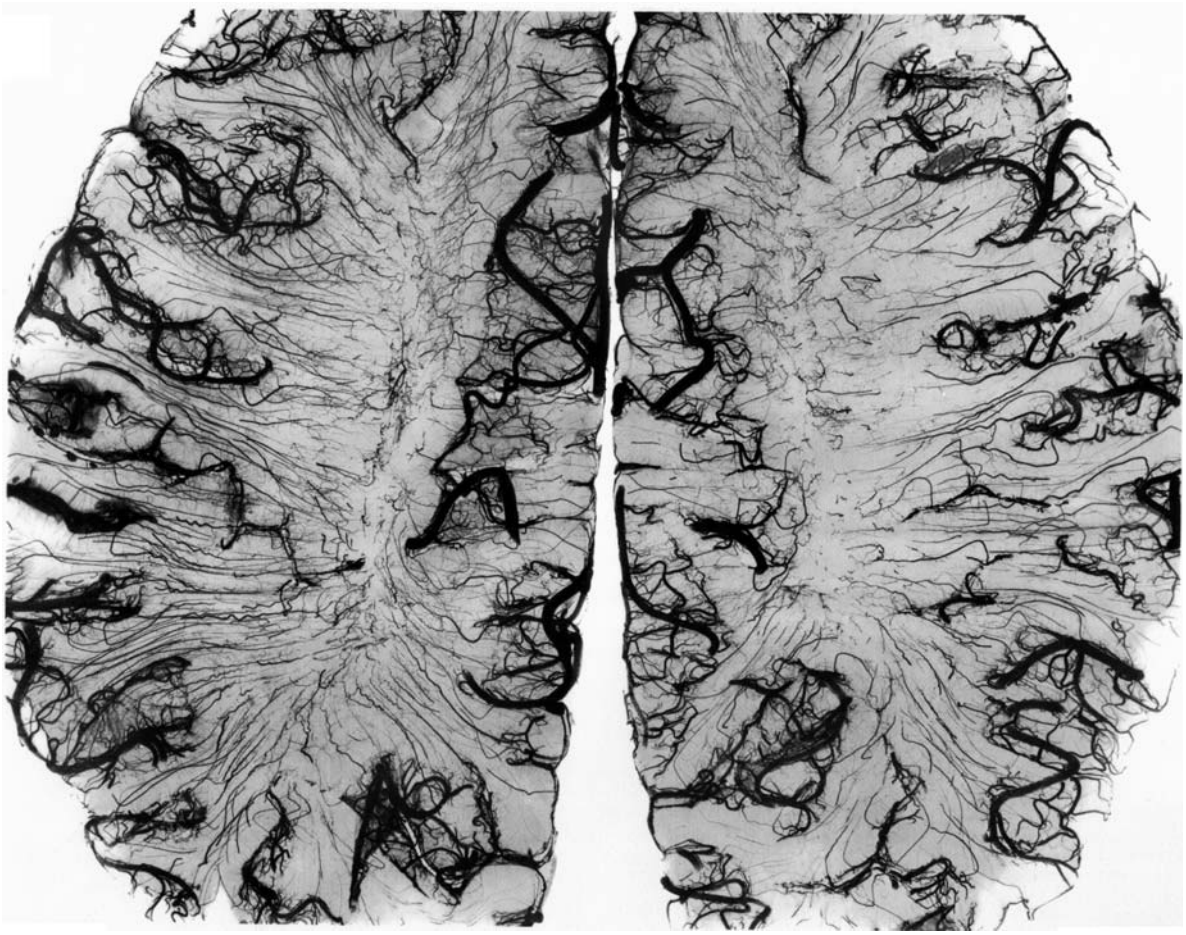

Fig. 3.90. The watershed junctional zones in the deep white matter, showing a roughly symmetrical disposition, as seen on the axial cut through the centrum semiovale. (From Salamon 1971)

of which arborize in the cortex while the longer ones supply the subcortical deep white matter (Fig. 3.89). These cortical branches are not end arteries and show anastomoses which may compensate to a variable extent the occlusion of one of these vessels with the blood supply from adjacent branches. The watershed zones, which may show ischemia in the case of hypotension, correspond to the areas of the cerebral cortex, the basal ganglia and the internal capsule situated between the territorial distributions of two of the primary arteries (Fig. 3.87,3.90).

B Vascular Supply of the Posterior Fossa

The vascular supply of the posterior fossa is provided by two vertebral arteries, which join at the level of the pontomedullary junction to form the basilar artery. Branches of the vertebral and basilar arteries can be classified into three types: the penetrating arteries, which penetrate the brainstem in its ventral aspect at the midline; The short circumferential and the long circumferential arteries. At each level of the brain stem, one circumferential artery is markedly developed and provides the blood supply for that portion of the brain stem and cerebellum. At the level of the medulla, the posterior inferior cerebellar artery supplies part of the medulla and the suboccipital surface of the cerebellum. The pons and petrosal surface of the cerebellum are supplied by the anterior inferior cerebellar artery, and the midbrain and tentorial surface of the cerebellum are supplied by the superior cerebellar artery.

1 The Posterior Inferior Cerebellar Artery

The posterior inferior cerebellar artery (PICA) is the largest branch of the vertebral artery, arising most commonly from its intradural segment. The PICA is divided into five segments according to Rhoton: an

anterior medullary segment, beginning at the origin of the PICA and terminating at the level of the inferior olive, continues with the second or lateral medullary segment which ends at the level of the lower cranial nerves. The third, or tonsilomedullary, segment is closely related to the tonsils, forming a caudal loop. The fourth, or retrotonsilar, segment starts at the midlevel of the tonsil and ends where the artery exits to become hemispheric. The last segment, the hemispheric segment, supplies the occipital surface of the vermis and cerebellar hemisphere.

The vascular territory of the PICA is highly variable and reflects the high degree of variability of this artery. It appears to be in balance with other major vessels in the posterior fossa. It supplies the lateral medullary area in 50% of cases. Its cerebellar territory includes the globose and emboliform nuclei.

2 The Anterior Inferior Cerebellar Artery

The anterior inferior cerebellar artery (AICA) originates from the basilar artery at the level of the pontomedullary sulcus and curves in a caudal direction around the pons towards the cerebellopontine angle. At this level it divides into superior and inferior trunks. The inferior trunk passes below the flocculus and vascularizes the inferior portion of the petrosal surface of the cerebellar hemisphere. The superior trunk has an upward curve and anastomoses with the superior cerebellar artery.

3 The Superior Cerebellar Artery

The superior cerebellar artery (SCA) originates from the superior segment of the basilar artery, usually a few millimeters before it divides into the posterior cerebral arteries. Duplication of the SCA is common and noted in 80% of cases. The course of the SCA is parallel to the postcerebral artery and is separated from the latter by the third nerve. Both arteries sweep around the brain stem towards the quadrigeminal plates. There, the SCA makes a sharp upward turn to reach the cerebellar hemisphere. It supplies the lower midbrain, upper pons, the dentate nucleus and the tentorial surface of the cerebellar hemisphere.

C The Cerebral Venous System

The cerebral venous system comprises the superficial cerebral veins and the deep cerebral veins, all of which, like dural sinuses, are devoid of valves. These two venous systems are very richly anastomosed (Fig. 3.91). The superficial cerebral veins are extremely variable, most running upward to end in the superior longitudinal sinus. In general, these veins drain the blood from the cortex and subcortical white matter to the superior sagittal sinus or the basal sinuses. The deep cerebral veins drain the choroid plexus, the diencephalon, the basal ganglia and the periventricular and deep white matter into the internal cerebral veins and the great cerebral vein.

The superficial cerebral veins form a network in the pia mater and then converge to form larger confluents which empty into the dural sinuses. These veins drain the blood from the lateral and medial aspects of the cerebral hemisphere into the superior sagittal sinus. There are about 10 to 15 superficial cerebral veins, the locations of which are extremely variable, most of them running upward before entering the superior sagittal sinus against the flow of the blood stream. Some of the veins of the medial hemispheric surface may drain into the inferior sagittal sinus. The largest of these veins is the superior anastomotic vein, or vein of Trolard, which anastomoses with the inferior anastomotic vein, or vein of Labbé. Both are variable in position, size and configuration. These two veins connect the superficial middle cerebral vein with the superior sagittal and transverse sinuses. The middle cerebral vein courses downward and forward in the lateral fissure before ending in the sphenoparietal or the cavernous sinus. The inferior aspect of the brain shows extensive venous plexus draining into the basal sinuses. The veins originating from the anterior temporal lobe and interpeduncular fossa drain into the cavernous and sphenoparietal sinuses. The orbital region may drain into the sagittal sinuses. The transverse and the petrosal sinuses collect the venous flow from the tentorium cerebelli. Note that the cortical regions of the medial and inferior aspects of the hemispheres may drain through anastomotic channels into the deep cerebral venous system.

The deep cerebral veins, angiographically more important than the superficial veins, comprise the insular and striate veins, the internal cerebral veins, the basal vein of Rosenthal and the great cerebral vein of Galen.

The insular veins present a similar configuration to the arterial branches of the middle cerebral artery even assuming a similar triangular configuration, “the venous sylvian triangle”. These veins drain into the deep middle cerebral vein, which in turn drains into the basal cerebral vein or the sphenoparietal sinus. The striate veins and veins originating from the

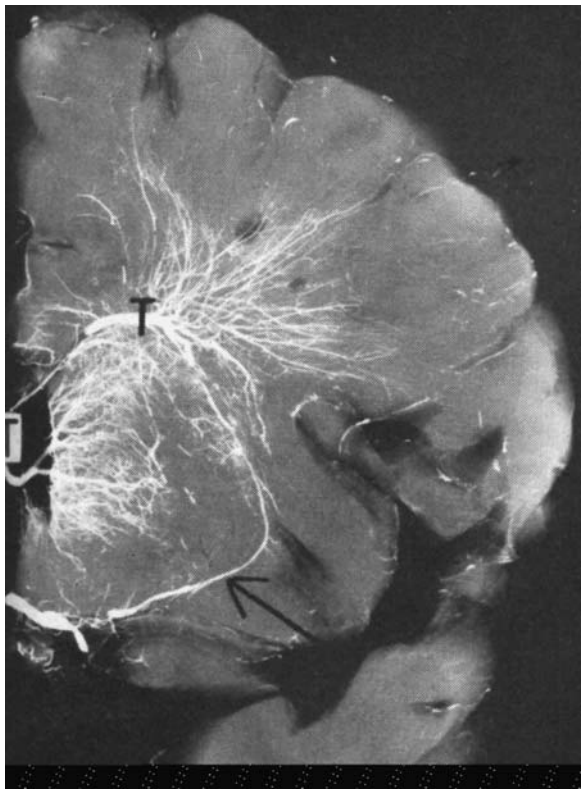

A

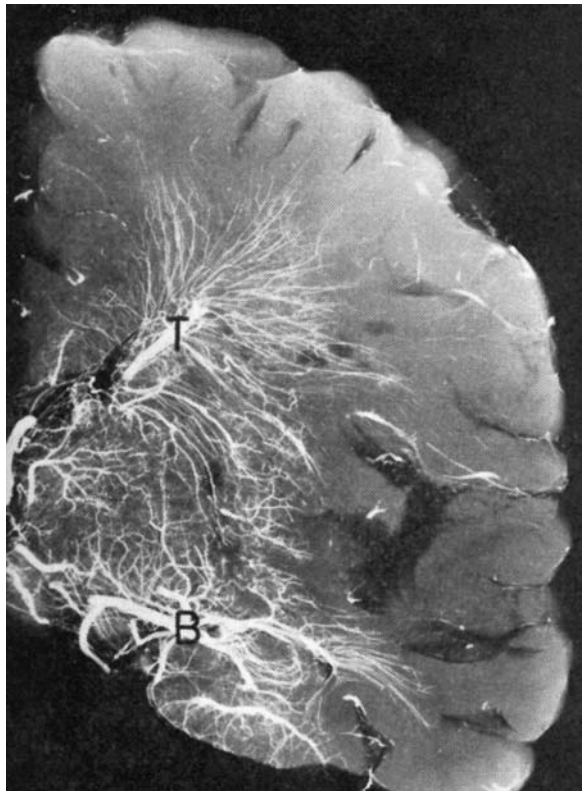

B

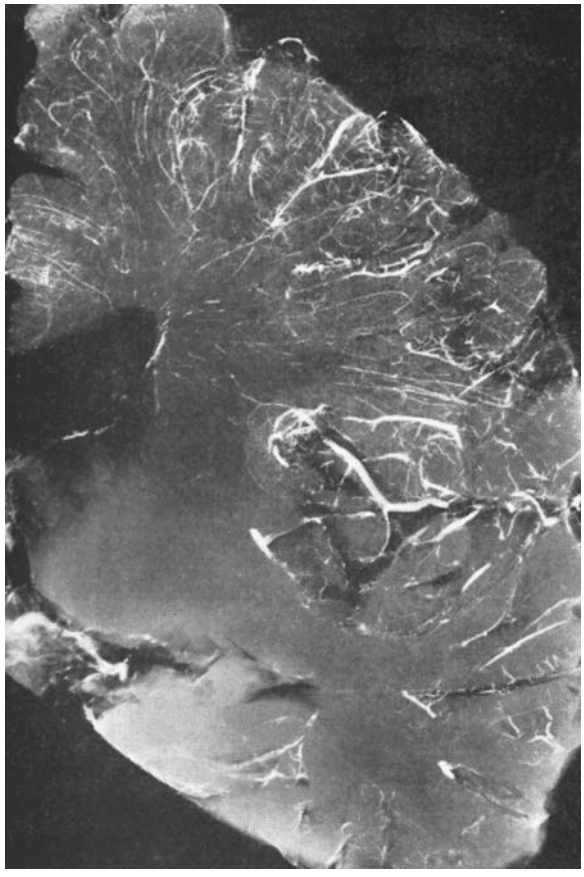

C

Fig. 3.91A–C. Coronal cuts of 1 cm thickness through head of the caudate (**A**) and the thalamus (**B**). *B*, basal vein; *T*, terminal vein; *I*, internal cerebral vein. **C** Coronal cut of 1 cm thickness through the posterior thalamus after contrast injection into the superior longitudinal sinus. (From Hassler 1966)

inferior aspect of the frontal lobe are also drained through the deep middle cerebral vein. An uncal vein coursing from the medial aspect of the temporal lobe drains into the sphenoparietal or cavernous sinus.

The paired internal cerebral veins, located just off the midline in the tela choroidea of the roof of the third ventricle, extend from the interventricular foramina of Monro over the superior and internal aspect of the thalamus to reach the upper portion of the quadrigeminal cistern. There they join to form the great cerebral vein of Galen. The latter follows a concave upward curve and ends in the straight sinus. The main tributary of the internal cerebral veins are: (1) the thalamostriate vein, which runs forward in the groove formed by the caudate nucleus and the thalamus; (2) the choroidal vein, which courses along the lateral border of the choroid plexus extending to the inferior horn of the lateral ventricle and draining the choroid plexus and the adjacent hippocampal regions; (3) the septal vein, which drains the rostral portion of the corpus callosum and the septum lucidum before joining the internal cerebral vein at the interventricular foramen; and (4) the epithalamic vein, which drains the dorsal portion of the diencephalon before joining the internal cerebral vein. The ventral portions of the diencephalon are drained into the pial venous plexus of the interpeduncular region. The lateral ventricular vein runs over the posterior superior aspect of the thalamus and joins the internal cerebral vein.

The basal vein of Rosenthal originates from the medial aspect of the anterior portion of the temporal lobe. It receives a small anterior cerebral vein which accompanies the anterior cerebral artery and drains the orbitofrontal region, the anterior corpus callosum and corresponding portions of the cingulate gyrus. The deep middle cerebral vein, situated in the depth of the lateral fissure, drains the insula and the opercular cortex. The inferior striate veins leave the striatum through the anterior perforated substance to drain into the deep middle cerebral vein. All these veins join the basal vein which passes backward around the brainstem to join the great cerebral vein of Galen.

The great cerebral vein of Galen is formed by the union of the paired internal cerebral veins, the paired basal veins, the paired occipital veins, which drain the internal and inferior aspects of the occipital lobes and the adjacent parietal lobes, and the posterior callosal vein, which drains the splenium and the adjacent internal brain areas. The great cerebral vein is a short vein located beneath the splenium of the corpus callosum. It drains into the rectus sinus.

References

Aresu M (1914) La superficie cerebrale nell'uomo. Arch Ital Anat Embr 12:380–433

Ariens Kappers CU (1947) Anatomie comparée du système nerveux. Masson and Cie, Paris (with the collaboration of E.H. Strasburger)

Ariens Kappers CU, Huber GC, Crosby EC (1936) Comparative anatomy of the central nervous system of vertebrates, including man, vols 1 and 2. Macmillan, New York

Bailey P (1948) Concerning the organization of the cerebral cortex. Tex Rep Biol Med 6:34–56

Bailey P, von Bonin G, Mc Culloch WS (1950) The isocortex of the chimpanzee. University of Illinois Press, Urbana, Ill

Bailey P, von Bonin G (1951) The isocortex of man. University of Illinois Press, Urbana, Ill

Baillarger JGF (1840) Recherches sur la structure dela couche corticale des circonvolutions du cerveau. Mem Acad R Med 8:149–183

Beccari N (1911) La superficie degli emisferi cerebrali dell'uomo nelle regioni prossime al rinecefalo. Arch Ital Anat Embr 10:482–543

Benedikt M (1906) Aus meinem Leben. Stulpnagel, Vienna

Betz W (1874) Anatomischer Nachweis zweier Gehirnzentra. Centr Med Wissensch 12:578–580, 595–599

Brissaud E (1893) Anatomie du cerveau de l'homme. Masson, Paris

Broca P (1878) Nomenclature cérébrale. Rev Anthropol 2:3

Brodmann K (1909) Vergleichende Lokalisationslehre der Großhirnrinde. Barth, Leipzig

Cabanis EA, Doyon D, Halimi PH, Iba-Zizen MT, Sigal R, Tamraz J (1988) Atlas d'IRM de l'encéphale et de la moëlle. Masson, Paris

Calori L (1870) Del cervello nei due tipi brachicefalo. zzz

Campbell AW (1905) Histological studies on the localization of cerebral function. Cambridge University Press, Cambridge

Chi T, Chang C (1941) The sulcal pattern of the Chinese brain. Am J Phys Anthropol 28:167–209

Chi JG, Dooling ED, Gilles FH (1977) Gyral development of the human brain. Ann Neurol 1:86

Chusid TG, Sugar O, French JD (1948) Corticocortical connections of the cerebral cortex lying within the arcuate and lunate sulci of the monkey (Macaca mulatta). J Neuropathol Exp Neurol 439–446

Comair Y, Hong SC, Bleasel A (1996a) Invasive investigation and surgery of the supplementary motor area. In: Lüders HO (ed) Advances in neurology, vol 70. Lippincott-Raven, Philadelphia

Comair YG, Choi HY, Tamraz J (1996b) Cortical anatomy: sulcal and gyral patterns. In: Wyllie E (ed) The treatment of epilepsy: principles and practice, 2nd edn. Lea and Febiger, Philadelphia

Connolly CJ (1950) External morphology of the primate brain. Thomas, Springfield, Ill

Cunningham DJ (1890) The intraparietal sulcus of the brain. J Anat Physiol 24:137–155

Cunningham DJ, Horsley V (1892) Contribution to the surface anatomy of the cerebral hemispheres. Royal Irish Academy, Dublin

Déjerine J (1895) Anatomie des centres nerveux, vol 1 and 2. Rueff, Paris

Delmas A, Pertuiset B (1959) Topométrie crânio-encéphalique chez l'homme. Masson, Paris
Duvernoy H, Cabanis EA, Iba-Zizen MT, Tamraz J, Guyot J (1991) The human brain surface three-dimensional sectional anatomy and MRI. Springer, Vienna New York
Eberstaller O (1884) Zur Oberflächen-Anatomie der Grosshirn-Hemisphären. Wien Med Bl 7:644–646
Eberstaller O (1890) Das Stirnhirn. Ein Beitrag zur Anatomie des Oberfläche des Großhirns. Urban and Schwarzenberg, Vienna
Ecker A (1869) Die Hirnwindungen des Menschen. Vieweg, Braunschweig
Elze K (1929) Einige Fasersysteme des menschlichen Grosshirns mit der Abfaserungs-methode untersucht. Z Anat Entwicklungsgesch 88:166–178
Filimonoff IN (1947) A rational subdivision of the cerebral cortex. Arch Neurol Psychiatr 58:296–311
Flechsig P (1898) Neue Untersuchungen über die Markbildung in den menschlichen Grosshirnlappen. Neurol Centrlbl 17:977–996
Giacomini C (1878) Guida allo studio delle circonvoluzioni cerebrali dell'uomo. Camilla e Bertolero, Turin, pp 96
Gillilan (1974) Potential collateral circulation to the human cerebral cortex. Neurology 24:941–948
Geyer H (1940) Über Hirnwindungen bei Zwillingen. Z Morphol Anthropol 38:51–55
Gratiolet P (1854) Mémoire sur les plis cérébraux de l'homme et des primates. Bertrand, Paris
Hassler H (1966) Deep cerebral venous system in man. Neurology 16:505–511
Henneberg R (1910) Messung der Oberflächenausdehnung der Grosshirnrinde. J Psychol Neurol 17:144–158
Heschl RL (1878) Über die vordere quere Schläfenwindung des menschlichen Grosshirns. Braumuller, Vienna
Higeta K (1940) Morphologische Untersuchungen des Gehirns bei den japanischen Zwillingsfeten. Okajimas Fol Anat Jpn 19:239–284
His W (1904) Die Entwicklung des menschlichen Gehirns während der ersten Monate. Hirzel, Leipzig
Holl M (1908) Die Insel des Menschen und Affenhirns in ihren Beziehung zum Schlafenlappen. Sitz Berl Akad Wissensch Wien Math Naturw Kl 117(3):365–410
Huang CC (1991) Sonographic cerebral sulcal development in premature newborns. Brain Dev 13:27
Huxley TH (1861) On the brain of Ateles paniscus. Proc Zool Soc Lond pp 247–260
Jaeger R (1914) Inhaltsberechnungen der Rinden und Marksubstanz des Grosshirns durch planimetrishce Messungen. Arch Psychiatr Nervenkrankh 54:261–272
Jefferson G (1913) The morphology of the sulcus interparietalis. J Anat Physiol 47:365–380
Jensen J (1870) Die Furchen und Windungen der menschlichen Grosshirnhemispharen. Allg Z Psychiatr 27:473–515
Jensen J (1875) Untersuchungen uber die Beziehungen zwischen Grosshirn und Geistesstörung an sechs Gehirnen geisteskranker Individuen. Arch Psychiatr Nervenkrankh. 5:587–757
Kanai T (1938) Über die Furchen und Windungen der Orbitalfläche des Stirnhirns bei Japanern. Okajimas Fol Anat Jpn 18:229–306
Karplus JP (1905) Über Familienähnlichkeiten an den Grosshirnfurchen des Menschen. Arb Neurol Inst Wien Univ 12:1–58
Karplus JP (1921) Zur Kenntnis der Variabilität und Vererbung am Zentralnervensystem des Menschen und einiger Sauger, 2nd edn. Deuticke, Leipzig
Kaufman E (1887) Über Mängel des Balkens im menschlichen Gehirn. Arch Psychiatr Nervenkrankh 18:769
Klingler J (1935) Erleichterung der makroskopischen Präparation des Gehirns durch den Gefrierprozess. Schw Arch Neurol Psychiatr 36:247–256
Kohlbrugge JHF (1906) Die Grosshirrfurchen der Javanen. Verh K Akad Wetens, Sect II, Amsterdam Deel 12(4):195 (9 plates)
Kraus WM, Davison C, Weil A (1928) The measurement of cerebral and cerebellar surfaces. Arch Neurol Psychiatr 19:454–477
Kükenthal W, Ziehen T (1895) Untersuchungen über die Grosshirnfurchen der Primaten. Jen Z Naturwiss 29:1–122
Landau E (1910) Über die Orbitalfurchen bei den Esten. Z Morphol Anthropol 12:341–352
Landau E (1911) Über die Grosshirnfurchen am basalen Teile des temporooccipitalen Feldes bei den Esten. Z Morphol Anthropol 13:423–438
Landau E (1914) Über die Furchen an der Lateralfläche des Grosshirns bei den Esten. Z Morphol Anthropol 16:239–279
Landau E (1919) The comparative anatomy of the nucleus amygdalae, the claustrum and the insular cortex. J Anat 53:351–360
Larroche J-C, Feess-Higgins A (1987) Development of the human foetal brain. An anatomical atlas. Editions INSERM. Masson, Paris
Lazorthes G, Gouazé A, Salamon G (1976) Vascularisation et circulation cérébrales. Masson, Paris
Leboucq G (1929) Le rapport entre le poids et la surface de l'hemisphere cerebral chez l'homme et les singes. Mem Acad R Belge Cl Sc 10(9):57
Leuret F, Gratiolet P (1839) Anatomie comparée du système nerveux, considérée dans ses rapports avec l'intelligence, vol 1 and 2. Baillière, Paris. Atlas. Masson, Paris
Lorente de No R (1933) Studies on the structure of the cerebral cortex. I. The area endorhinalis. J Psychol Neurol 45:381–438
Ludwig E, Klingler J (1956) Atlas cerebri humani. Karger, Basel
Marchand F (1895) Die Morphologie des Stirnlappens und der Insel der Anthropomorphen. Arb Pathol Inst Marb 2:1–108
McLardy T (1950) Uraemic and trophic deaths following leucotomy: neuro-anatomical findings. J Neurol Neurosurg Psychiatry 13:106–114
Meynert T (1867/1868) Der Bau der Grosshirnrinde und seine örtlichen Verschiedenheiten, nebst einem pathologisch-anatomischen Corollarium. Vierteljahrsch Psychiatr 1:77–93, 125–217, 381–403; 2:88–113
Meynert T (1877) Neue Studien über die Associationsbundel des Hirnmantels. Sitz Berl K Akad Wiss Wien Kl 101(3):361–380

Naidich P, Valavanis G, Kubik S (1995) Anatomic relationships along the low-middle convexity. I. Normal specimens and magnetic resonance imaging. Neurosurgery 36(3):517–531

Nieuwenhuys R, Voogd J, Van Huijzen C (1988) The human central nervous system. A synopsis and atlas, 3rd edn. Springer, Berlin Heidelberg New York

Ono N, Kubik S, Abernathy DG (1990) Atlas of the cerebral sulci. Thieme, Stuttgart

Onufrowicz W (1887) Das balkenlose Mikrocephalengehirn Hofmann. Arch Psychiatr Nervenkrankh 18:305–328

Paturet G (1964) Traité d'anatomie humaine, vol 4: système nerveux. Masson, Paris

Perlmutter D, Rhoton AL Jr (1976) Microsurgical anatomy of the anterior cerebral-anterior communicating-recurrent artery complex. J Neurosurg 45(3):259–272

Pfeifer RA (1936) Pathologie der Hörstrahlung und der corticale Hörsphäre. In: Foerster O (ed) Handbuch der Neurologie, vol 6. Springer, Berlin, pp 533–626

Ramon y Cajal S (1911) Histologie du système nerveux de l'homme et des vertébrés, vol II. (translated by L. Azoulay) Maloine, Paris

Retzius G (1896) Das Menschenhirn. Studien in der makroskopischen Morphologie, vol 1. Norstedt, Stockholm

Rose M (1926) Über das histogenetische Prinzip der Einteilung der Grosshirnrinde. J Psychol Neurol 32:97–158

Rössle R (1937) Zur Frage der Ähnlichkeit des Windungsbildes an Gehirnen von Blutsverwandten, besonders von Zwillingen. Sitz Ber Preuss Akad Wissensch pp 146–68

Salamon G (1971) Atlas of the arteries of the human brain. Sandoz, Paris

Salamon G, Raynaud C, Regis J et al (1990) Magnetic resonance imaging of the pediatric brain. An anatomical atlas. Raven, New York

Sano F (1916) The convolutional pattern of the brains of identical twins. Philos Trans R Soc Lond B 208:37–61

Schlesinger B (1953) The insulo-opercular arteries of the brain, with special reference to the angiography of striothalamic tumors. Am J Roentgenol 70:555–563

Schnopfhagen F (1890) Die Entstehung der Windungen des Grosshirns. J Psychiatr 9:197–318

Shellshear JL (1926) The occipital lobe in the brain of the Chinese with special reference to the sulcus lunatus. J Anat 61:1–13

Slome I (1932) The bushman brain. J Anat 67:47–58

Symington J, Crymble PT (1913) The central fissure of the cerebrum. J Anat 47:321–39

Szikla G, Bouvier G, Hori T, Petrov V (1977) Angiography of the human brain cortex: atlas of vascular patterns and stereotactic cortical localization. Springer, Berlin Heidelberg New York

Talairach J, Szikla G, Tournoux P, Prossalentis A, Bordas-Ferrer M, Covello L, Iacob M, Mempel E (1967) Atlas d'anatomie stéréotaxique du télencéphale. Masson, Paris

Tamraz J (1983) Atlas d'anatomie céphalique dans le plan neuro-oculaire (PNO). MD Thesis, Schering, Paris (1986)

Tamraz J (1991) Morphometrie de l'encephale par resonance magnetique: application à la pathologie chromosomique humaine, à l'anatomie comparée et à la teratologie. These Doct Sci Paris V, Paris

Tamraz J, Rethoré M-O, Iba-Zizen M-T, Lejeune J, Cabanis EA (1987) Contribution of magnetic resonance imaging to the knowledge of CNS malformations related to chromosomal aberrations. Hum Genet 76:265–273

Tamraz J, Saban R, Reperant J, Cabanis EA (1990) Définition d'un plan de référence céphalique en imagerie par résonance magnétique: le plan chiasmato-commissural. CR Acad Sci Paris 311(III):115–121

Tamraz J, Saban R, Reperant J, Cabanis EA (1991) A new cephalic reference plane for use with magnetic resonance imaging: the chiasmato-commissural plane. Surg Radiol Anat 13:197–201

Tamraz J, Rethoré M-O, Lejeune J, Outin C, Goepel R, Stievenart JL, Iba-Zizen M-T, Cabanis EA (1993) Morphométrie encéphalique en IRM dans la maladie du cri du chat. A propos de sept patients, avec revue de la littérature. Ann Génét 2:75–87

Testut L, Latarjet A (1948) Traité d'anatomie humaine. Tome 2: système nerveux central, 9th edn. Doin, Paris

Turner OA (1948) Growth and development of the cerebral cortical pattern in man. Arch Neurol Psychiatr 59:1–12

Turner OA (1950) Some data concerning the growth and development of the cerebral cortex in man II. Postnatal Psychiatr (Chic) 64:378–385

Turner W (1891) The convolutions of the brain. J Anat Physiol 25:105–153

van Bork-Feltkamp AJ (1930) Utkomsten van een onderzoek van een 60-tal hersenen van chineezen. Versluis Uitgevers-Maatschappij, Amsterdam

Vint FW (1934) The brain of the Kenya native. J Anat 68:216–223

Vlahovitch B, Gros C, Fernandez-Serrats A, Adib-Yazdi IS, Billet M (1964) Repérage du sillon insulaire supérieur dans l'angiographie carotidienne de profil. Neurochirurgie 10:91–99

Vlahovitch B, Gros C, Fernandez-Serrats A (1965) Les repères de l'insula dans la partique de l'angiographie carotidienne. Expansion Scientifique Française, Paris

Vlahovitch B, Frerebeau P, Kuhner A, Billet M, Gros C (1970) Etude des lignes supra et infra-insulaires dans l'angiographie carotidienne normale et pathologique. Neurochirurgie 16:127–183

Vogt C, Vogt O (1919) Allgemeinere Ergbnisse unserer Hirnforschung. J Psychol Neurol (Lpz) 25:279–461

von Bonin G, Bailey P (1947) The neocortex of macaca mulatta. University of Illinois Press,Urbana, Ill (Illinois Monographs in the Medical Sciences, vol V, no 4)

von Economo C (1927) L'architecture cellulaire normale de l'ecorce cerebrale. Masson, Paris

von Economo C (1929) The cytoarchitectonics of the human cerebral cortex. Oxford University Press, London

von Economo C, Koskinas GN (1925) Die Cytoarchitektonik der Hirnrinde des erwachsenen Menschen. Textband und Atlas. Springer, Vienna New York

Wagner H (1864) Massbestimmungen der Oberfläche des Gehrins. Wigand, Cassel

Weinberg R (1905) Die Gehirnform der Polen. Ztschr Morphol Anthropol 8:123–214; 279–424

Wernicke C (1876) Das Urwindungsstystem des menschlichen Gehirns. Arch Psychiatr Nervenkr 6:298–326

Wernicke C (1881–83) Lehrbuch der Gehirnkrankheiten, vol 1–3. Fischer, Kassel

Wilder BC (1886) The paroccipital. A newly recognized fissural integer. J Nerv Ment Dis 8:301–315
Willis T (1664) Cerebri anatome, cui accessit nervorum descriptio et usus. Martyn and Allestry, London
Zenker W (1985) Benninghoff Makroskopische und mikroskopische Anatomie des Menschen. Nervensystem. Urban and Schwarzenberg, Munich
Zernov D (1877) The individual types of the brain sinuosity. University of Moscow, Moscow
Zuckerkandl E (1906) Zur Anatomie der Fissura calcarina. Arb Neurol Inst Wien Univ 13:25-61